THE UNIVERSITY OF MICHIGAN

INDUSTRY PROGRAM OF THE COLLEGE OF ENGINEERING

ANALYSIS OF THE EFFECT OF MEAN STRESS ON THE FATIGUE STRENGTH OF NOTCHED STEEL SPECIMENS WITH PARTICULAR REGARD TO THE INFLUENCE OF LOCAL PLASTIC STRAIN

Robert E. Little

A dissertation submitted in partial fulfillment
of the requirements for the degree of
Doctor of Philosophy in the
University of Michigan
Department of Mechanical Engineering
1963

August, 1963

IP-630

ACKNOWLEDGEMENTS

The writer gratefully acknowledges all those who aided in this study and those associated with his doctoral studies, in particular the following:

Professor Charles Lipson, Chairman of the Doctoral Committee for his encouragement and constructive criticism.

Professor Robert C. Juvinall, Doctoral Committee member for his encouragement and constructive criticism.

Professor Clarence A. Siebert, Doctoral Committee member for his assistance in the metallurgical area of this study.

Professors Samuel K. Clark and Joseph E. Shigley, Doctoral Committee members for their advice and assistance.

Professor Gordon J. Van Wylen, Chairman of the Department of Mechanical Engineering for his aid, counsel, and encouragement.

The National Science Foundation and the Horace H. Rackham School of Graduate Studies for predoctoral fellowships.

The Department of Mechanical Engineering for support of this study and for providing financial support through a teaching fellowship and an instructorship.

S. Roll and R. S. Shoberg for their help in making the specimens and mounting the strain gages. T. A. Despres and W. Mitchell for their stimulating discussions of fatigue.

The Dearborn Center of the University for use of the facilities of the Engineering Mechanics Laboratory.

The Industry Program of the College of Engineering for its assistance in preparing this dissertation.

TABLE OF CONTENTS

TABLE OF CONTENTS (CONT'D)

LIST OF TABLES

LIST OF FIGURES

LIST OF FIGURES (CONT'D)

CHAPTER I

INTRODUCTION

Since the beginnings of the Industrial Revolution, engineers have been confronted with the problem of preventing fatigue in various metals, particularly steel. Prevention of fatigue is of prime importance in design because fatigue failure is an abrupt failure which may occur in metallic machine components as a result of alternating, repeated, or spectral stressing under normal operating conditions.

Although many studies have been made of fatigue failure in machine components and in laboratory specimens, the body of existing knowledge is not adequate to serve as a basis for a fundamental understanding of the effect on the fatigue mechanism of superimposing a steady or mean stress upon the alternating stress. The primary objective of this study, therefore, has been to examine existing knowledge about fatigue, and through experimental work based on what is already known, to arrive at a more accurate means of predicting the effect of mean stress on the ability of a metal to resist failure by fatigue.

Traditionally, the most satisfactory approach to predicting the effect of mean stress has been the use of the modified Goodman diagram, which depicts an empirical relationship between the allowable or "working" alternating stress and the given superimposed mean stress. A major end-product of this study is the development of a similar diagram which, however, incorporates several modifications to treat factors not previously considered.

All such diagrams, which are termed working stress diagrams, are based on the pioneer work by Wöhler[1] about 1860 which showed that fatigue failure in steel is caused by alternating stressing. Wöhler's work led to the development of the S-N curve which is a plot of the imposed alternating stress, S_a, versus the number of stress cycles to failure, N. The S-N curve has become the basic element in diagrams depicting the fatigue behavior of engineering materials.

The S-N Curve

Figure 1.1 shows the general form of Wöhler's results schematically. The amplitude of the alternating stress which leads to failure after N stress cycles is termed the fatigue strength for a life of N cycles. Mild steels, under normal conditions, exhibit a knee in the S-N curve, a point at which the curve becomes horizontal. The amplitude of the alternating stress corresponding to the horizontal portion of the curve is termed the fatigue limit. It is generally accepted that if the amplitude of the imposed alternating stress is smaller than the fatigue limit, then no failure will take place, no matter how many stress cycles are imposed on the material.

Although the most common fatigue tests pertain to zero mean stress, this mode of stressing is relatively rare in practice. In general, a periodic stress is considered as having an alternating stress component (S_a) and a mean stress component (S_m) and is termed a cyclic stress. Thus, it is necessary to stipulate the value of the mean stress as well as the magnitude of the alternating stress

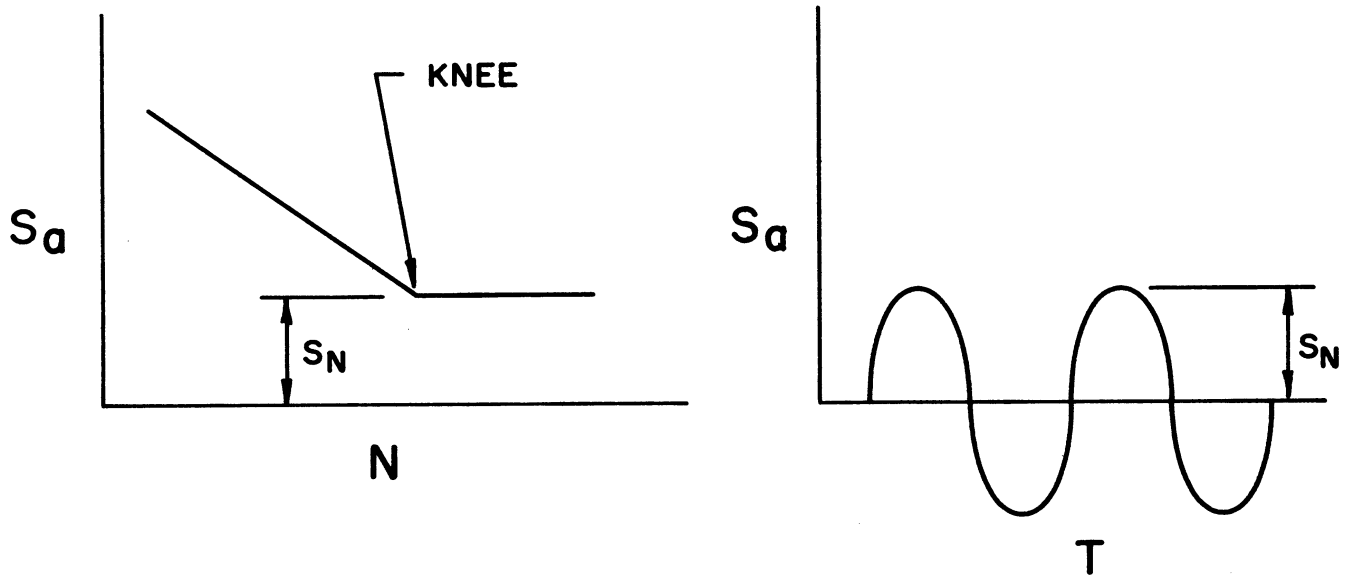

Figure 1.1 Wöhler curve or S-N curve. Corresponding alternating stress-versus-time diagram shown which pertains to the fatigue limit, S_n, of mild steel.

to define the cyclic stress and, consequently, to define the fatigue strength and the fatigue limit.

Wöhler discovered that the fatigue limit is reduced somewhat when tensile mean stress is superimposed on the material. This change in the fatigue limit, as related to various levels of mean stress, is refereed to as the effect of mean stress on fatigue.

Traditionally, the study of the effect of mean stress on fatigue has involved the testing of unnotched laboratory specimens. These specimens, which have a uniform cross-section, are used to develop the S-N curves of Figure 1.2. The over-all results of these fatigue tests can be summarized graphically in the form of an allowable or "working" stress diagram, such as the Goodman[2] diagram of Figure 1.3. The Goodman diagram shows that the allowable alternating stress decreases as the superimposed tensile mean stress increases.

An alternate method of plotting the Goodman relationship appears in Figure 1.4. This method was first used by Haigh[3] and by Soderberg.[4]

Working Stress Diagrams

No theory of fatigue adequately describes the effect of mean stress; practical working stress diagrams, such as Figure 1.3, are empirical and are developed by plotting fatigue data. Unfortunately, sufficient uniform data do not exist for all materials and all possible modes of loading to permit the extensive development of working stress diagrams. However, when sufficient uniform data exist, as is the case

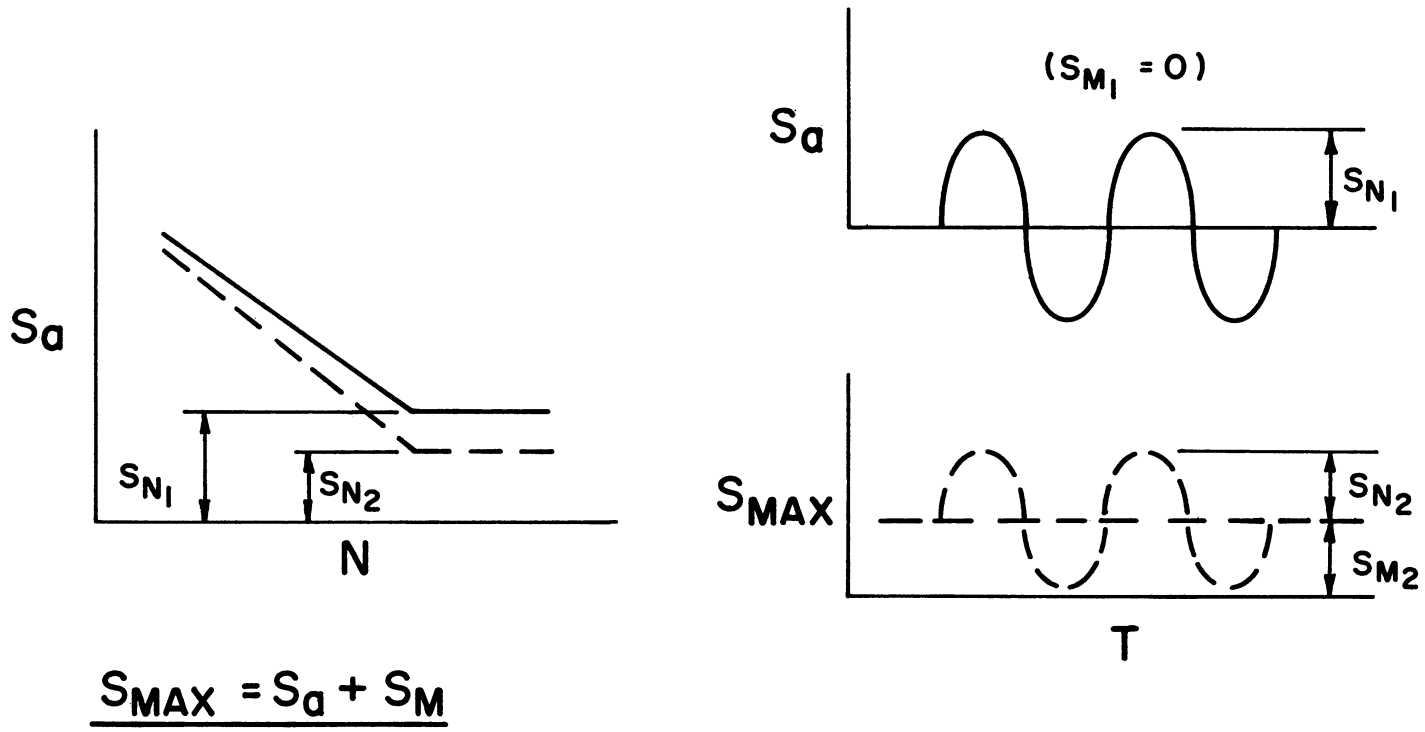

Figure 1.2 S-N curves showing effect of tensile mean stress. Alternating and cyclic stress-versus-time diagrams shown which pertain to the fatigue limits.

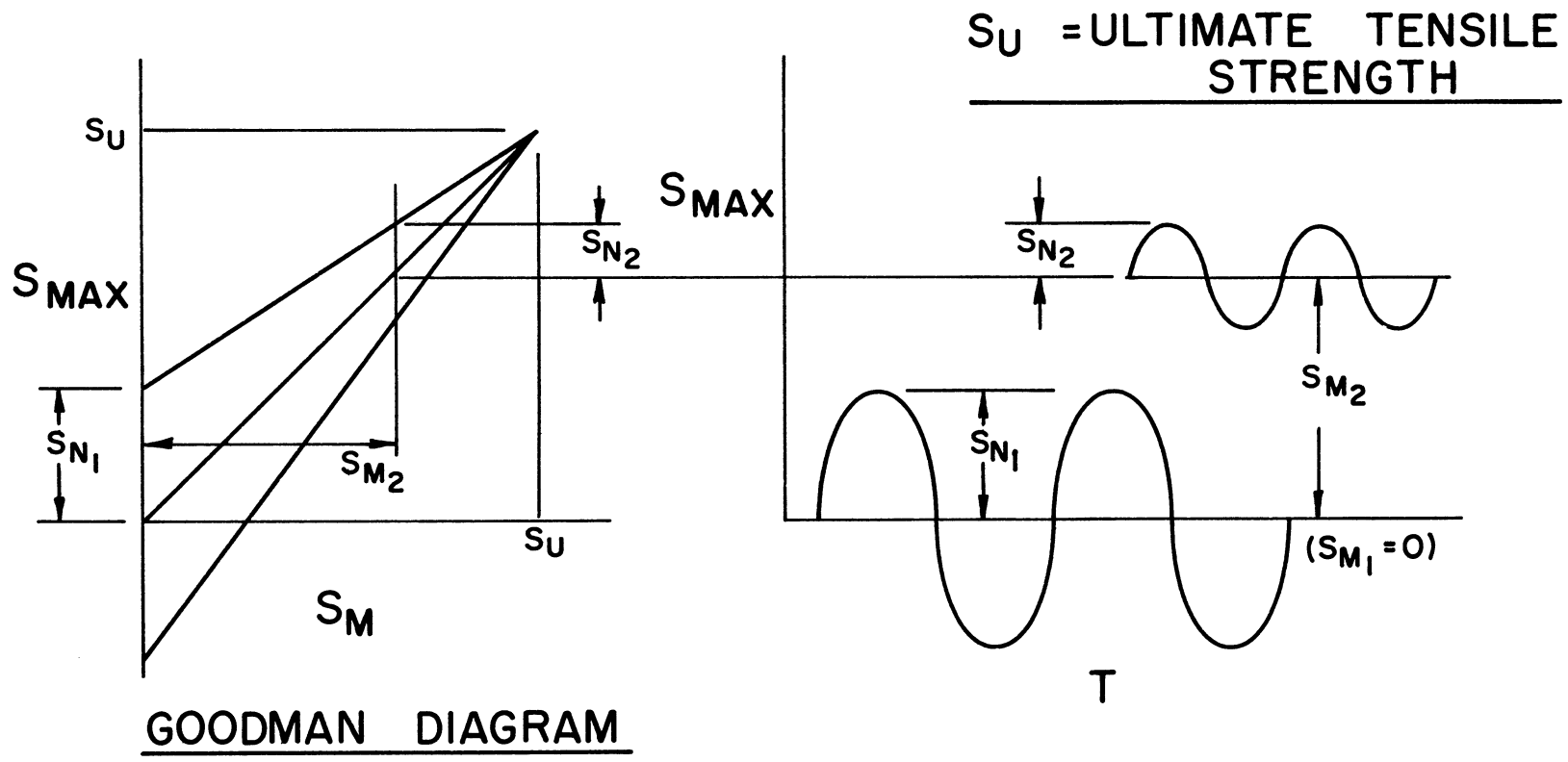

Figure 1.3 Goodman diagram representation of the effect of tensile mean stress on fatigue. See Figure 1.2. Diagram shows that as the mean stress increases, the allowable alternating stress decreases.

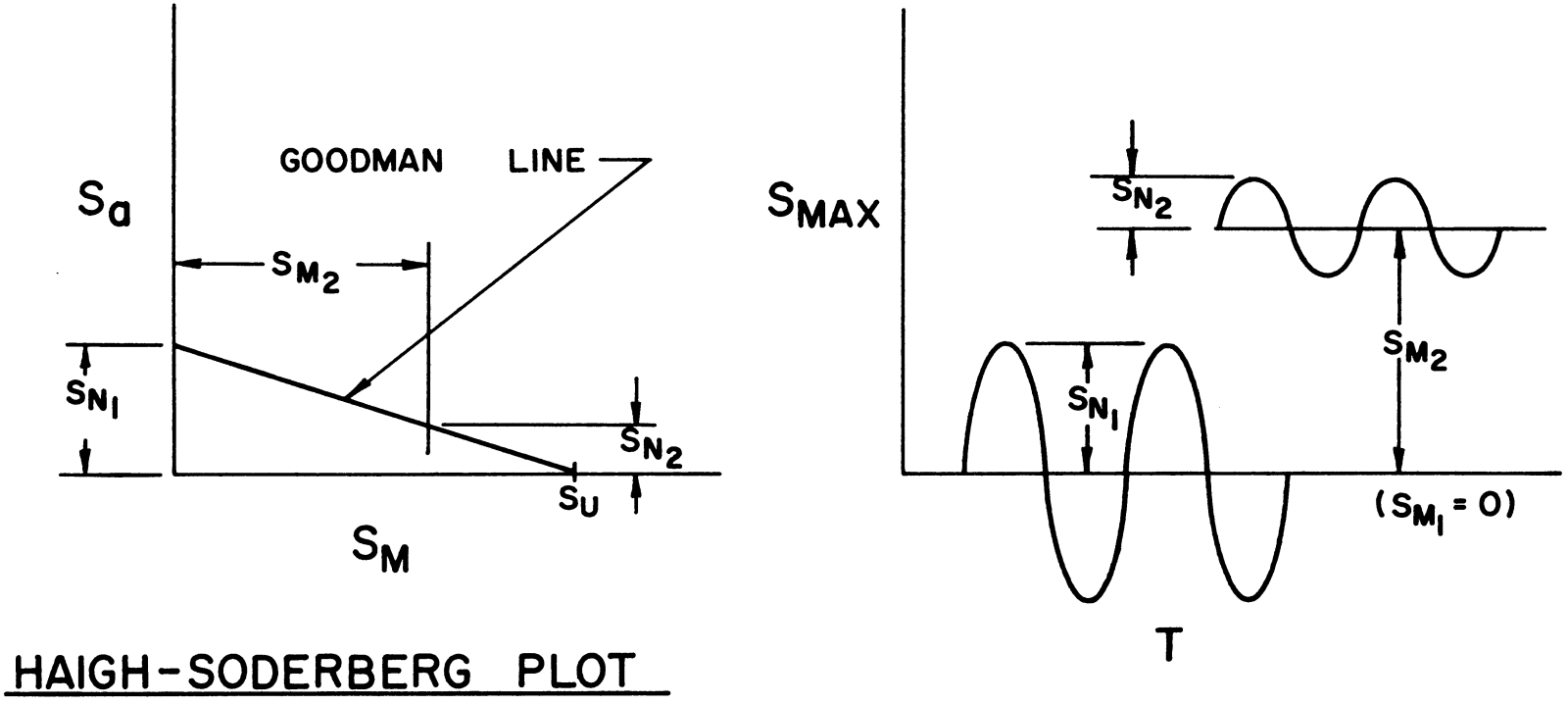

HAIGH-SODERBERG PLOT

Figure 1.4 Haigh-Soderberg method of plotting the Goodman relationship. See Figure 1.3. This method is used in this study.

for mild steel, the most practical approach in plotting these diagrams is to use the static strengths of the material as reference values. By this means, these diagrams can be used to estimate the mean stress fatigue behavior of similar materials by relating the appropriate static strengths.

In practice, the Goodman diagram of Figure 1.3 is modified to exclude maximum cyclic stresses (the mean stress plus the alternating stress) which exceed the static yield strength. These maximum stresses, although momentary, can induce very large deformations, particularly in the case of axial loading. These deformations precede failure by fatigue and therefore may become more critical than fatigue. Thus, strictly speaking, working stress diagrams pertain only to the domain of cyclic stress in which fatigue failure occurs without significant prior deformation.

Although working stress diagrams can be used to obtain a qualitative notion of the effect of mean stress on the fatigue limits of machine components, experience has shown that further experimental work is required to obtain quantitative correlation. In other words, the unnotched laboratory specimens used to develop the working stress diagrams do not correlate closely enough to actual machine components to permit direct use of these laboratory data in design analysis. The major factor preventing the direct use of laboratory data is that machine components have stress raisers (notches), while conventional laboratory specimens do not.

Effect of Notches

The term notch is used to identify all geometric stress raisers such as holes, grooves, fillets, keyways, and splines. The influence of notches on the fatigue limit of a material cannot be quantitatively deduced from theory and must be determined by fatigue testing. To simplify test procedures, vertually all tests of this type have been conducted with a zero mean stress. These tests have shown that

$$K_f = 1 + (K_t - 1)q, \qquad (1.1)$$

where K_f = the fatigue strength reduction factor, which which is defined as the ratio of the unnotched fatigue strength for N cycles, to the notched fatigue strength for N cycles. This definition is also valid for the ratio of the fatigue limits, although the conventional terminology is somewhat inconsistent and the term fatigue limit reduction factor is more precise.

K_t = the geometric stress concentration factor, as determined by theory or test. This factor is generally based on the maximum principal stress and on the minimum cross-sectional area.

q = the notch sensitivity index calculated from test results using Equation (1.1). This index, discounting scatter in the data, ranges between zero and unity for different materials and notches.

With the appropriate notch sensitivity data, Equation (1.1) can be used to estimate the influence of any given notch on the fatigue limit at zero mean stress of any given material. However, because zero mean stress applications are rare, this method of estimating these fatigue limits has limited practical application.

Because this study deals with estimating the fatigue limit of notched specimens under various levels of mean stress, the use of

Equation (1.1) will be extended to relate the nonzero notched and unnotched fatigue limits.

Objectives of Study

This study places particular emphasis on the influence of the notch when the maximum cyclic stress is such that localized plastic strain (localized yielding) takes place at the root of the notch. The influence of localized yielding has been discussed qualitatively in the literature, but little experimental work has actually been done and no quantitative analysis exists for steel specimens. Consequently, a major objective of this study is to further the understanding of the influence of localized plastic strain on the fatigue limit of notched steel specimens.

Because improved understanding of localized plastic strain has definite practical application, another objective of this study is to utilize this knowledge to improve the ability to predict the fatigue limit of notched steel specimens under various levels of tensile mean stress. This ability, in many cases, can lead to more reliable design analyses.

Scope of Study

This study involves two basic areas: first, a literature survey and analysis of these data; then, an experimental study to extend the results of the literature survey.

The analysis of existing data involves three steps, as discussed in Chapter III. First, existing mean stress data for

unnotched steel laboratory specimens are compiled and plotted in the form of a working stress diagram. Then, this diagram is used in conjunction with the two most common methods of relating notched and unnotched fatigue limits to predict the fatigue limits of notched steel specimens. Finally, these predicted results are compared to existing data for notched specimens.

It will be seen in Chapter III that the predicted results correlate relatively well with the meager existing data for low mean stress levels; but the correlation is poor at very high mean stress levels because localized yielding takes place at these high mean stress levels and introduces an influence that was not considered in predicting these fatigue limits. Hence, the problem is to determine the influence of localized plastic strain on the fatigue limit at high mean stress levels and to relate this influence to existing data by modifying existing methods of analysis.

In the second area of this study, the influence of localized plastic strain is determined by conducting two series of fatigue tests. Each test series is conducted at a high level of mean stress: one series at the maximum mean stress level at which no localized plastic strain takes place, and the other test series at a higher mean stress level at which large localized plastic strain (approximately two per cent) takes place. (The fatigue specimen is a large mild steel plate with a one-inch-diameter central hole and is subjected to axial loading.)

In addition, the influence of cyclic loading on the local stress-strain behavior at the edge of the hole is determined by means of strain gages in order to relate this behavior to the observed fatigue limits.

The results from both areas of this study lead to the development of a method of predicting the fatigue limits of notched and unnotched steel specimens under various values of tensile mean stress. The development of this method involves the modification of existing approaches, models, and diagrams. Because these modifications necessitate introducing new definitions, and revising certain diagrams, Chapter II will consider these matters.

CHAPTER II

EXPLANATION OF TERMS AND DIAGRAMS[1]

In order to treat the influence of localized yielding on fatigue, it is necessary to define the ideal phenomenon and to distinguish between cyclic stresses which lead to ideal localized yielding and those which do not. An ideal model of localized yielding is used because it can illustrate the principles involved in the following discussion, without becoming entangled in the more complex aspects of the real phenomenon. Consequently, a discussion of the real phenomenon is postponed until Chapter VI when it is possible to augment that discussion by introducing the results of pertinent tests conducted in the second part of this study.

Ideal localized yielding occurs, by definition, when the maximum principal cyclic stress at the root of the notch exceeds the static yield strength of the material. Ideal yielding is independent of the state of stress, the principal stress gradient, the microstructure and grain size, and the size of the specimen.

Prior to discussion of the cyclic stresses which lead to ideal localized yielding and those which do not, methods of extending the definition of the fatigue strength reduction factor, K_f, to non-zero mean stress situations will be explained in order to develop background which will aid in distinguishing between these cyclic stresses.

---

[1] A summary of the basic terminology is given in Appendix A.

K_f For Nonzero Mean Stress Situations

The fatigue strength reduction factor has been defined previously for the case of alternating (fully reversed) stressing as the ratio of the unnotched fatigue strength to the notched fatigue strength: see Terminology (Appendix A) or see Chapter I, Effect of Notches. Figure 2.1 shows this definition graphically. Just as K_f is determined from the S-N curves of Figure 2.1, the corresponding factor for nonzero mean stress situations should be determined from S-N curves which pertain to the desired level of mean stress. However, mean stress data for notched specimens are very limited, perhaps because mean stress tests generally require expensive test equipment. In the absence of sufficient data, it has been the practice to extrapolate existing zero mean stress data to nonzero mean stress applications by using various empirical approaches.

The ASTM Manual on Fatigue Testing[5] suggests two approaches to extension of the definition of the fatigue strength reduction factor to nonzero mean stress situations. These approaches, which will be referred to as the internal yielding approach and the modified elastic approach, are outlined below.

According to the internal yielding approach (the most common approach), the fatigue strength reduction factor is defined as the ratio of the nominal alternating stress, S_a, for a polished unnotched specimen to that for a notched specimen; S_a is taken at a given life, N, from the S-N curves for the notched and unnotched specimens which pertain to the same value of nominal mean stress. The internal yielding approach is shown in Figure 2.2. In this definition, it follows

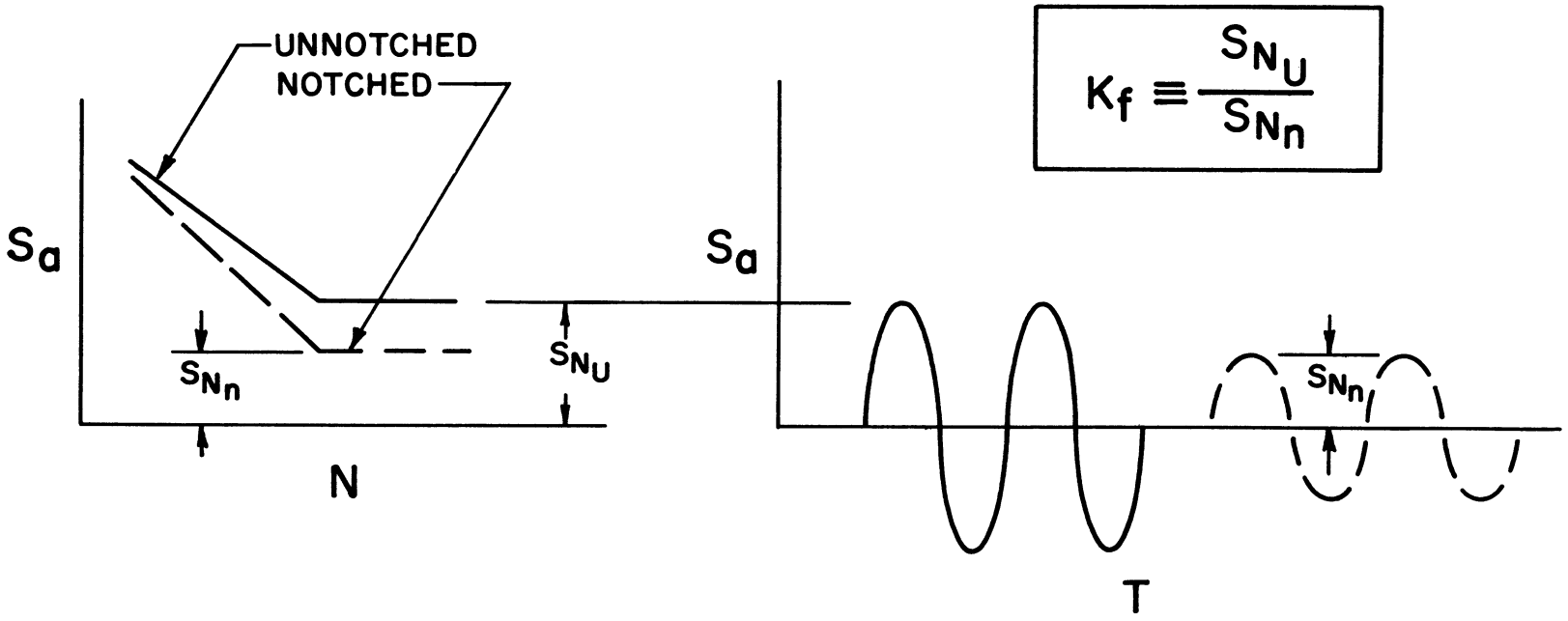

Figure 2.1 Definition of K_f for fully reversed stressing. It is assumed that the test conditions are identical for the notched and unnotched specimens.

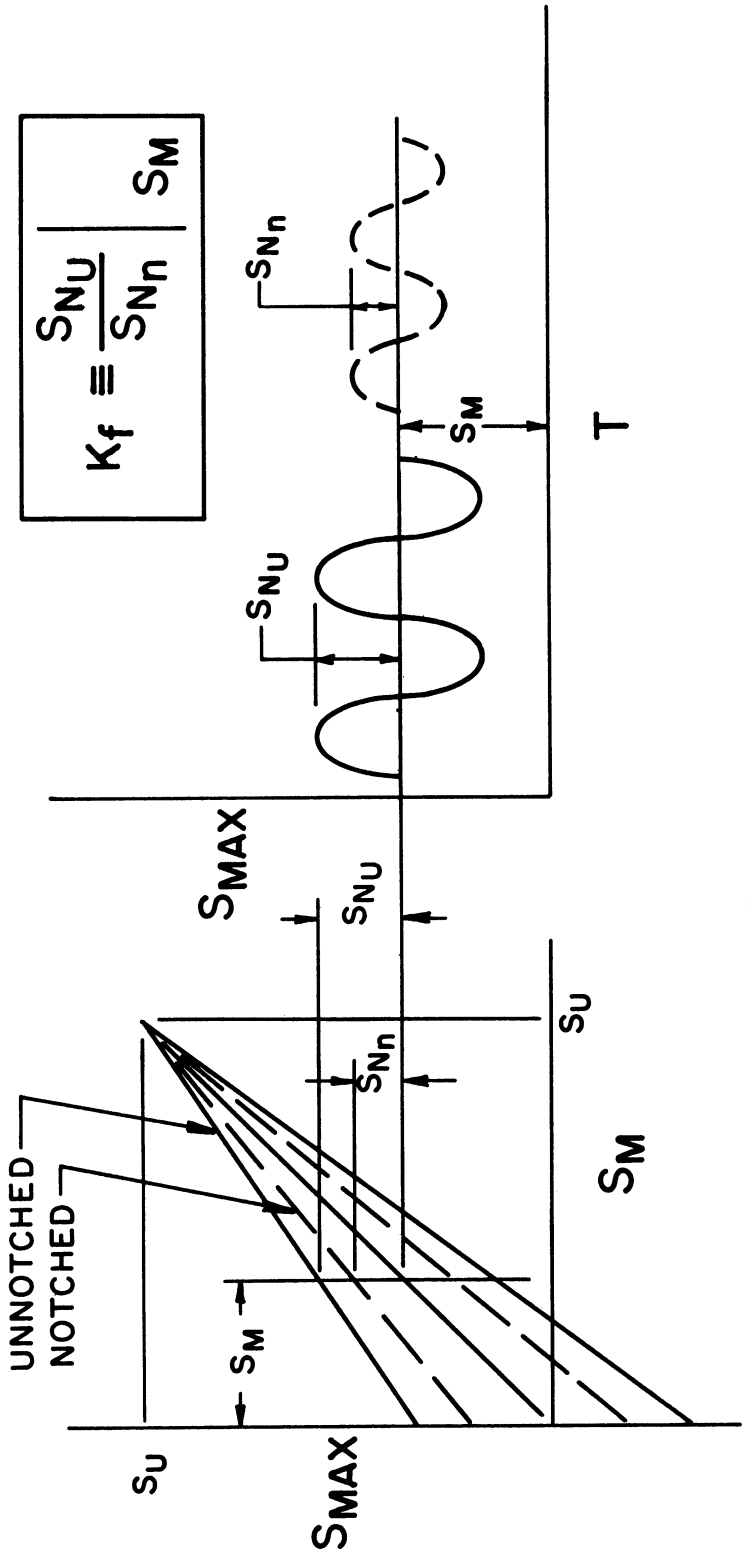

Figure 2.2 Definition of K_f according to the internal yielding approach. This definition is valid for finite life when the notched and unnotched specimens are compared at the same fatigue life.

that the local increase in stress at the notch affects only the nominal alternating stress and has no effect on the nominal mean stress. This approach has given the best available estimate of the early mean stress data for notched specimens and has been rationalized by stating that the local increase in mean stress is mitigated by localized yielding at minute imperfections in the material, hence the terminology, internal yielding approach.

According to the modified elastic approach, the fatigue strength reduction factor is defined as the ratio of the maximum nominal stress, S_{max}, for a polished unnotched specimen to that for a notched specimen, S_{max} being taken at a given life, N, from the S-N curves for notched and unnotched specimens which pertain to the same value of the stress ratio, R. The stress ratio is defined as the algebraic ratio of the minimum cyclic stress to the maximum cyclic stress. The modified elastic approach is shown in Figure 2.3. In this definition, it follows that the local increase in stress at the notch affects both the nominal alternating stress and the nominal mean stress. Because the effective increase in local stress can be determined, according to this definition, by multiplying K_f times the nominal cyclic stress, the terminology modified elastic approach has been used to describe this approach. (If K_t, rather than K_f, could be used, this approach would be an elastic approach.)

Strictly speaking, both of these approaches are valid only for limited ranges of mean stress because neither can be justified by existing fatigue data which pertain to very large maximum cyclic stresses of a magnitude approaching the tensile strength of the material.

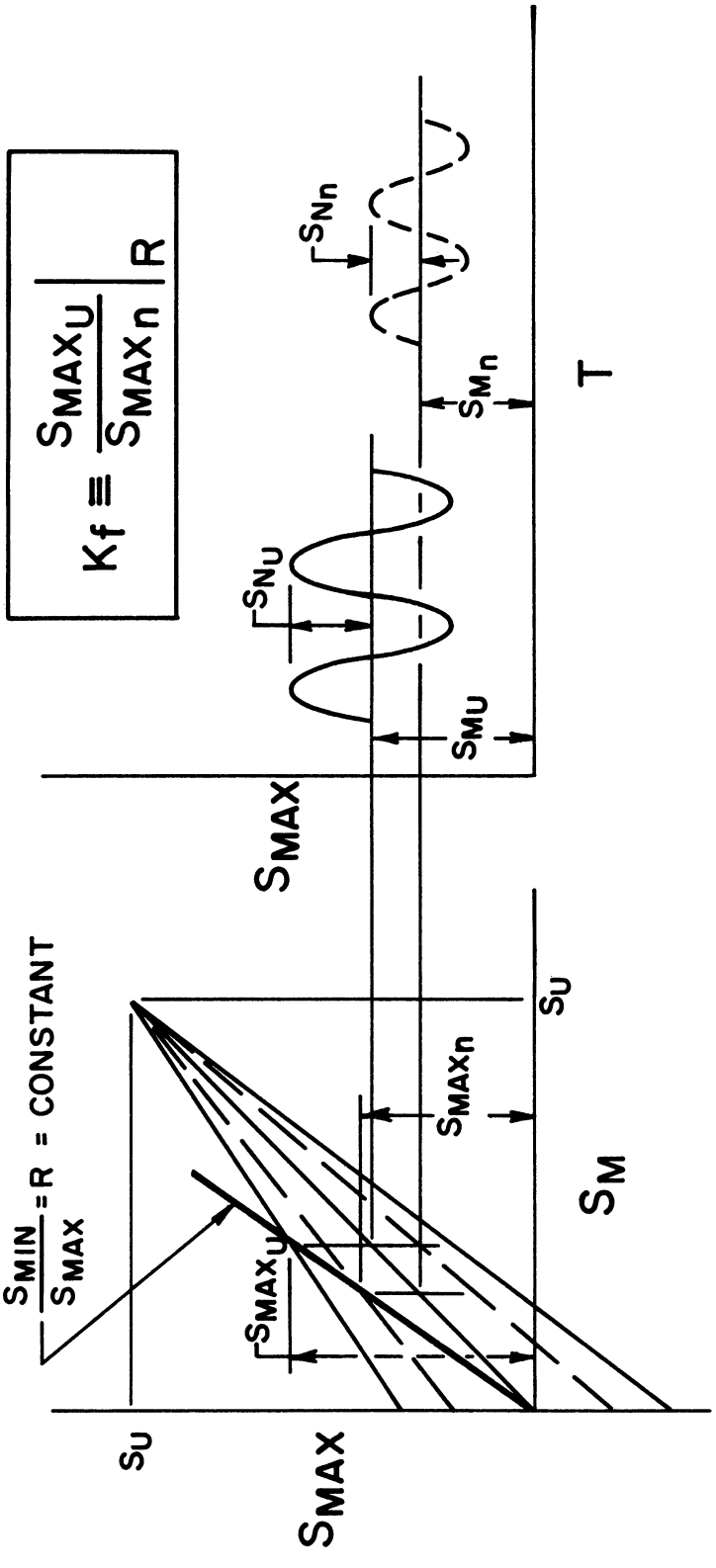

Figure 2.3 Definition of K_f according to the modified elastic approach. This definition is valid for finite life when the notched and unnotched specimens are compared at the same fatigue life.

In other words, there is no correlation between the effect of a notch on the fatigue strength and the effect on the tensile strength.

Both fatigue strength reduction factors defined by these two approaches are also valid for the ratio of the fatigue limits, although the conventional terminology is somewhat inconsistent and the term fatigue limit reduction factor is more precise.

The elastic approach and the internal yielding approach give equal values for the fatigue strength reduction factor in two special cases: when the mean stress is zero, and when the fatigue strength is independent of the mean stress. (In the latter case, limitations imposed by static strength of the material bound the domain of mean stress in which these approaches can be compared.)

Deformation Limitations for Unnotched Specimens

No specific deformation limitations have been imposed on the maximum cyclic stress in the discussion, so far, in order to simplify the working stress diagrams of Figures 2.2 and 2.3. However, because cyclic stresses which exceed the static tensile yield strength may induce very large permanent deformations, some deformation criterion must be established. This criterion can be taken as limiting the maximum allowable cyclic stress to be less than the static tensile yield strength. This criterion, which in essence approximates the cyclic yield strength by the static yield strength, applies to unnotched specimens. It will be discussed in more detail in Chapter III.

This deformation limitation on the maximum cyclic stress is represented by the line S_y-P in Figure 2.4. In this working stress

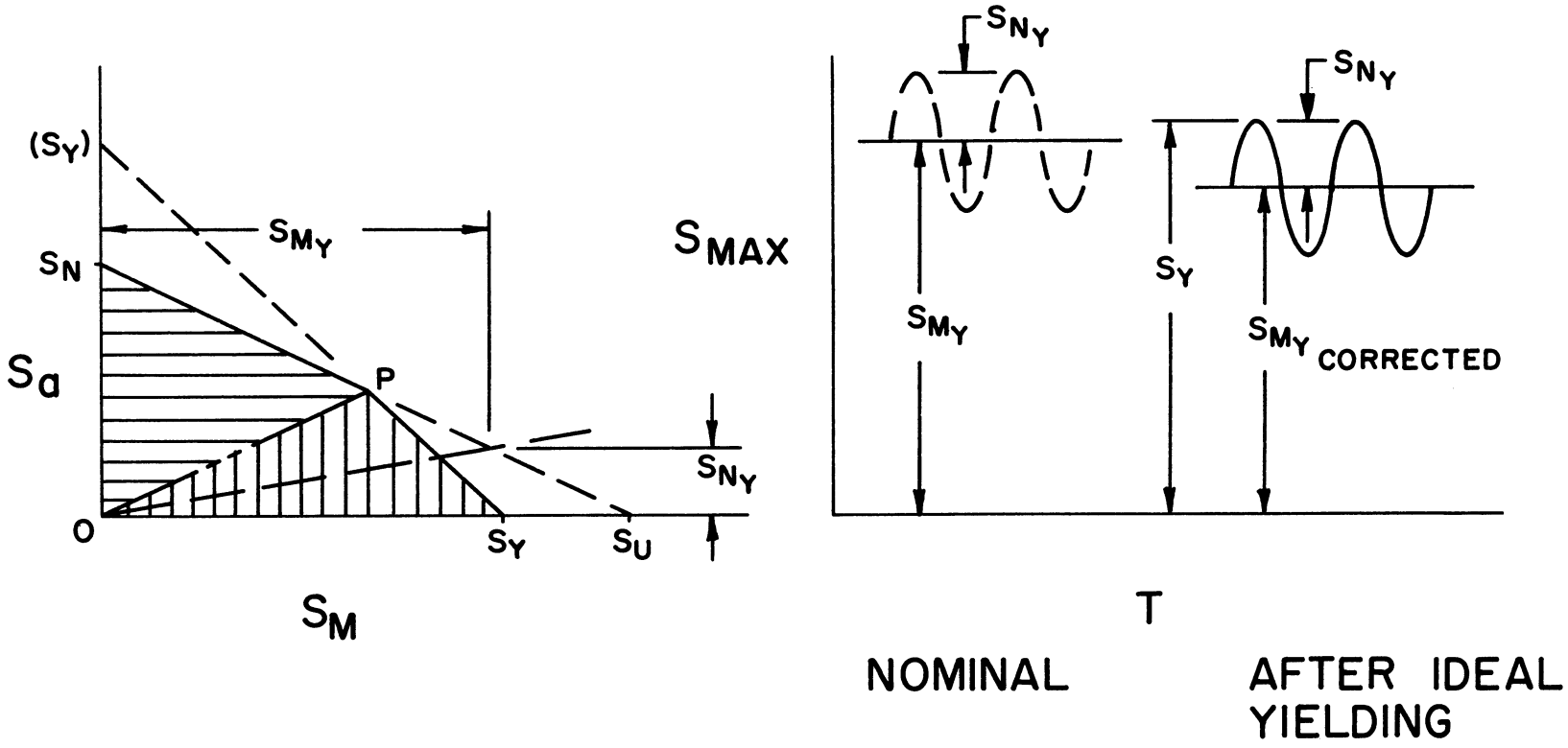

Figure 2.4 Working stress diagram which distinguishes between fatigue- and deformation-limited ranges of stress. Fatigue failure occurs without prior permanent deformation along line S_n-P; however, permanent deformation precedes fatigue failure along line P-S_y.

diagram, fatigue failure occurs along line S_n-P without prior plastic deformation. However, along line S_y-P, plastic deformation precedes fatigue failure. Hence, the domain bounded by 0-S_n-P-0 is termed the fatigue-limited range of stress; the domain bounded by 0-P-S_y-0 is termed the deformation-limited range of stress. Nominal stress calculations are questionable in the domain of stress beyond line S_y-P because yielding takes place there, and hence Hooke's law does not apply.

Cyclic Stress Domains for Notched Specimens

When the working stress diagram of Figure 2.4 is analyzed using the modified elastic approach, the locus of notched fatigue failure, line S_n/K_f-Q, can be predicted as shown in Figure 2.5. However, it can be seen that the stress at the root of the notch exceeds the static yield strength along line U-Q. Therefore, in the ideal case, yielding takes place for cyclic stressing corresponding to line U-Q. Consequently, the domain 0-S_n/K_f-U-0 is termed the fatigue-limited range of stress for notched specimens. It can be seen that if the notch sensitivity index, q, is unity, in other words, if $K_t = K_f$, then points U, T, and Q are coincident; if the notch sensitivity index is zero, that is, if $K_t \neq K_f = 1$, then points U, S_n/K_f, and S_n are coincident. For intermediate values of q, ideal localized yielding first occurs at point U on line (S_y/K_T) - S_y/K_t. As shown in Figure 2.5, ideal localized yielding can take place under fully reversed stressing. Point U is the critical point which (along with point 0) establishes the boundary of the domain of stress for

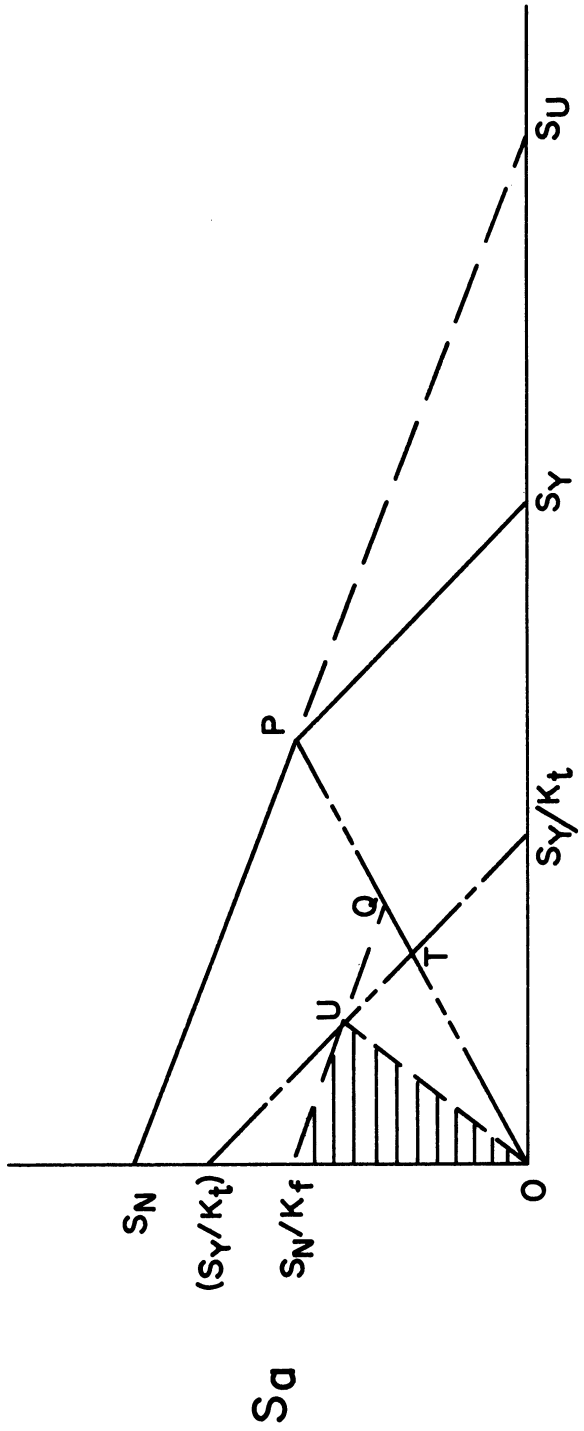

Figure 2.5 Working stress diagram for notched specimens developed using modified elastic approach. Nominal stress calculations are valid for domain O-S_n/K_f-U-O. See Figure 2.4.

which the nominal stress-versus-time diagram of Figure 2.4 is valid and is termed the ideal local yield point.

If this diagram were developed by using the internal yielding approach, the slope of line S_n/K_f-U-Q would be slightly smaller, and point Q would lie directly below point P. These changes do not affect the fatigue-limited range of stress significantly and therefore are not shown.

Regardless of the approach used to develop the working stress diagram for notched specimens, the stress domain to the right of line O-U cannot be termed the deformation-limited range of stress because these deformations are localized and need not be so large as to be considered as representing a mode of failure. This study places particular emphasis on developing the fatigue failure locus in the stress domain to the right of line O-U, that is, in the domain where localized yielding takes place. First, however, it is necessary to establish the lines S_n-P and S_n/K_f-U in order to investigate this domain of stress. These lines are established in the next chapter by compiling existing mean stress data for mild steel. After these lines have been established, the results of the experimental portion of this study will be presented in order to develop the domain of stress to the right of line O-U in Figure 2.5.

CHAPTER III

THE EFFECT OF MEAN STRESS ON FATIGUE

The first extensive series of fatigue tests were conducted by A. Wöhler[1] during the period when he was chief locomotive superintendent of the Royal Lower Silesian Railway. As evidenced by the materials that he tested, Wöhler's primary interest in fatigue was associated with the service failure of railroad car axles and springs. As these components are subjected to very large mean stresses in service, this interest in these failures apparently led to his pioneer fatigue tests on the effect of mean stress on fatigue.

Wöhler's tests, which were conducted over a period of twelve years, established several of the basic concepts of fatigue, in addition to ascertaining that increasing the tensile mean stress decreases the fatigue limit of unnotched steel specimens. Although he also established that sharp notches cause a marked decrease in the fully reversed fatigue limit, Wöhler did not conduct sufficient tests on notched specimens to determine the effect of mean stress as he had done for unnotched specimens.

Since Wöhler's time, many working stress diagrams have been proposed to deal with the effect of mean stress on the fatigue limits of unnotched specimens.

Various Working Stress Diagrams

Figure 3.1 shows a representative sample of working stress diagrams which have been proposed to deal with fatigue in mild steel

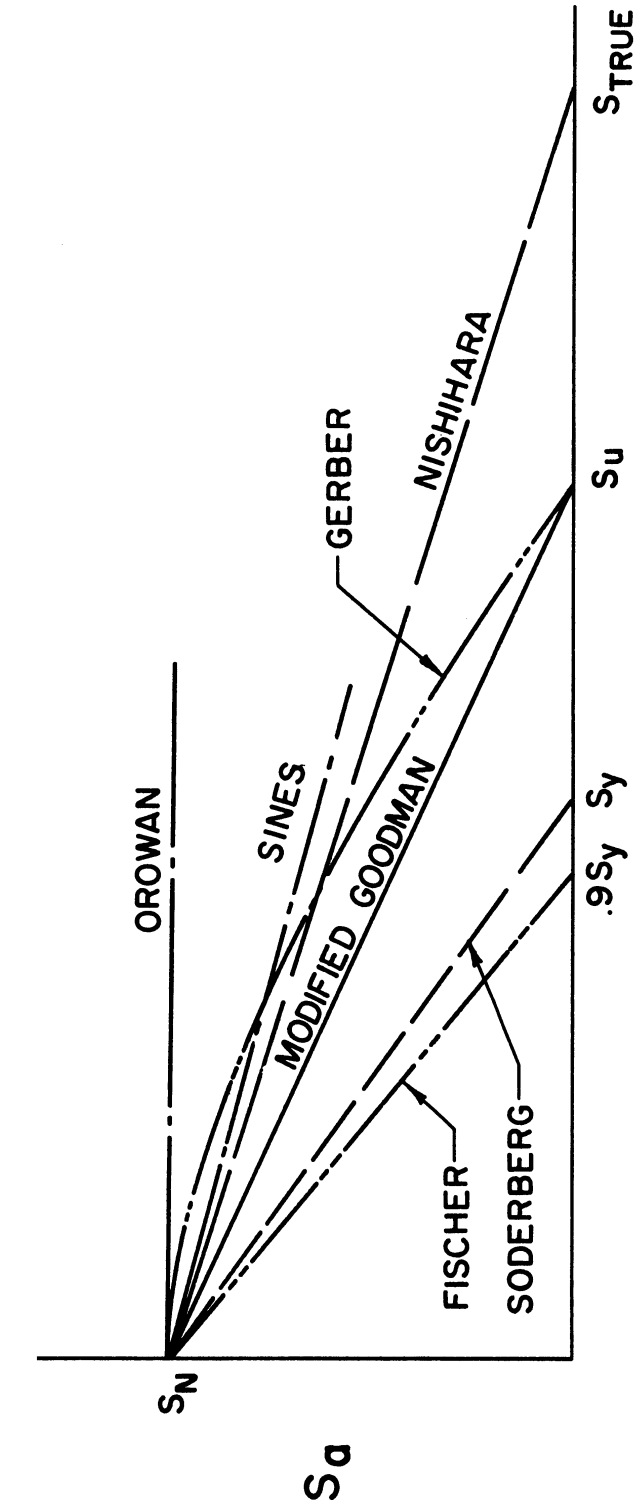

Figure 3.1 Various working stress diagrams for mild steel under axial loading. See text for discussion.

under axial loading. The Fischer,[6] Soderberg,[4] and the modified Goodman[7] diagrams are basically intended for design purposes and are somewhat conservative. The Nishihara,[8] Gerber,[9] and Sines[10] diagrams are based on the trends of a limited amount of fatigue data. The Orowan[11] diagram is based on his well-known theory of fatigue failure.

In addition to these diagrams, Smith,[12] Pomp and Hempel,[13] Peterson,[14] Gunn,[15] Heywood,[16] Stulen and Cummings,[17] Kitagawa and Morohashi,[18] Yokobori,[19] and Nakinishi[20] have developed working stress diagrams for various materials under various modes of loading.

As can be seen in Figure 3.1, these diagrams predict substantially different effects of mean stress on fatigue. The fact that there are so many diagrams indicates clearly that the effect of mean stress has not been resolved to the satisfaction of these investigators.

Grover[21] recently pointed out that a good part of the difficulty encountered in treating notched specimens stems from the lack of knowledge as to the effect of mean stress on unnotched specimens. In other words, a good part of the difficulty arises from not knowing which diagram of Figure 3.1 to use as a basis to analyze the behavior of notched specimens. Thus, the problem faced in dealing with notched specimens is that it is first necessary to be able to predict the effect of mean stress on unnotched specimens; yet, this effect for unnotched specimens had not been resolved. Therefore, the first part of this study must deal with unnotched specimens before these results can be extended to notched specimens.

The working stress diagram for unnotched specimens which is used in this study is developed in the next section by compiling existing mean stress data.

Compilation of Mean Stress Data

It became apparent while compiling the axial mean stress data that these data display a very large scatter when plotted in the form of a working stress diagram and that no precise diagram can be established with confidence if all data are weighed equally. However, by limiting the compilation to only data for which no plastic deformation took place prior to fatigue failure, the scatter is reduced markedly. While it is not evident in all test results, there are considerable data which show that plastic deformation prior to fatigue failure changes the effect of mean stress on fatigue. A few of these tests are discussed below in order to establish the method used in compiling existing data.

O'Connor and Morrison[22] have shown that reductions in area of approximately seventy per cent can take place under axial fatigue loading even though the maximum cyclic stress does not exceed the static yield strength. In their tests on an alloy steel, the fatigue limits associated with plastic deformation were substantially lower than the fatigue limits associated with only "elastic" deformations. Pomp and Hempel[23] found similar results for a spring steel; but, on the other hand, they found an increase associated with plastic deformation for two mild steels. However, Gough and Wood[24] found a marked decrease in the fatigue limit associated with plastic deformation in tests on a mild steel. In general, plastic deformation decreases the fatigue limit;

but, this decrease can in some cases be more than offset by the strengthening effect of strain hardening.

As far back as 1929, Thorne[25] reported that the trend of mean stress data appeared to change when the maximum cyclic stress equals or exceeds the static yield strength. Smith's[12] well-known plot of torsional mean stress data shows this change in trend as well as a large increase in scatter when the maximum cyclic stress exceeds .9 S_{ys}.

Inclusion of fatigue data associated with plastic deformation in a mean stress compilation introduces two opposing effects, plastic strain versus strain hardening, which tend to confuse the issue and which increase the scatter in a plot of these data. Furthermore, unnotched specimens and notched specimens cannot be related theoretically unless both specimens are subject to similar plastic deformation. Because plastic deformation in notched specimens takes place in a very small volume at the root of the notch, while plastic deformation in unnotched specimens generally takes place in a much larger volume, particularly in the case of axial loading; the situation in which notched and unnotched specimens undergo similar plastic deformation is extremely rare.

Several investigators have questioned whether axial fatigue data associated with plastic deformation has any practical value in the case of unnotched specimens: Cazaud,[26] Herold,[27] and Owen[28] have recommended limiting the maximum cyclic stress to practical values in dealing with working stress diagrams. German industrial standards follow this recommendation.[29]

The tests and recommendation mentioned above led to the method adopted in this study of limiting the compiled data to that for which it can be established that no permanent deformation took place prior to fatigue failure. Tests by Smith,[30] Brown,[31] Gough and Wood,[24] Pomp and Hempel,[23] O'Connor and Morrison,[22] Tapsell,[32] Ono,[33] and Haigh and Robertson[34] show that the cyclic yield strength for relatively mild steel is approximately equal to the static lower yield strength. However, tests by Bairstow,[35] Lidstrom and Lazan,[36] Blatherwick and Olsen,[37] Karamoto and Nishioka[38] and Forrest[39] show that very small permanent deformations can occur at an even lower cyclic stress. Therefore, a value of $.9\ S_y$ was arbitrarily taken in this compilation to be the maximum permissible cyclic stress (unless specific attention had been given to plastic deformation during the test).

Table 3.1 gives this compilation for axial fatigue tests on relatively mild steels. These data are plotted in Figure 3.2.

In addition to the tests listed in Table 3.1, several other tests[50-60] were reviewed but were not compiled because of insufficient data or because the cyclic stressing exceeded $.9\ S_y$. In general, these data support the working stress diagram developed in Figure 3.2. Only two tests[46,61] which apparently are not associated with plastic deformation give results which fall substantially below the working stress line drawn in Figure 3.2. These two tests did not have the study of mean stress as their primary objective; hence, some of these data are meager and have not been plotted in Figure 3.2.

TABLE 3.1

Compliation of pertinent mean stress data. Axial fatigue tests on unnotched steel specimens with ultimate tensile strengths under approximately 175 ksi: data compiled for cyclic stressing such that S_{max} is less than approximately .9 S_y.

Investigator, Year and Reference No.	Material (Type of steel or per cent carbon.)	S_u	S_y	S_n	S_m/S_u	S_a/S_n
		--- in ksi ---			-- ratio --	
J. H. Smith, 1910, 30.	Ni	71.7	68.6	43.5	.272	.902
B. P. Haigh, 1915, 40.	.13 C	56.5	47.1	29.1	.196	.943
R. M. Brown, 1928, 31.	.29 C:					
	11 per cent cold drawn	86.0	72.1	34.9	.156 .313	.994 .948
	23 per cent cold drawn	97.6	85.2	40.3	.138 .275 .413	.982 .898 .839
	35 1/2 per cent cold drawn	103.7	84.0	42.6	.130 .259	.982 .945
H. F. Moore, 1933, 41.	"Rail steel"	130 est	78 est	45.5	.162	.924
A. Pomp and M. Hempel, 1936, 23.	.17 C	79.8	54.7	43.6	.112	.956
	.44 C	126.2	79.3	56.3	.073 .130	.952 .937
	NiCr	128.0	110.4	67.3	.198 .383	.918 .865
	.11 C	52.6	33.2	20.1	.190	.902
	.47 C	137.5	95.0	31.4	.351	.818

TABLE 3.1 (Cont'd)

Investigator, Year and Reference No.	Material (Type of steel or per cent carbon.)	S_u	S_y	S_n	S_m/S_u	S_a/S_n
		---	in ksi	---	-- ratio --	
A. Pomp and M. Hempel, 1936, 13.	.47C: 10 per cent cold drawn	121.8	118.0	35.6	.328 .605	.942 .875
H. J. Gough and W. A. Wood, 1939,24.	.12 C	59.4	37.0	27.6	.106	.959
T. Nishihara and T. Sakurai, 1939, 8.	.41 C	101.2	55.5	36.2	.123	.933
M. Hempel and J. Luce, 1941, 42.	.64 C	113.8	58.7	41.3	.125	.932
	CrMo	114.5	95.5	57.0	.211	.850
	CrMo	136.0	121.5	69.8	.314	.877
	NiCrMo	149.5	127.5	78.3	.333	.854
H. J. Grover, S. M. Bishop and L. R. Jackson, 1951, 43.	CrMo	117.0	98.5	46.3	.048 .104 .216 .366	1.087 1.048 1.034 .888
B. Taylor, 1952, 44.	.16 C	67.2	45 est	35.5	.083	.974
W. J. Trapp and R. T. Schwartz, 1953, 45.	NiCrMo	158.5	146.9	70.0	.362	.822
T. T. Oberg and E. J. Ward, 1953, 46.	NiCrMo	146.5	126.0	67.0	.362	.791

TABLE 3.1 (Cont'd)

Investigator, Year and Reference No.	Material (Type of steel or per cent carbon.)	S_u	S_y	S_n	S_m/S_u	S_a/S_n
		---	in ksi	---	-- ratio --	
W. N. Findley, 1954, 47.	NiCrMo	120 est	100 est	57.0	.333	.954
J. W. Fitchie, 1955, 48.	NiCr	118.8	98.5 est	53.8	.094 .113 .113	1.000 1.000 1.000
H. C. O'Connor and J. L. M. Morrison, 1956, 22.	NiCrMo	125.2	119.0	70.1	.179 .358	.913 .869
J. Morrow and G. M. Sinclair, 1958, 49.	NiCrMo	141.0	129.0	57.0	.426	.790

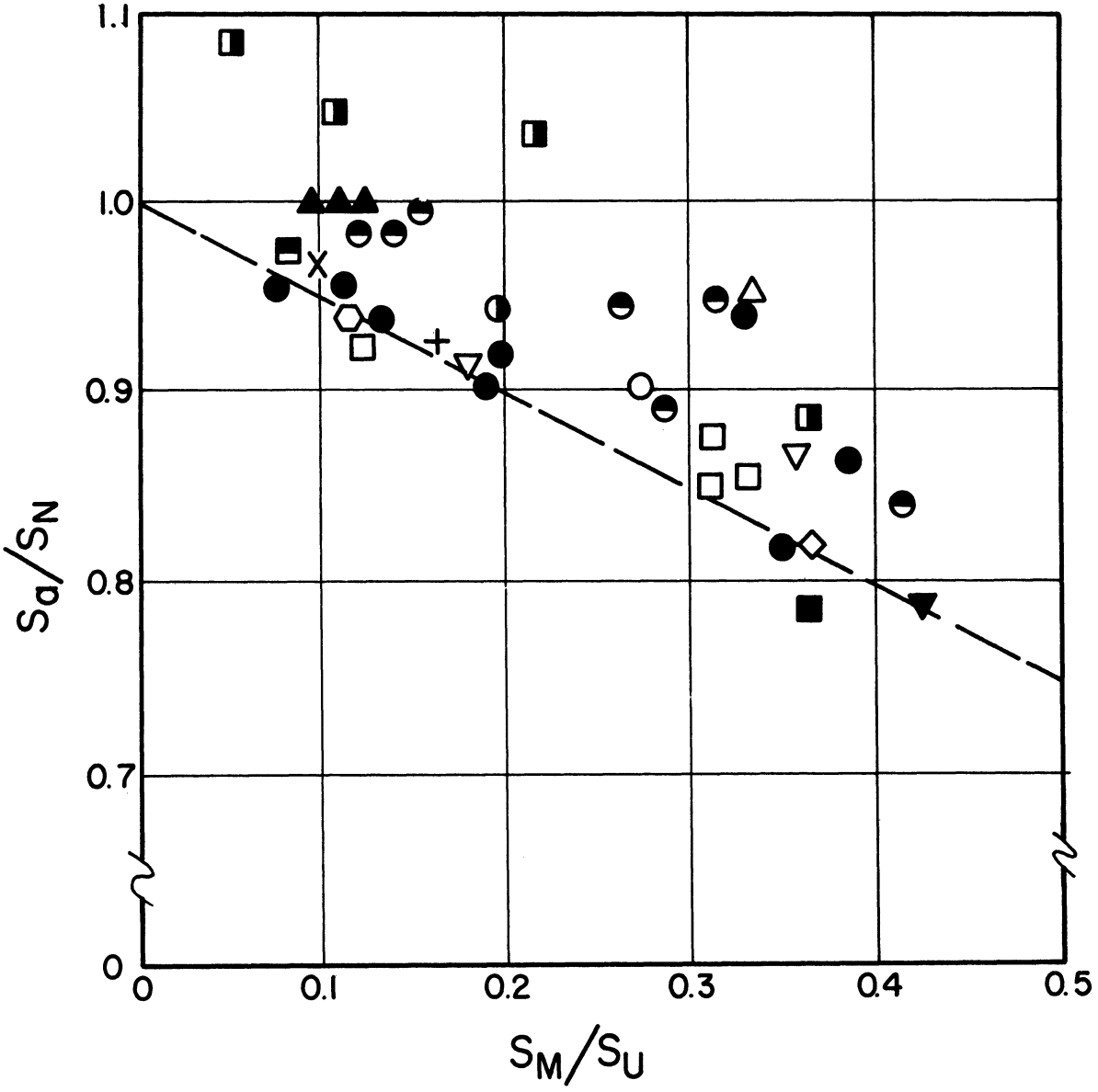

Figure 3.2 Effect of mean stress on fatigue. Plot of the compilation listed in Table 3.1.

The data by Grover, Bishop, and Jackson[43] are the only data in over thirty mean stress tests examined which show that a tensile mean stress increased the fatigue limit. These data pertain to sheet specimens which were restrained from buckling by the use of guides. Therefore, there is a distinct possibility that these guides influenced the test result for fully reversed stressing in an adverse manner. One way or the other, the tensile mean stress data display a trend consistent with the other data.

Further support for the "elastic" working stress diagram of Figure 3.2 is given by mean stress tests[13,62-64] which do not include data on the fully reversed fatigue limits (these values can be estimated and then the given mean stress data can be compared to the elastic diagram).

Working stress diagrams similar to that of Figure 3.2 have been developed in this study for bending and torsional fatigue.[65] These diagrams are discussed briefly in Chapter VI.

Prediction of Notched Data

The elastic working stress diagram (for axial loading) of Figure 3.2 relates the allowable alternating stress, S_a, to the mean stress, S_m, by

$$S_a/S_n = 1 - .5\, S_m/S_u \qquad (3.1)$$

where

S_n = the fully reversed fatigue limit

S_u = the ultimate tensile strength.

This diagram can be modified to treat notched specimens by using the two approaches discussed in Chapter II, K_f for Nonzero Mean Stress Situations. Figure 3.3 shows that the internal yielding approach and the modified elastic approach give similar results. (In the case of bending and torsional fatigue, these results are almost identical.) The reason for the close agreement is that these results can only be compared within a limited stress domain and the effect of mean stress on fatigue is relatively small within this domain.

To extend these approaches to the stress domain to the right of line O-U'-U in Figure 3.3 involves extrapolation which cannot be supported by simple elastic theory. In other words, the notched specimens under stressing in the stress domain to the right of line O-U'-U cannot be directly related in terms of elastic stress to the unnotched specimens under stressing in the fatigue-limited range of stress for cyclic stressing which leads to localized yielding. To deal with this situation, either an empirical approach must be used or the simple elastic theory must be modified to account for the influence of localized yielding. While empirical approaches are justified in many cases, it will be shown in this study that elastic theory, modified local yielding and other practical considerations, can be used to analyze the behavior of notched specimens.

Therefore, the empirical internal yielding approach to treating notched specimens is rejected in this study and the modified elastic approach is accepted. Because more experimental support for accepting the modified elastic approach will be presented in

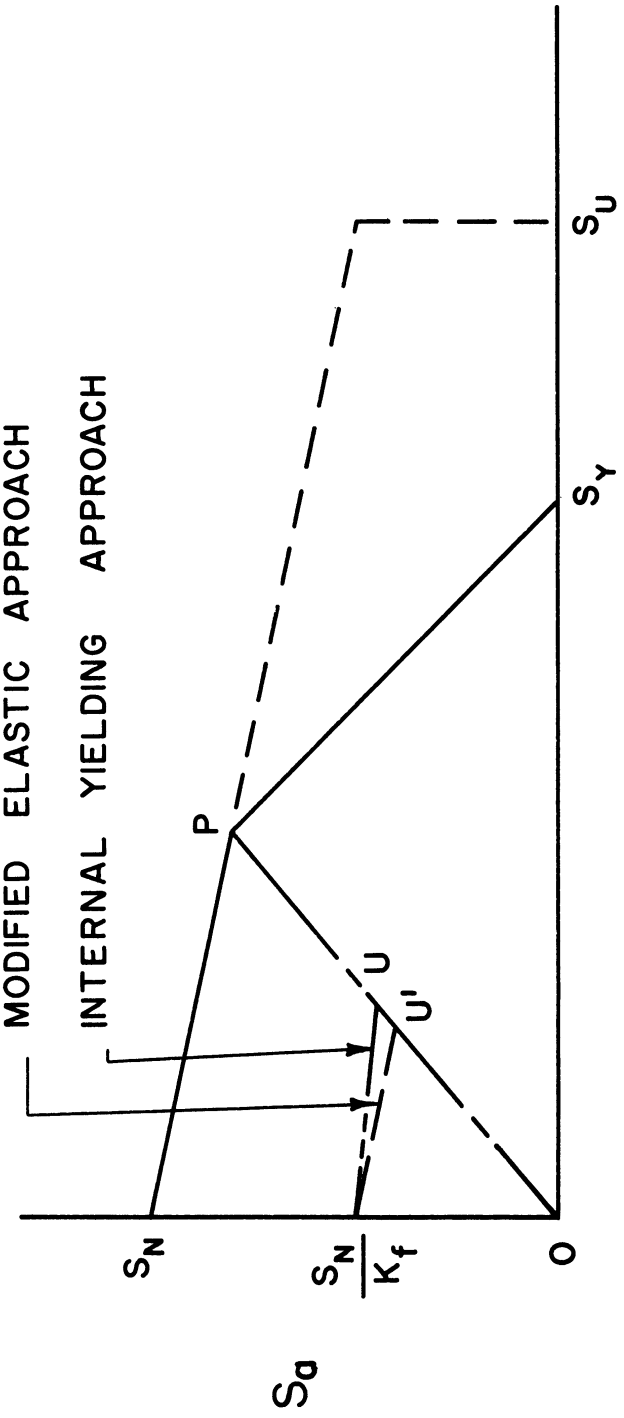

Figure 3.3 Modification of elastic working stress diagram to treat notched specimens. Both the internal yielding and the modified elastic approaches give approximately the same predicted locus for fatigue failure of notched specimens.

Chapter VI, at this time only the data by Pomp and Hempel[13] is given in Figure 3.4 to support this approach.

Notched data of a slightly different type will be presented here in order to establish clearly that neither the internal yielding approach nor the modified elastic approach can be used to analyze data which pertain to very high mean stress levels. Tests by Pomp and Hempel[13] on mild steel bolts show no effect of mean stress at high mean stress levels. In addition, tests on galvanized steel wire under axial stressing with high mean stress components by Shelton and Swanger[66] also show little or no effect of mean stress. See Tables 3.2 and 3.3. While the stress raisers in these tests are not precisely defined and while no fully reversed fatigue limits are given, these results are adequate to establish the effect of mean stress at very high mean stress levels. Neither the modified elastic nor the internal yielding approach gives predicted results (by extrapolation) which correlate to these data. Therefore, this study deals with experimentally determining the fatigue behavior in this range of stress in a situation which is amenable to stress analysis and subsequently with the analysis of these data.

Area of Experimental Study

The stress domain investigated in this study is the domain of cyclic stress in Figure 3.3 which is bounded by lines O-U'-U-P-S_y-O. As previously mentioned, it will be seen in Chapter VI that elastic theory, modified by practical considerations, can be used to analyze the behavior of notched specimens in this stress domain. Before proceeding to the experimental work, some related literature will be

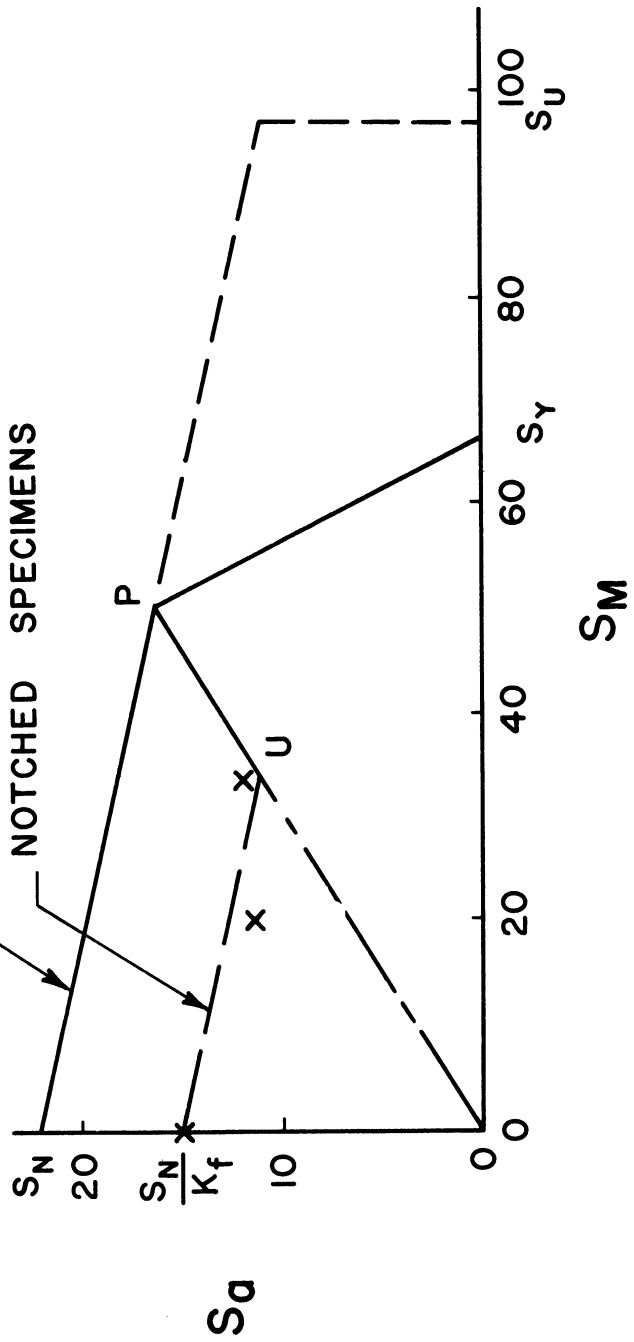

Figure 3.4 Comparison of data and locus predicted by the modified elastic approach. Reference 23. (Strengths in kg/mm^2.)

TABLE 3.2

Mean stress data for mild steel bolts. Axial fatigue tests on 1" and on 1 1/8" bolts (with mild steel nuts .8 X D) without initial tightening tension. Reference 13.

Type of Steel	S_u	S_y	S_m	S_a	Remarks
	---------- in ksi ---------				
.07 C	60.9	41.6	9.6	5.6	1" bolts.
			27.8	5.0	
.03 C	64.1	44.6	7.7	4.3	1 1/8" bolts.
			26.5	3.6	
.30 C	101.2	78.4	9.3	5.1	1" bolts.
			61.9	5.1	
.33 C	119.8	97.6	8.7	4.3	1 1/8" bolts.
			49.5	5.3	
			64.0	5.1	

TABLE 3.3

Mean stress data for galvanized wire. Axial fatigue tests on heat-treated and on cold-drawn galvanized (solid) steel wire with tensile strengths of approximately 225 ksi. Reference 66.

Type of Wire	S_m	S_a	Remarks
	--- in ksi ---		
Heat-treated	49	26 1/2	Rotating beam fatigue tests give fatigue limit of 110 ksi for specimens machined from this wire.
	68	24 1/2	
	88	23	
	107	23 1/2	
	133	25	
	153	24	
Cold-drawn	50	30	Rotating beam fatigue limit for specimens machined from this wire equals 118 ksi.
	73	24	
	90	24	
	110	25	
	135	21 1/2	
	156	22	

reviewed in order to develop more fully the nature of the practical considerations involved in this problem and to support the discussion of the experimental results.

Related Literature--The Behavior of Steel Under Cyclic Loading

It has been shown that large plastic deformations can take under cyclic stressing approximately equal to the static yield strength. However, large plastic deformation represents only one aspect of the behavior of steel under cyclic stressing: the general cyclic behavior of steel under other ranges of mean stress is reviewed below.

While it is known that various forms of sub-microscopic inelastic and anelastic mechanisms are present at virtually all levels of stressing,[67] for all practical purposes these mechanisms can be ignored in the case of static loading below the proportional limit. However, these mechanisms must be considered in the case of cyclic loading because minute inelastic behavior "accumulates" during cyclic stressing.[68] Hence, inelastic action that may be neglected in any one cycle can become quite important over a number of cycles.

A steel that displays a linear stress-strain relationship during the first cycle can develop a pronounced hysteresis loop after several cycles even though the maximum cyclic stress is below the static yield strength.[69] Therefore, the criterion for linear elastic behavior is more restricted for the case of cyclic stressing than for static stressing. The upper limit of cyclic stress for linear behavior, which corresponds to the proportional limit for static stress, is called the cyclic stress sensitivity limit.[37] (The term "cyclic

stress sensitivity limit" is more precisely used to specify the fully reversed stress below which internal damping, by static and/or dynamic hysteresis, is not affected by the number of imposed stress cycles.)[67]

Because the stress-strain relationship is non-linear for cyclic loading above the cyclic stress sensitivity limit, curves have been developed to depict the relationships involved.

The cyclic stress-strain locus curves are developed by obtaining a series of stress-strain hysteresis loops for different ranges of stress (or strain) on different specimens. The individual loops which pertain to the same number of cycles are superimposed on a common origin and curves are drawn through the maximum points of these loops, one curve for each specified number of cycles. These curves are called the cyclic stress-strain locus curves. Figure 3.5 shows these curves for a 1018 steel under fully reversed axial strain.[37]

A shorter approach utilizes just one specimen which is subjected to a range of stress that is gradually increased while the maximum cyclic strains are measured. Figure 3.6 shows a plot of the amplitude of cyclic stress versus the amplitude of cyclic strain for a 1017 steel obtained under fully reversed axial stress.[39] This plot is called the dynamic stress-strain curve.

Since these approaches are relatively recent, curves for various materials and various values of mean stress are not yet available. However, this information can often be deduced from the early literature in which the hysteresis loops were given for an extensive number of stress cycles.[30]

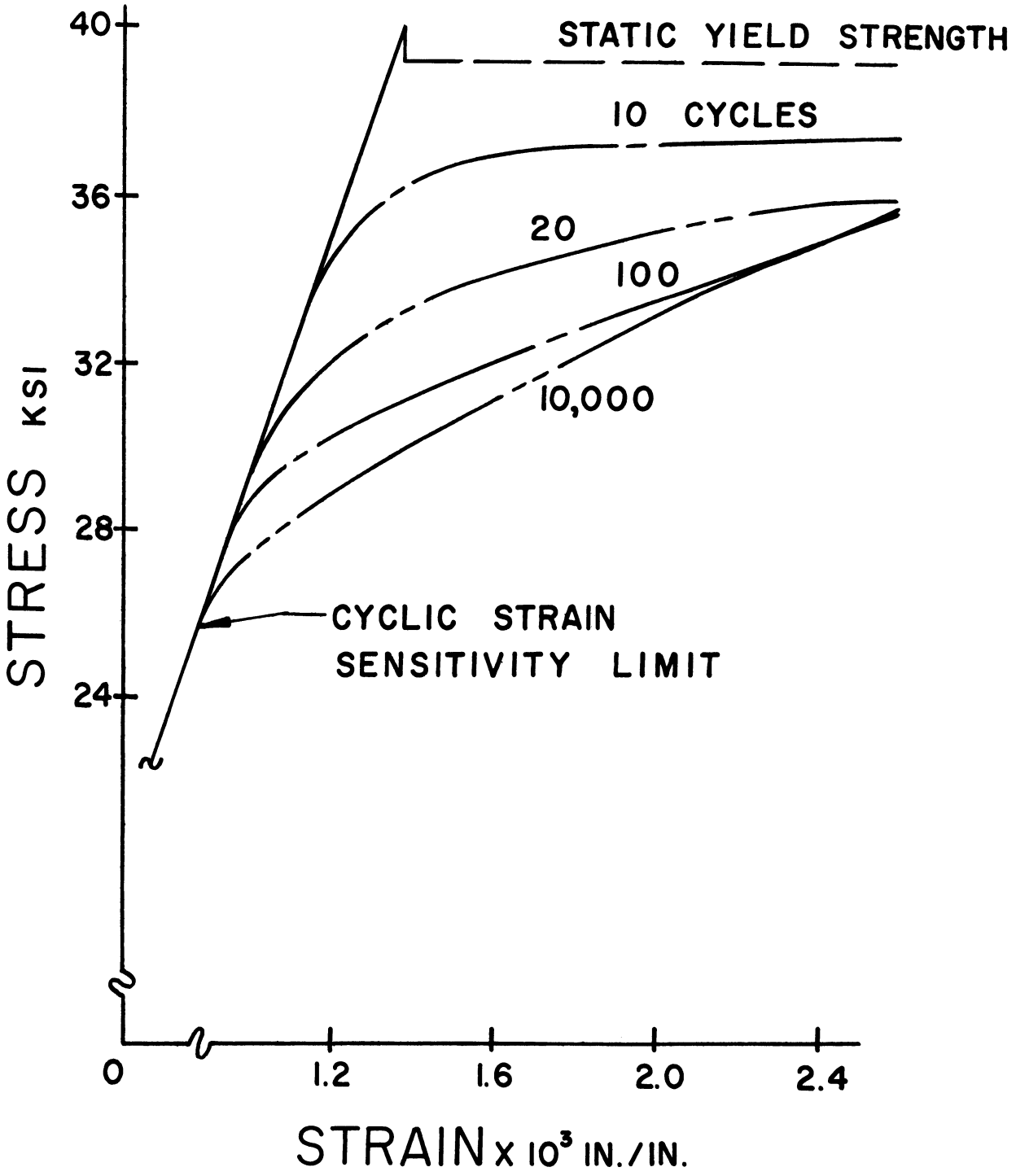

Figure 3.5 Cyclic stress-strain locus curves. Reference 37.

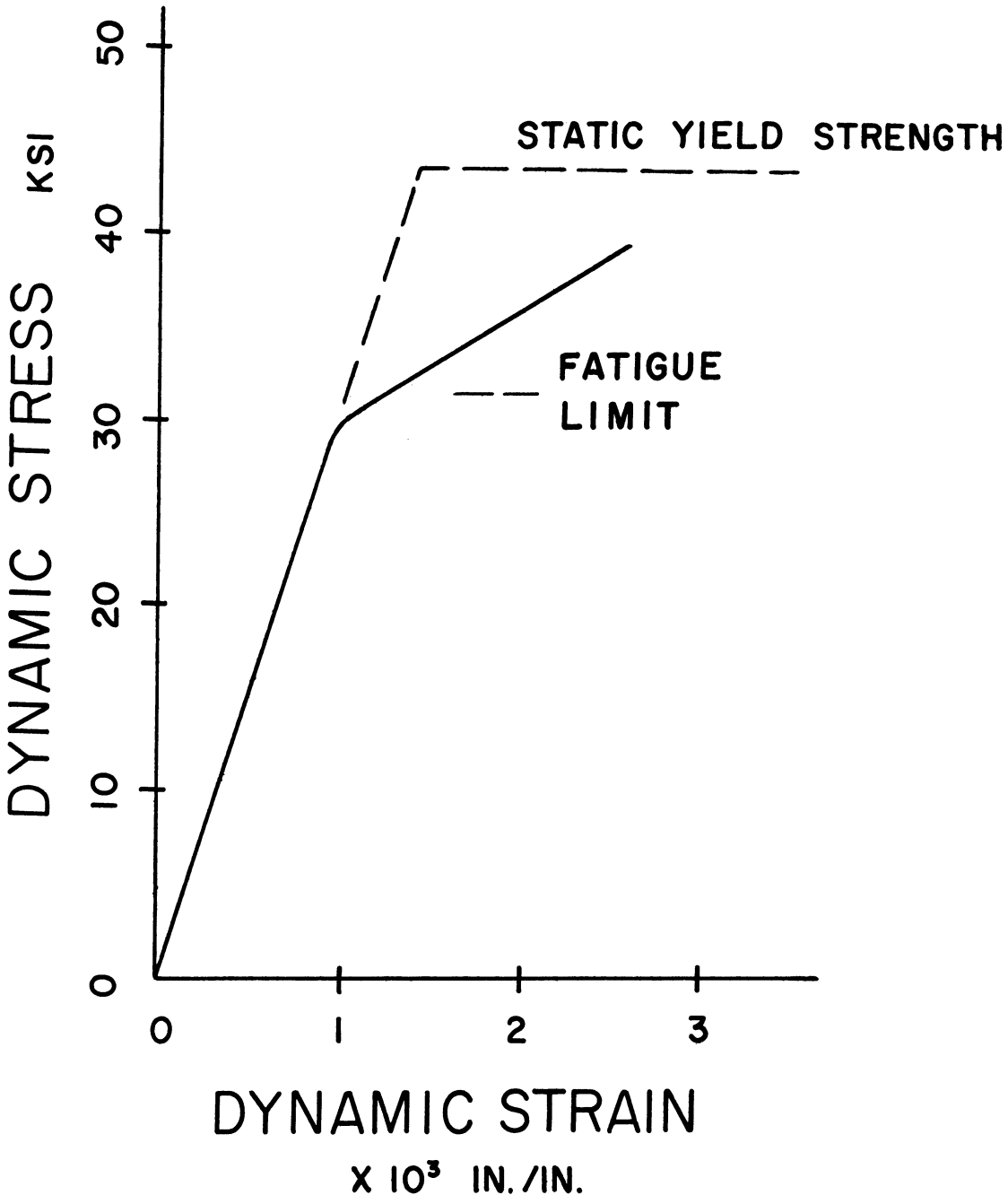

Figure 3.6 Dynamic stress-strain curve. Reference 39.

Few data exist which pertain directly to the cyclic behavior at the root of a notch.

Wever and Martin[70] studied the effect of cyclic stress on a flat sheet specimen with a central hole (K_t approximately equal 2.7). The specimen, of Ni-Cr steel with a yield strenght of 95,000 psi and an ultimate strength of 132,000 psi, was packed in steel chips after machining and heated to about 1200° F to remove residual stresses. Under a nominal static stress of 14,200 psi, the calculated stress at the edge of the hole is about 38,400 psi: this stress was determined to be 33,500 psi on the basis of X-ray strain data. This specimen was then subjected to an alternating stress of 7,100 psi which was superimposed on the static stress. After 15,000,000 cycles, the alternating stress was discontinued, and the stress (under the static load) was determined as before. However, the stress at the edge of the hole was then approximately 15,000 psi and was no longer the maximum observed stress. The maximum observed stress occurred away from the edge of the hole and was approximately the same magnitude as it had been before cyclic loading. When the static load was removed, compressive residual stresses were found at the edge of the hole. The over-all strain distribution resembled that which results from overstrain in tension.

Other investigations have determined by X-ray diffraction techniques that compressive residual stresses are introduced into the surface of the specimen by cyclic loading.[71-73] These tests are discussed by Vitovec.[74]

Blatherwick and Olson[37] observed a change in the strain distribution under fully reversed cyclic loading of a notched axial specimen. This was accomplished by mounting foil strain gages at the root of the notch and across the face of the specimen. They use the cyclic stress-strain locus curves of Figure 3.2 to adduce evidence of stress redistribution.

Bennett[75] studied the effect of rotating bending on SAE 4130 steel specimens that had been vacuum-annealed at 1650°F. He found that the surface strain (measured by X-ray) varies as a function of the number of cycles imposed. One particular specimen, after having undergone more than 50,000,000 cycles of stress at 35,000 psi, yielded under a static bending stress of only 30,000 psi.

Taira and Murakami[76] conducted reversed bending tests on two annealed steels. By means of etching techniques, they found that compressive residual stresses of 10,000 to 20,000 psi are introduced into the surface layers by the alternating bending even though, in some cases, the imposed stress is less than one-half the static yield strength.

Mason and Inglis[77] observed that the stress-strain behavior of rotating bending specimens changes under cyclic loading. By using mirrors and "projecting" the deflection on a screen, they ascertained that the specimens deflect at right angles with the applied moment as well as in the expected direction. They deduced that hysteresis causes the plane of the deflection to be different than the plane of the bending.

Gough and Tapsell[78] and Frith[79,80] conducted bending and torsional fatigue tests on both solid and hollow specimens. During these tests, as near as can be ascertained, all conditions were identical: same material from the same source, same machine, same outside diameter and surface finish, and so forth. Yet, for 37 tests, the hollow specimens were found to be weaker in 34 tests and the strengths were found to be the same in one test. This very skewed distribution correlates to the work by Mason and Inglis[77] who found that surface strains are larger for hollow specimens than for solid specimens when the calculated stresses are the same. They showed that the fatigue strength is related more closely to the observed strain than to the calculated stress. (Of 63 tests compiled[77-81] for both hollow and solid specimens for various test conditions, only 3 tests show the solid specimens to be weaker.)

In general, the same type of cyclic stress-strain behavior occurs at higher values of stress, except that the changes are more pronounced. The high cyclic strain fatigue tests by Coffin,[82] Low,[83] Johansson,[84] Coffin and Tavernelli,[85] and by Benham and Ford[86] show that strain plotted versus fatigue life, on log-log coordinates, gives a straight line relationship. The tests of Johansson are of particular interest because the load variation during testing is also given and the variation is of a different form for different steels.

Morrow and Sinclair[49] studied stress relaxation for hollow axial fatigue specimens subjected to various levels of mean stress. They observed little or no relaxation in less than a million cycles

for specimens that did not undergo gross yielding on the first cycle. However, for specimens that exhibited yielding on the first cycle, the stress continued to relax during cyclic loading. They conclude that the mean stress may also be completely removed during cyclic loading of soft steel.

Recently, a few analyses of fatigue data make an attempt to account for the influence of plastic strain on fatigue.[15,87,88]

The above review of cyclic dependent material properties shows that the stress-strain relationship changes under cyclic loading and that residual stresses are introduced into the surface by cyclic loading. Hence, fatigue is a process which involves a changing strength as well as a changing localized stress even though the applied loads are unchanged. Therefore, simple theory must be modified somewhat to treat the real rather than the ideal situation.

The view of the fatigue process which envisions a continually changing material behavior has received considerable experimental support recently in the field of electron transmission studies of thin films. These studies have shown that the internal structure of the material changes under cyclic loading and that various dislocation mechanisms interact and lead to the formation of a "sub-structure". Despres[89] has shown that the change in internal structure is related to both the alternating stress level and the number of imposed stress cycles.

In the over-all, the basic effect of tensile mean stress on fatigue is to raise the maximum cyclic stress and thus to alter the

internal structure of the material by promoting minute inelastic and anelastic behavior which can culminate in fatigue failure. Unfortunately, this statement cannot be made more specific because the mechanism of fatigue is not understood at present, not is it even known that a single mechanism exists.

Mechanism of Fatigue

Although the mechanism of fatigue cannot presently be related directly to the effect of mean stress on fatigue, no literature review on fatigue can be complete withour giving attention to this topic. Therefore, the following representative review is in order.

The first fundamental study of the mechanism of fatigue failure was conducted by Ewing and Humfrey[90] in 1902. They found that slip occurred during the cyclic stressing of steel above its fatigue limit and that these slip bands broadened under continued stressing. Finally, cracks formed in the slip bands and spread from grain to grain until fracture resulted. However, at stress levels below the fatigue limit, no appreciable slip occurred. This work led to the attrition theory of fatigue.

Other early theories of fatigue were proposed by Beilby,[91] Rosenhain,[92] Haigh,[93] Griffith,[94] Jenkin,[95] and Gough and Hanson.[96] The work by Gough and Hanson is still of basic interest today in that considerable attention was given to the mechanism of slip.

In 1939, Orowan[11] proposed a fatigue model in which cumulative strain hardening in localized areas led to fracture. However,

it has since been shown that repeated plastic strains need not result in fatigue failure.[97]

In recent years, significant progress has been made toward an understanding of the mechanism of fatigue failure. This progress has been experimental as well as theoretical in nature.

One major experimental advance has been the discovery that extrusion[98] and intrusion[99] of material occur along slip bands during cyclic loading. Since fatigue cracks have been shown to take place in slip bands, it is thought that fatigue cracks result from voids left behind by extrusions[100] or from the growth of intrusions.[99] Wood[101] has proposed a model in which "notches" are produced by the action of alternating slip.

Another major advance was the discovery that extrusions, intrusions, and fatigue cracks can be formed at extremely low temperatures.[102] Hence, it would seem that thermally activated processes such as chemical processes and movement of vacancies cannot be of primary importance in the fatigue mechanism. In addition, the surface structure of the slip bands does not appear to be affected in a marked nammer by the temperature at which the tests are conducted (from 4.2° K to 293° K).[103]

Apparently, on the basis of the results of the low temperature studies, most investigations are now being conducted in the area of possible slip mechanisms.[104-107] In this area, it appears the electron transmission studies will eventually lead to a better understanding of fatigue.

CHAPTER IV

EXPERIMENTAL EQUIPMENT AND PROCEDURE

Fatigue Machine

A Sonntag Universal Fatigue Testing Machine, model SF-10-U, with a five-to-one multiplying fixture was used for the fatigue tests. This machine produces an axial alternating load superimposed on an axial mean load.

The basic machine has a dynamic capacity of $\pm$ 5,000 lbs. Hence, for cyclic loading with the five-to-one fixture in place, the maximum load is 50,000 lbs. The instruction manual lists the accuracy of loading at $\pm$ 2 per cent. The corresponding maximum amplitude of the over-all change in length of the fatigue specimen is $\pm$ .038 inch.

This machine applies the alternating load by means of a rotating eccentric and a flex-plate network. The static load is applied by springs and is maintained at a constant level by means of a differential transformer which senses specimen elongation and automatically adjusts the load accordingly.

The fatigue tests were conducted in the Engineering Mechanics Laboratory located at the Dearborn Center of The University of Michigan.

Material

The steel used in this study is a AISI 1008 steel. An analysis, performed by the Detroit Testing Laboratory, gave the

composition as: C .03, Si .06, Mn .42, P .015 and S .025.

This material was purchased in the form of an 11 gage, 4' x 10' cold finished sheet. It was sheared by the supplier as shown in Figure 4.1.

Tensile tests were conducted on specimens of the material in the "as received" condition and on specimens that had been heated in boiling water for about 6 hours. It was determined that this steel displayed a small amount of strain-aging.

The tensile specimen used in these tests is shown in Figure 4.2. The results of these tests, which were conducted using a 60 ton Southwark Emery hydraulic tensile testing machine, are given in Tables 4.1 and 4.2.

In order to reduce the change in static properties due to strain-aging, during the period of testing, the fatigue specimens (and the remaining tensile specimens) were heated in water at approximately 180° F for 8 hours. Table 4.3 lists the results of tensile tests performed shortly after this aging process.

It also seemed advisable to test tensile specimens at approximately the half-way point during the fatigue tests and after the fatigue test had been concluded in order to determine if strain-aging had occurred during that period. These results are given in Tables 4.4 and 4.5. It can be demonstrated, by comparing the results listed in Tables 4.3 and 4.5, that no marked change took place during the period of testing. These three series of tests were conducted using a 120 ton Southwark Emery hydraulic tensile testing machine.

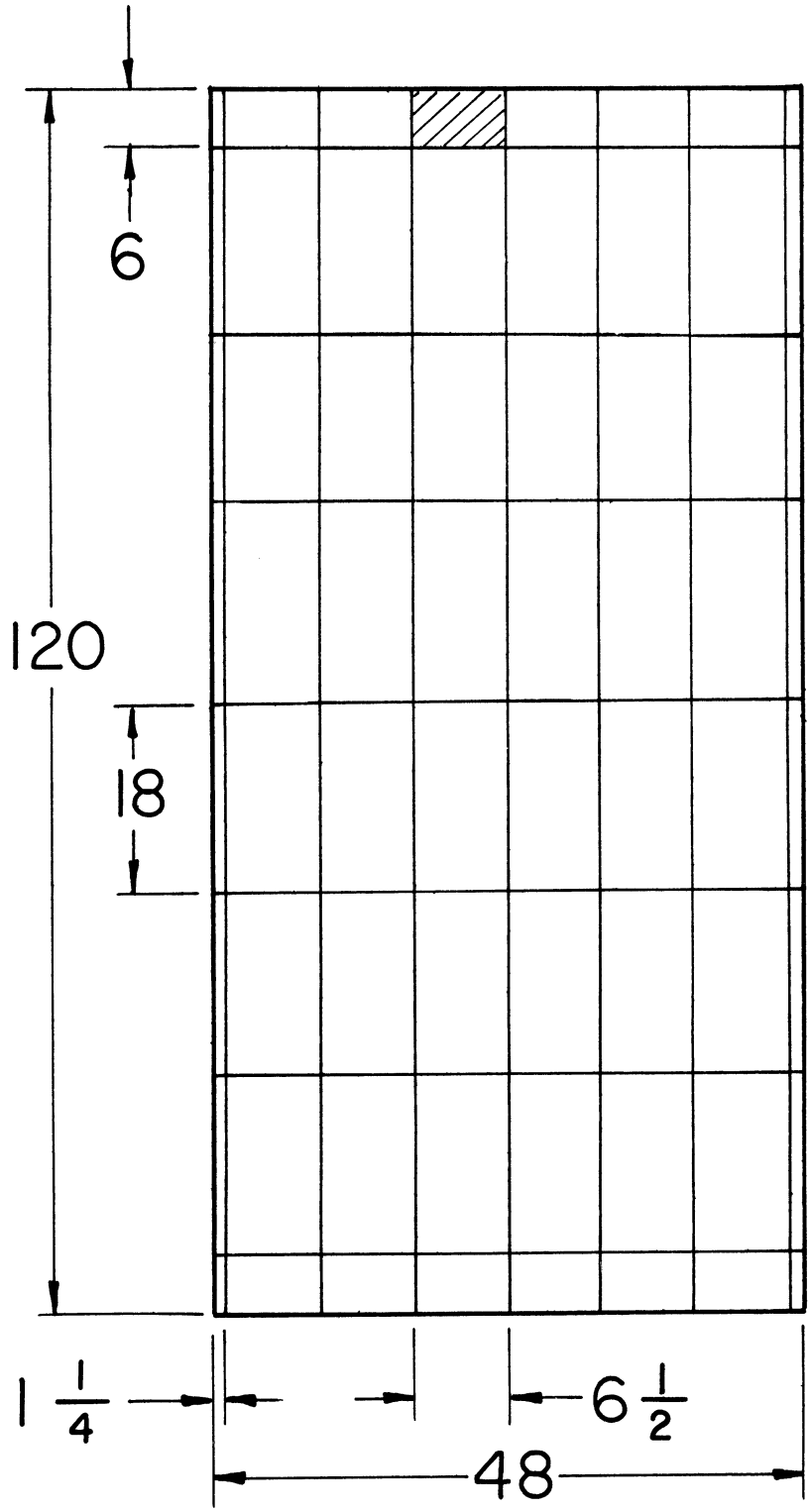

Figure 4.1 Sheet stock showing orientation of specimen blanks. Smaller end blanks used for tensile specimens.

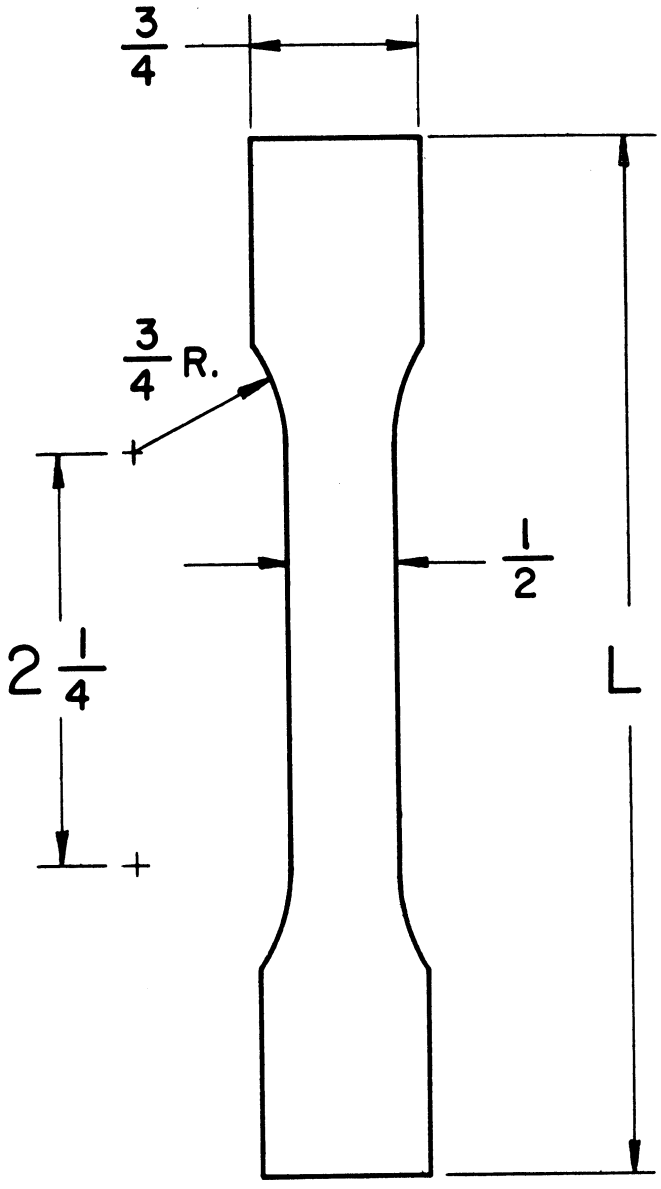

Figure 4.2 Tensile specimen. See Figure 4.1. L equals 6" for longitudinal specimens and L equals 6-1/2" for transverse specimens.

TABLE 4.1

Tensile test data. Material as received.

Specimen Number	Upper Yield Strength	Lower Yield Strength	Ultimate Tensile Strength	Elongation
	---------- in ksi ----------			per cent
Longitudinal				
1	34.6	34.2	47.1	36
2	32.7	32.3	47.4	37
3	35.2	34.6	46.7	36
4	33.0	32.3	47.1	37
5	33.3	32.7	47.1	37
6	34.9	33.3	47.1	36
Average	33.8	33.2	47.1	36 1/2
Deviation	+1.4	+1.4	+0.3	+ 1/2
	-1.1	-0.9	-0.4	- 1/2
Transverse				
1	32.3	31.2	46.4	39
2	35.2	33.6	47.4	38
3	30.7	30.4	45.4	40
4	32.7	30.7	46.7	39
Average	32.7	31.5	46.5	39
Deviation	+2.5	+2.1	+0.9	+1
	-2.0	-1.1	-1.1	-1

TABLE 4.2

Tensile test data. Material aged in boiling water for approximately 6 hours.

Specimen Number	Upper Yield Strength	Lower Yield Strength	Ultimate Tensile Strength	Elongation
	---------- in ksi ----------			per cent
Longitudinal				
1	37.4	36.2	47.7	37
2	37.8	35.8	46.4	37
3	37.1	35.2	47.1	38
Average	37.4	35.7	47.1	37
Deviation	+0.4 -0.3	+0.5 -0.5	+0.6 -0.7	+1 -0
Transverse				
1	35.2	34.4	47.1	40
2	33.3	33.0	46.7	41
3	35.2	34.9	46.7	40
Average	34.6	34.1	46.8	40
Deviation	+0.6 -1.3	+0.8 -1.1	+0.3 -0.1	+1 -0

TABLE 4.3

Tensile test data. Specimens aged in water at approximately 180° F for approximately 8 hours. Tests conducted within 48 hours.

Specimen Number	Upper Yield Strength	Lower Yield Strength	Ultimate Tensile Strength	Elongation
	---------- in ksi ----------			per cent
Longitudinal				
1	36.7	35.2	48.3	37
2	35.7	34.7	47.2	37
3	35.5	34.5	46.9	40
4	35.9	34.4	47.4	38
5	36.0	34.9	47.7	38
Average	36.0	34.7	47.5	38
Deviation	+0.7	+0.5	+0.8	+2
	-0.5	-0.3	-0.6	-1

TABLE 4.4

Tensile test data. Specimens aged in water at approximately 180° F for approximately 8 hours. Tests conducted after approximately 3 months.

Specimen Number	Upper Yield Strength	Lower Yield Strength	Ultimate Tensile Strength	Elongation
	---------- in ksi ----------			per cent
Transverse				
1	34.3	32.7	47.1	41
2	35.7	33.3	46.7	40
3	35.7	33.3	46.4	40
4	34.9	33.6	47.4	40
5	35.2	33.3	47.1	42
Average	35.2	33.2	46.9	41
Deviation	+0.5	+0.4	+0.5	+1
	-0.9	-0.5	-0.5	-1

TABLE 4.5

Tensile test data. Specimens aged in water at approximately 180° F for approximately 8 hours. Tests conducted after approximately 10 months.

Specimen Number	Upper Yield Strength	Lower Yield Strength	Ultimate Tensile Strength	Elongation
	---------- in ksi ----------			per cent
Longi-tudinal				
1	35.2	34.9	47.7	37
2	36.2	35.4	47.1	38
3	35.2	33.0	----	--
4	34.7	33.5	----	--
5	35.5	34.4	----	--
Average	35.4	34.2	47.4	37 1/2
Deviation	+0.8	+1.2	+0.3	+ 1/2
	-0.7	-1.2	-0.3	- 1/2

Note: The lower yield strengths for specimens 3, 4 and 5 under load with a zero strain rate were 32.5, 32.0 and 33.1 ksi, respectively.

The aged longitudinal tensile specimens displayed an average lower yield strength of 34,500 psi and an average ultimate strength of 47,500 psi. Figures 4.3 and 4.4 show the microstructure of this material. The ASTM grain size is approximately 8 to 9. The dark globules at the grain boundaries are carbides. A typical nominal stress-strain curve appears in Figure 4.5.

Piobert-Luders' Bands

Three specimens listed in Table 4.5 were not pulled to failure. These specimens were used to determine the plastic strain level within the Piobert-Luders' bands. The strain level within these bands will be used in Chapter VI to show that the localized plastic strain encountered in the fatigue tests conducted in this study is sufficiently large to treat all practical applications of fatigue analysis.

Two .031 inch gage length foil strain gages were mounted on one of these specimens. One gage was mounted at the center of the gage length and the other was mounted directly below it opposite a gage length prick-mark. This specimen was pulled until the upper yield was reached, and then elongated only a few thousandths of an inch further. The upper gage, which was mounted on the central elastic area, indicated a strain of approximately 1200 micro-inches per inch: the lower gage, over Piobert-Luders' bands, indicated over 20,000 micro-inches per inch strain.

These results show that the plastic strain associated with Piobert-Luders' bands is a minimum of two per cent for this material.

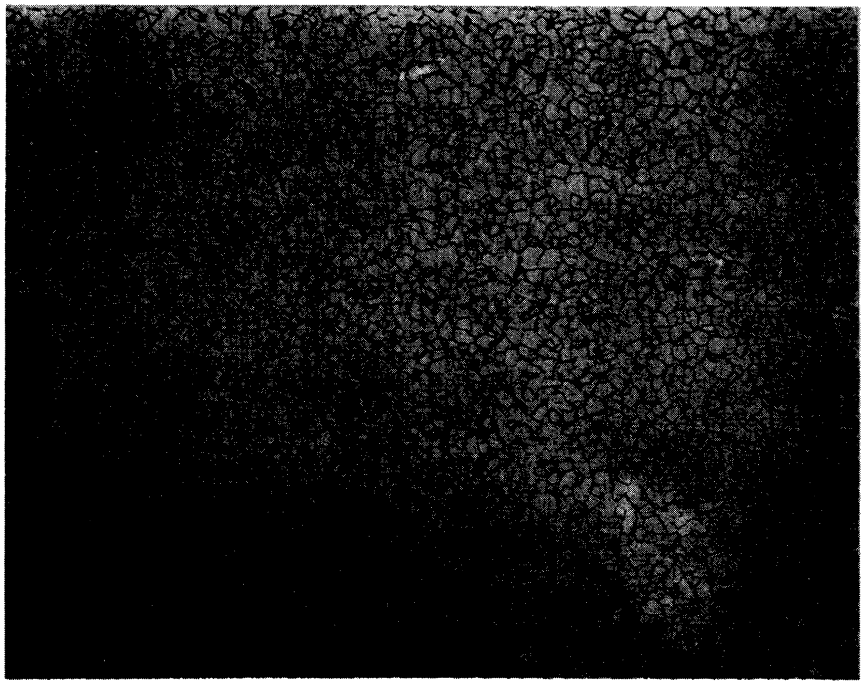

Figure 4.3 Microstructure X 100. Inclusions elongated in longitudinal direction.

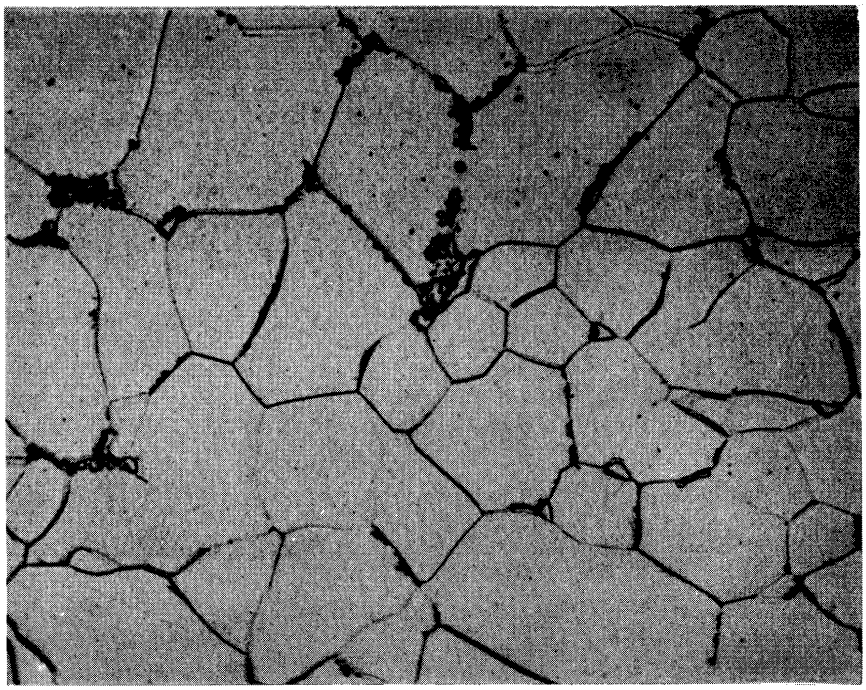

Figure 4.4 Microstructure X 1000.

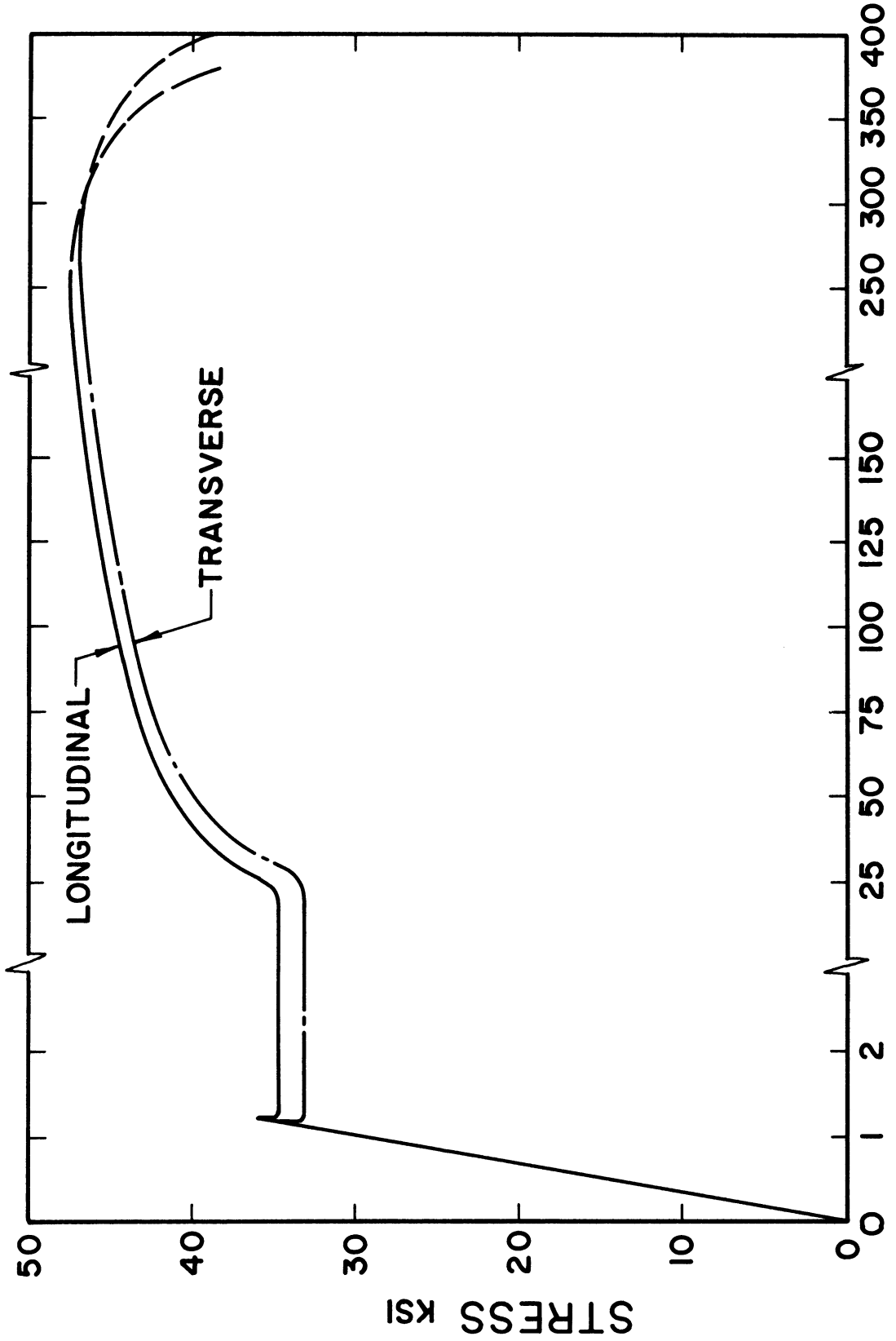

Figure 4.5 Nominal stress-strain curve. Average value of Young's modulus equals 28.7×10^6 psi. Average value of the yield point elongation approximately equal 2 1/2 per cent.

(In general, the strain level within these bands can be approximated as the yield point elongation.)[108-114]

Fatigue Specimen

Figure 4.6 shows the fatigue specimen used in this study. The notch, which is the central hole, has been treated both analytically and experimentally in the literature. This aspect is discussed in the next section.

The central hole was reamed, and then expansion reamed in order to remove only about .006 inch (total) on the final cut. The specimens were aged prior to final processing which involved removing large scratches with a fine file, and then polishing sucessively with 1, 0, 00, 000 and 0000 emery paper. The surface area of the hole within approximately 3/16 of an inch of the transverse center-line was examined with a magnifying glass to establish that no prominent grooves or scratches were present. The edge of the hole was given a small chamfer and was polished as outlined above to a radius of approximately .02 inch.

Determination of the Theoretical Stress-Concentration Factor

Kirsch's generalized (elastic) plane-stress solution of the problem of an infinite plate, with a central hole, subjected to uniform tension along one axis consists of finding a stress state such that equilibrium, compatibility, and the appropriate boundary conditions are satisfied. This solution is given in detail by Durelli, Phillips, and Tsao[115] along with a complete series of isobars, isotenics, etc. This solution yields a theoretical stress concentration factor of 3.0.

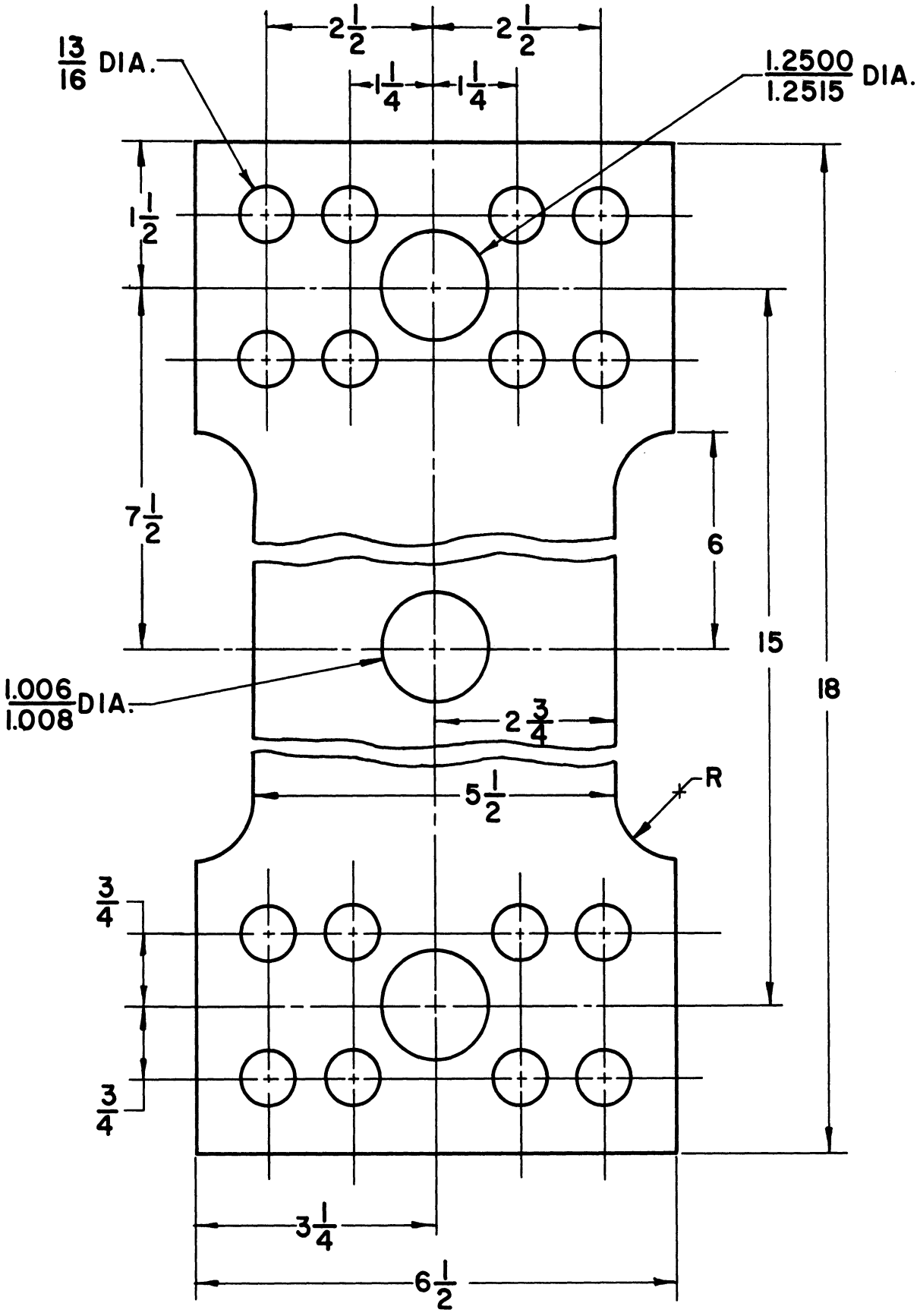

Figure 4.6 Fatigue specimen.

While the plane-stress approach is generally accepted to represent a close approximation to the actual state of stress in very thin members, it can be shown that the plane-strain approach yields the same theoretical stress-concentration factor as above[115] and that this factor is not influenced significantly by varying the thickness of the plate.[116,117] Mindlin[118] includes the effect of couple-stresses in a recent static solution. Pao[119] has developed a dynamic solution for this problem in which the dynamic stress concentration factor is approximately 3.0 for the stressing frequency used in this study.

Howland Solution

The fatigue specimens resemble the case of a central circular hole in a thin plate of finite width, of infinite length, which is subjected to uniform tension along one axis. See Figure 4.7.

Howland[120] found a stress function in the form of an infinite series which leads to a generalized (elastic) plane-stress solution that satisfies the appropriate boundary conditions. Basically, the approach was to let the first "term" of the series stress function be that of the Kirsch solution: then the coefficients of the second term were chosen such that normal and shear stresses "introduced" on the vertical edges (by the first term) were eliminated . . . however, the second term in turn "introduced" normal and shear stresses on the edge of the hole. The coefficients of the third term were chosen such that the latter stresses were eliminated, and so forth. This solution yields a theoretical stress-concentration factor of 2.55.

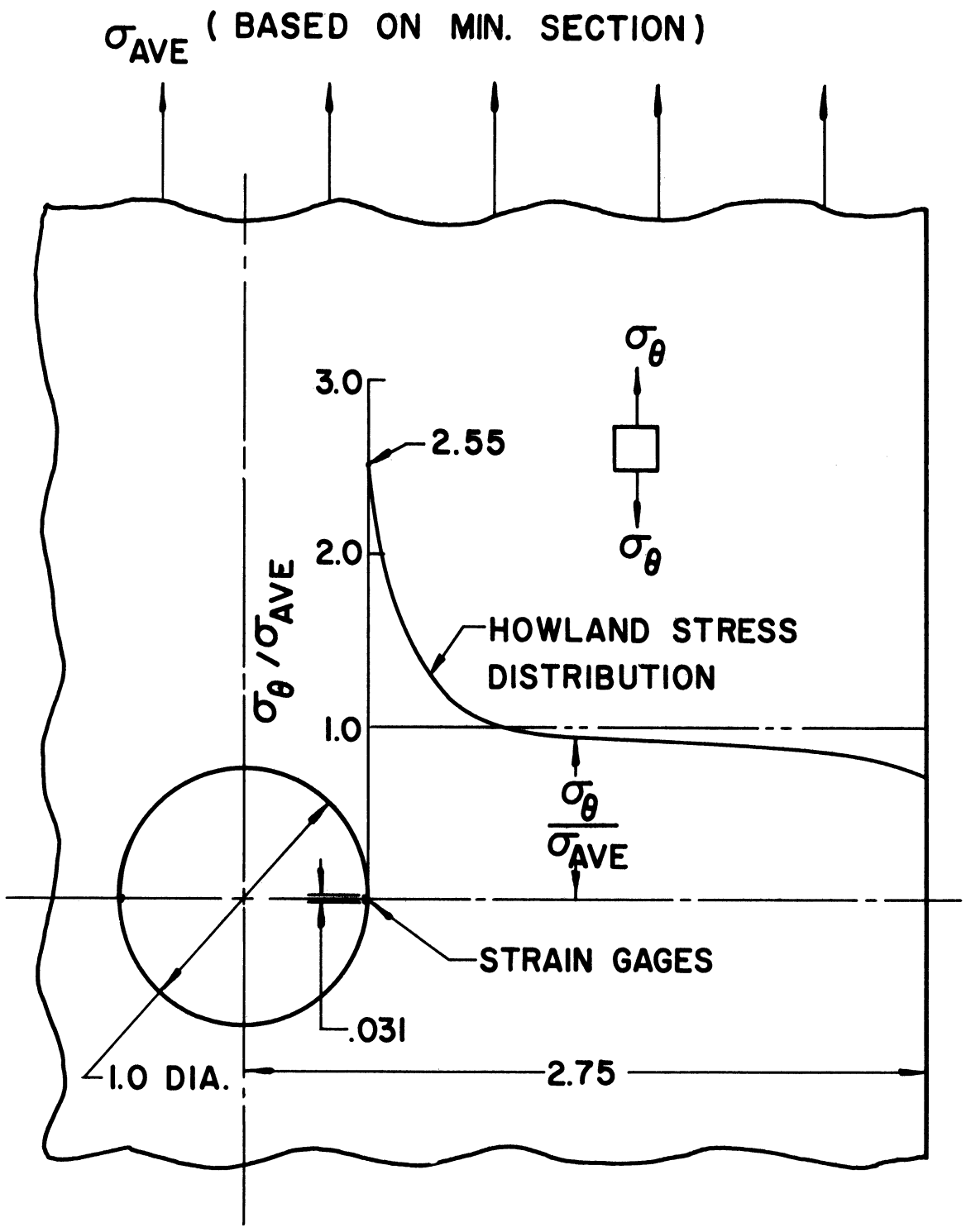

Figure 4.7 Transverse stress distribution. Stress element shown pertains only to longitudinal stress on the transverse center-line.

The Howland solution yields the stress distributions along the longitudinal axis shown by the solid lines in Figure 4.8: the corresponding Kirsch stress distribution along the center-line is represented by the dashed line. It can be seen that the tensile stress along the center-line approaches its limiting value more rapidly than in a plate of great width. These curves are presented to establish that the proportions of the fatigue specimen used in this study are adequate to approximate closely the ideal case of uniform tension near the fixture grips.

Experimental Support of the Howland Solution

Wahl and Beeuwkees[121] developed the empirical formula:

$$K = 3 - 3.13\,(a/b) + 3.76\,(a/b)^2 - 1.71\,(a/b)^3 \qquad (4.1)$$

from their photoelastic test results. This formula gives a value of the stress concentration factor of 2.55.

The recommended curves for two compilations of data[122,123] for various experimental approaches give stress concentration factors of 2.54 and 2.55, respectively. While these recommendations may have been influenced by the previously mentioned data and analytical results; both are adequately supported by other data . . . which varies between approximately plus and minus five per cent from the values cited above. (The stress concentration factor found by strain gage techniques during this study is 2.54.)

Procedure

As the objective of the fatigue tests is to ascertain the influence of localized yielding on the effect of mean stress, one

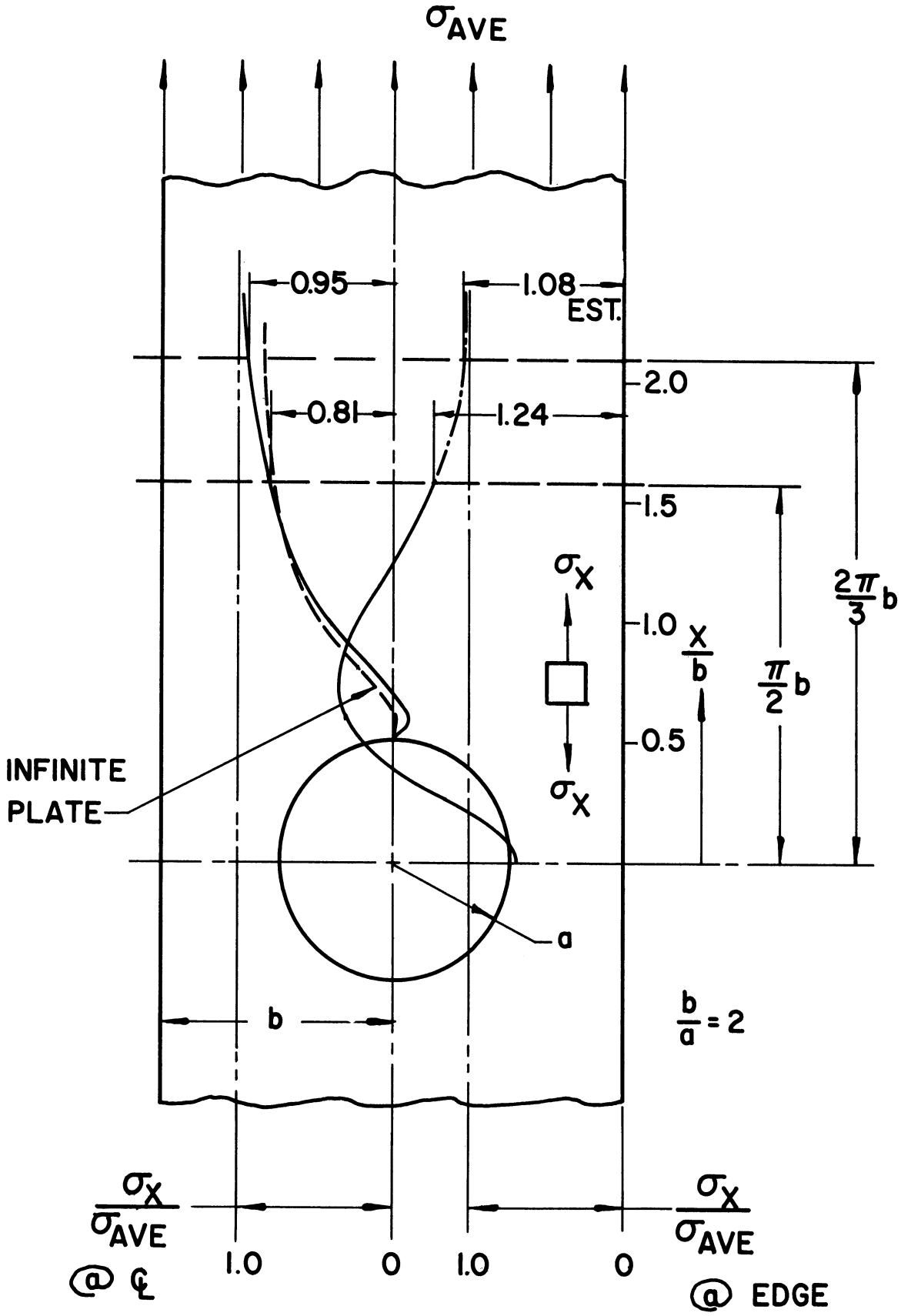

Figure 4.8 Longitudinal stress distribution. Stress element shown pertains only to the longitudinal stress along each edge and along the longitudinal center-line.

series of tests are conducted under conditions such that little or no plastic strain takes place and another series of tests are conducted under conditions such that very large localized plastic strain takes place. By selecting the maximum cyclic stress in the first series of tests to be approximately equal the stress at which localized yielding occurs, the basic difference between these series of tests is that localized yielding takes place in one but not in the other. Therefore, the influence of localized plastic strain can be determined by comparing the results of these two series of fatigue tests.

These two series of fatigue tests are shown schematically in Figure 4.9: the diagram on the left pertains to no localized yielding. In the first series of tests in which no localized yielding takes place, the specimens are loaded elastically to point A, after which the local strain follows the ideal hysteresis loop A-B-C-D-A. In the second series of tests in which large localized plastic strain takes place, the specimens are loaded such that localized yielding takes place at point A and continues to point B, after which the local strain follows the ideal hysteresis loop B-C-D-E-B. It is assumed in drawing these diagrams that the maximum value of the local stress is equal to the local yield strength: the nominal stress corresponding to large localized plastic strain is, of course, much larger than the nominal stress corresponding to no localized yielding.

Following the fatigue tests, static tests are conducted on virgin (non-fatigued) specimens in which the local cyclic stress-strain behavior is determined. In these tests, the local hysteresis

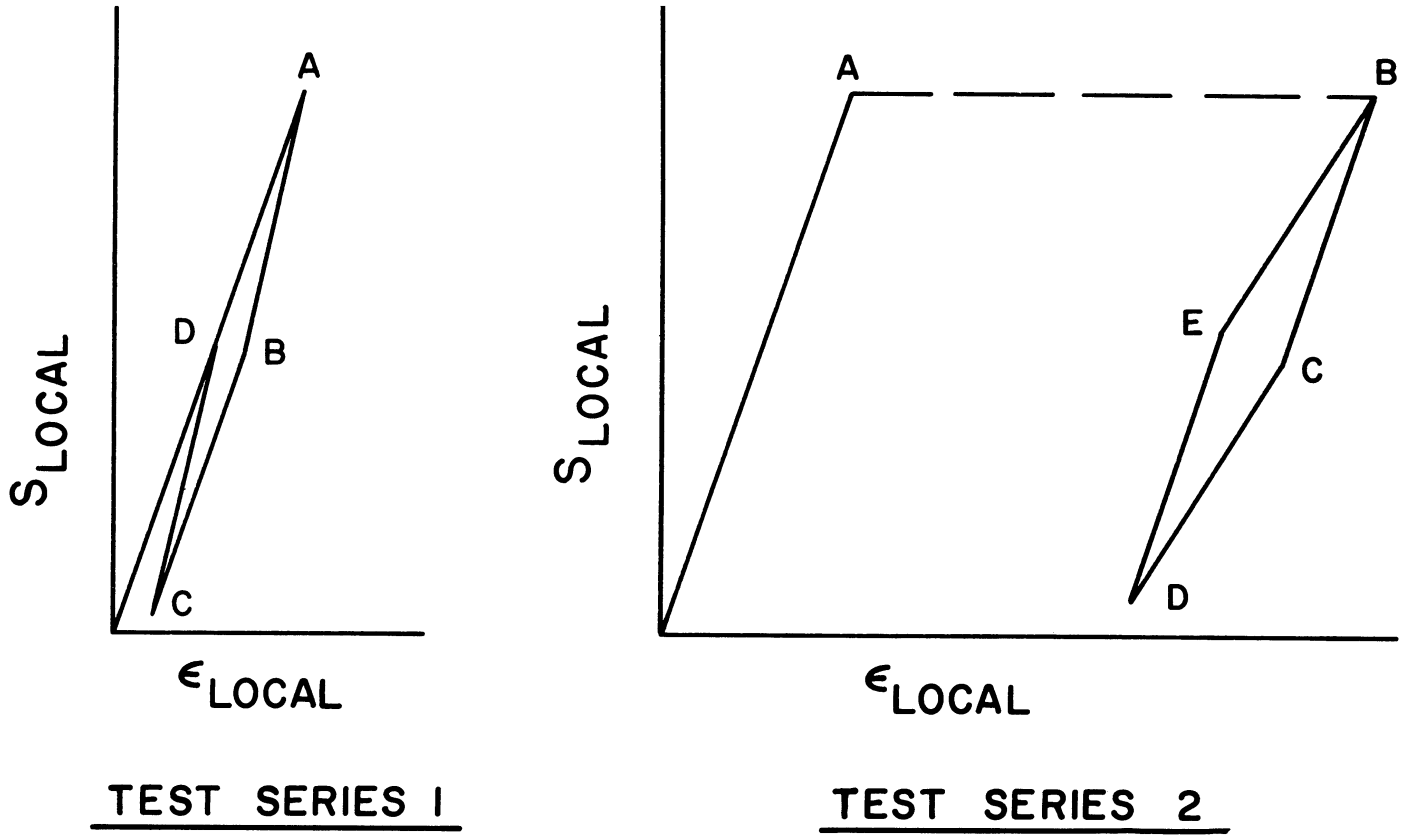

Figure 4.9 Ideal view of test procedure. The diagram on the left corresponds to the first series of fatigue tests in which no initial plastic strain takes place. The diagram on the right corresponds to the second series of fatigue tests in which large initial plastic strain takes place.

loops are measured by means of strain gages while the specimens are very slowly loaded and unloaded such that the maximum and the minimum nominal stresses correspond to values determined by the fatigue tests. These tests are conducted in order to compare these results to the results of similar tests on unbroken fatigue specimens which have withstood several millions of stress cycles.

The data from the static tests aid in analyzing the fatigue data and in developing an understanding of the local behavior.

CHAPTER V

TEST RESULTS

Preliminary Tests

Because it is necessary to select the first mean stress level in the fatigue tests such that little or no plastic strain takes place upon initial loading, the stress-strain behavior at the edge of the hole was established in preliminary tests by means of strain gages. It was determined that less than 100 micro-inches per inch plastic strain resulted from a maximum nominal stress of 21,000 psi.

It was also determined that the strains on either side of the hole were the same in the elastic range of stress within two per cent.

Fatigue Tests - Stress Ratio 0.0

The first fatigue specimen tested was cycled between 150 psi and 13,900 psi nominal stress. This small minimum stress insures that the specimen is always in tension. The 13,900 psi value was calculated using the Goodman diagram and the internal yielding approach modification to treat notched specimens. This specimen did not fail in five million cycles.

Table 5.1 lists the stress range for the subsequent specimens tested to establish the approximate fatigue limit. The estimated fatigue limit is 10,000 psi nominal, for a mean stress of 10,000 psi nominal.

As this fatigue cycle does not induce significant plastic strains, nine specimens were tested to determine this fatigue limit

TABLE 5.1

Preliminary fatigue tests. Stress ratio 0.0.

Specimen Number	Maximum Nominal Stress in psi.	Minimum Nominal Stress in psi.	Remarks
1	13,900	150	Did not fail in 5×10^6 cycles.
2	15,800	140	Did not fail in 5×10^6 cycles
3	17,600	200	Did not fail in 5×10^6 cycles.
4	19,500	150	Did not fail in 5×10^6 cycles.
5	21,650	160	Failed left hand side after 2.659×10^6 cycles.

more accurately. A stress ratio of 0.0 was used in these tests. The results are listed in Table 5.2.

The position of the loading platen was measured before and after each test. The maximum change in this position was .005 inch for the unbroken specimens. This reflects a maximum over-all change in length of only .001 inch; therefore, it could not be ascertained whether the dowel pin holes had elongated, whether the specimen had shifted slightly in the grips, or if the specimen had permanently elongated.

Figure 5.1 shows a typical failure. All broken specimens in this series failed in the same manner.

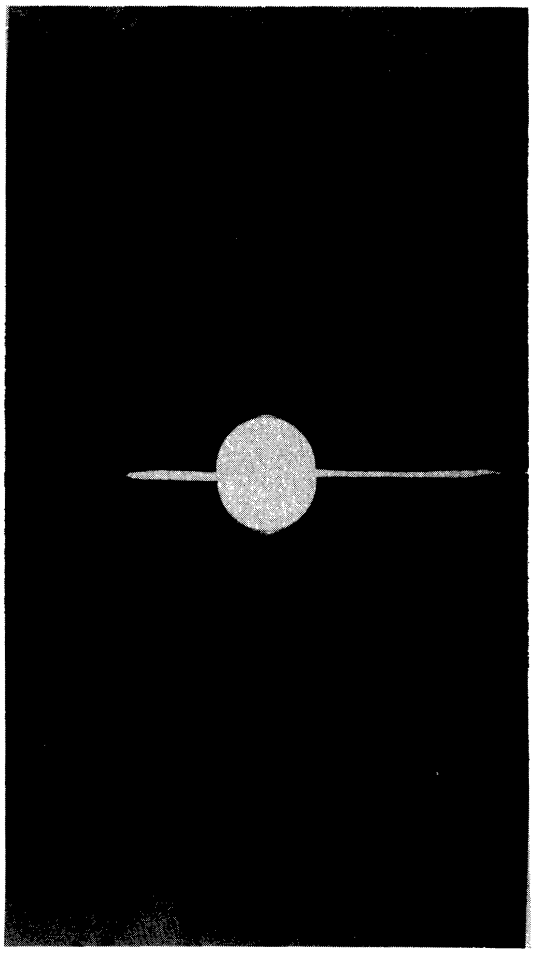

Figure 5.1 Typical fatigue failure. All broken fatigue specimens tested under a stress ratio of 0.0 failed in this manner.

Fatigue Tests -- Stress Ratio .33

The first specimen in this series was cycled between 9,250 and 27,750 psi nominal stress. Piobert-Luders' bands originated at the center-line of the hole at each edge and grew directly across the minimum section to a final length of approximately 3/4 of an inch. (These results agree with tests by Durelli, Kobayashi and Hofer[124], but do not conform to the theoretical results predicted by Nadai.[125]) These bands appeared within the first half-minute of testing and gradually grew during the first 20,000 to 50,000 cycles. Their appearance did not change during the remainder of the test.

Three more specimens were tested and these results indicated that the fatigue limit was 10,000 psi nominal, for a mean stress of 20,000 psi nominal. See Table 5.3.

At this point the supply of flat specimens was almost exhausted; therefore, the tests were continued using bowed specimens.

These tests gave results for the bowed specimens that could not be discerned in any manner from the results for flat specimens. See Table 5.3: specimens 5 through 7, inclusive.

Finally, a flat specimen was tested to establish a counterpart for the upcoming static tests. This test was discontinued after thirty million cycles.

In all, eight specimens were tested with a stress ratio of .33. The fatigue limit for this series is the same as for the first series, that is, 10,000 psi nominal.

Again, the position of the loading platen was measured before and after each test. The maximum change in this position

TABLE 5.2

Fatigue Data. Stress Ratio 0.0.

Specimen Number	Maximum Nominal Stress in psi.	Minimum Nominal Stress in psi.	Remarks
1	20,940	140	Failed right hand side after 4.87 x 10^6 cycles.
2	20,120	120	Did not fail in 10 x 10^6 cycles.
3	20,630	130	Failed right hand side after 3.898 x 10^6 cycles.
4	20,080	80	Did not fail in 10 x 10^6 cycles.
5	20,630	130	Failed right hand side after 7.148 x 10^6 cycles.
6	20,150	150	Failed left hand side after 9.325 x 10^6 cycles.
7	20,230	230	Failed left hand side after 2.638 x 10^6 cycles.
8	19,710	210	Did not fail in 15 x 10^6 cycles.
9	19,710	210	Did not fail in 15 x 10^6 cycles.

TABLE 5.3

Fatigue Data. Stress Ratio .33.

Specimen Number	Maximum Nominal Stress in psi.	Minimum Nominal Stress in psi.	Remarks
1	27,750	9,250	Did not fail in 15×10^6 cycles.
2	29,250	9,750	Did not fail in 15×10^6 cycles.
3	30,000	10,000	Did not fail in 15×10^6 cycles.
4	30,750	10,250	Failed left hand side after $5.784 \times 10^6 \times 10^6$ cycles.
5	30,000	10,000	Failed right hand side after 6.888×10^6 cycles.
6	30,000	10,000	Failed right hand side after 9.712×10^6 cycles.
7	30,000	10,000	Failed right hand side after 7.554×10^6 cycles.
8	29,250	9,750	Did not fail in 30×10^6 cycles.

was .009 inch for the unbroken specimens which corresponds to an elongation of .0018 inch for the specimen.

Figure 5.2 shows the appearance of a typical failure. All broken specimens in this series failed in the same manner.

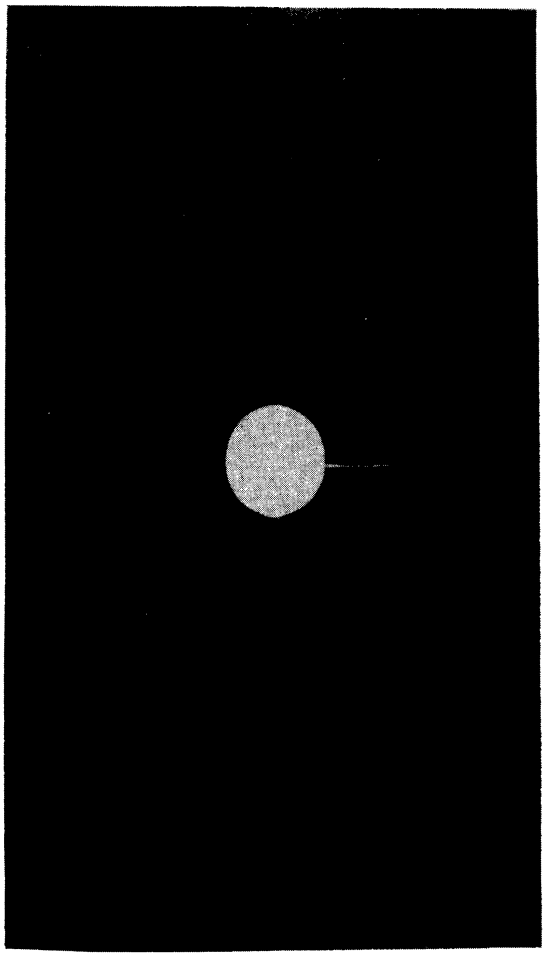

Figure 5.2 Typical fatigue failure. All broken fatigue specimens tested under a stress ratio of .33 failed in this manner.

Static Tests-Stress Ratio 0.0

Static tests were conducted on a virgin specimen and on fatigue specimen 4 of Table 5.2 in which .031 inch gage length foil strain gages were mounted on the inside surface on each side of the hole and on the face of the specimens. These specimens were very slowly loaded in a cyclic manner between zero and 20,000 psi nominal stress.

Figure 5.3 shows the local strain at the left hand side of the hole during the initial cycle for the virgin specimen. The horizontal jogs shown at 19,000 and 20,000 psi, represent strain readings taken immediately after the load was established, and 2 1/2 minutes later. Although these readings were relatively stable after 2 1/2 minutes, the initial anelastic behavior was marked.

Figure 5.4 shows the 10th cycle: this loop form was relatively stable during the first few cycles. The virgin specimen was then subjected to 10,000 fatigue cycles at 1800 CPM. Figure 5.4 also shows a typical cycle after this loading as well as a typical cycle after approximately 100,000 fatigue cycles at 1800 CPM (90,000 additional cycles).

The other cycle shown in Figure 5.4 pertains to fatigue specimen 4: the origin for this loop is not the same as for the preceding loops which pertain to the virgin specimen. All curves, however, pertain to the local strain at the left hand side of the hole.

Static Tests- Stress Ratio .33

Static tests were also conducted on a virgin specimen and on fatigue specimen 8 of Table 5.3. These specimens were very slowly

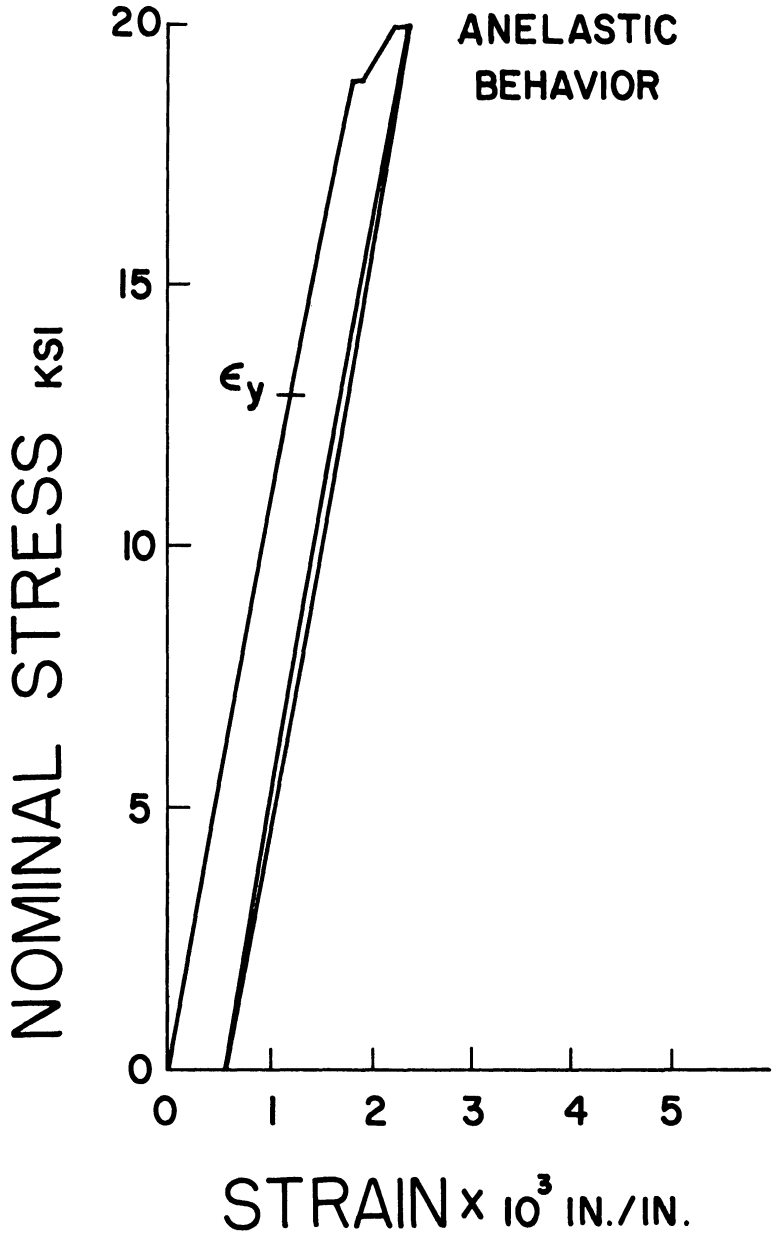

Figure 5.3 Local stress-strain curve. Note the anelastic behavior for local strains approximately 50 per cent greater than the yield point strain.

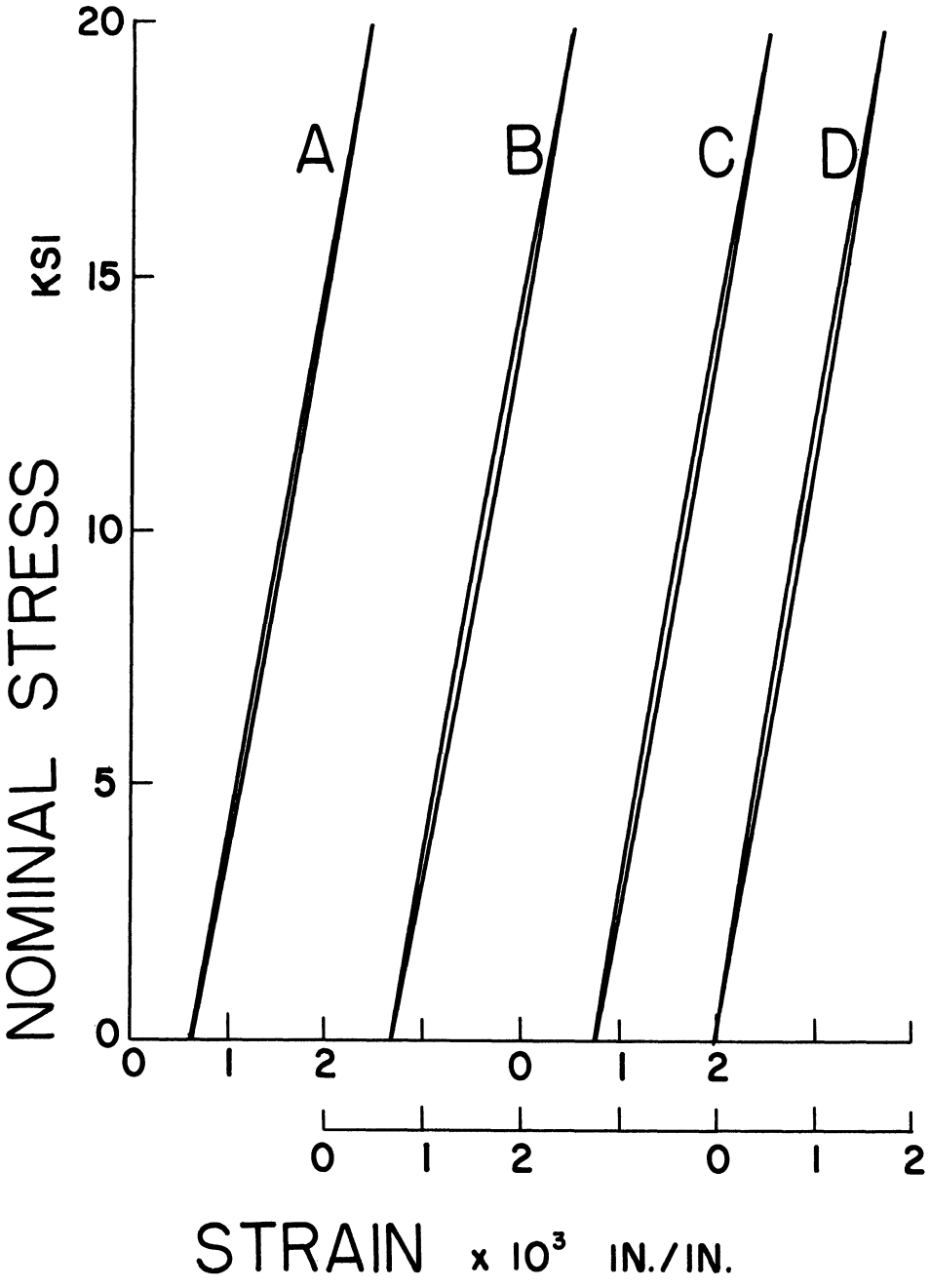

Figure 5.4 Subsequent hysteresis loops. Loop A pertains to the 10th cycle following initial loading. Loop B shows the local behavior after 10,000 (high speed) fatigue cycles and loop C corresponds to 100,000 fatigue cycles. Loop D pertains to a similar static test on a fatigue specimen that had not failed in 10 x 10^6 cycles.

loaded in a cyclic manner between 10,000 and 30,000 psi nominal stress.

Figure 5.5 shows the local strain at the left hand side of the hole during the initial cycle for the virgin specimen. Only very slight anelastic behavior was observed below 17,000 psi. The readings which are plotted above that value pertain to the strain level at 2 1/2 to 5 minutes after the loads were established.

Figure 5.6 shows a typical loop for the next few cycles as well as a typical loop after the specimen had undergone 100,000 fatigue cycles at 1800 CPM.

The other loop shown here is a typical cycle for fatigue specimen 8: the origin for this loop is not the same as for the preceding loops which pertain to the virgin specimen. All curves, however, pertain to the local strain at the left hand side of the hole.

Strain Redistribution During Cyclic Loading

Figure 5.7 shows typical plots of the strain distribution for the virgin specimens after the first cycle and after 100,000 cycles. Although the range of strain (the maximum strain minus the minimum strain) does not change noticeably, the maximum and the minimum strain gradually increase during cyclic loading. Approximately one-half of the total increase occurs in the first ten cycles.

No strain redistribution was observed during the static tests conducted on the specimen previously fatigue tested at the lower mean stress level. While some strain redistribution was noted for the fatigue specimen previously tested at the higher mean stress level, this specimen was unloaded between the fatigue and the static tests

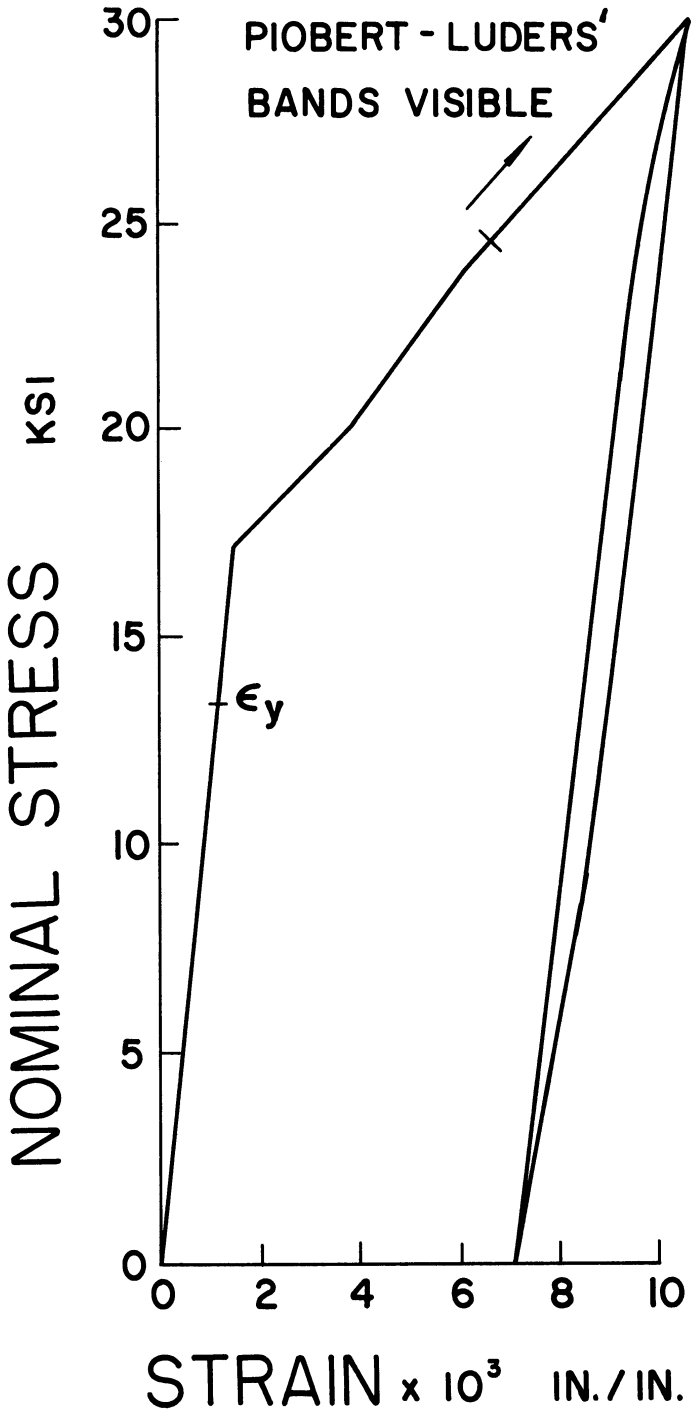

Figure 5.5 Local stress-strain curve. Piobert-Luders' bands were not visible immediately following gross plastic flow. Considerable anelastic behavior took place at stress levels associated with gross plastic flow.

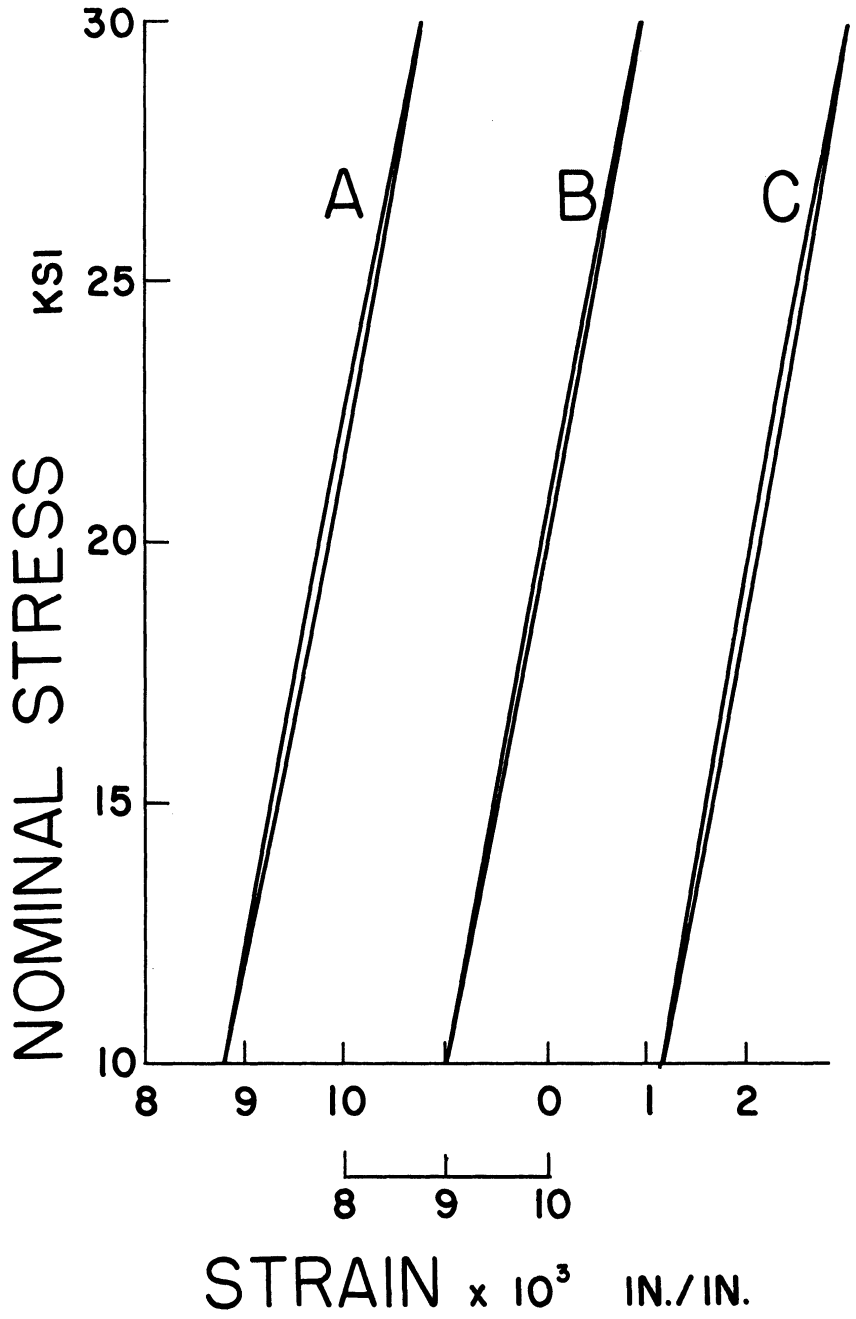

Figure 5.6 Subsequent hysteresis loops. Loop A pertains to the 10th cycle following initial loading. Loop B shows the local behavior after 100,000 (high speed) fatigue cycles. Loop C pertains to a similar static test on a fatigue specimen that had not failed in 30 x 10^6 cycles.

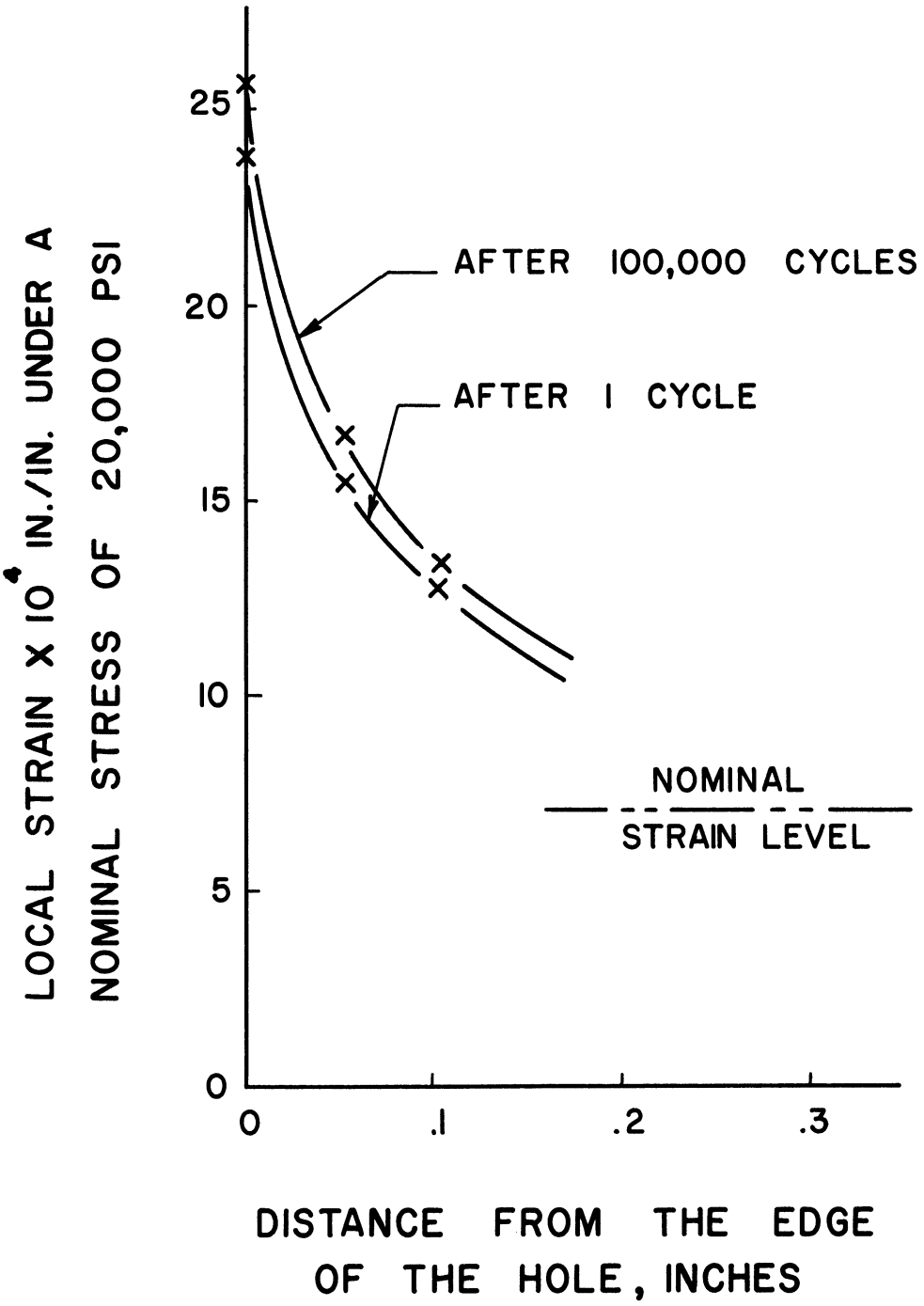

Figure 5.7 Strain redistribution under cyclic loading. The local strain increases for a given nominal stress as a function of the number of imposed stress cycles.

and this may have lead to yielding in compression as a consequence of unloading due to the Bauschinger effect. These results are not shown here because of this uncertainty and because the subsequent strain redistribution, although smaller, is of the form shown in Figure 5.7.

Load-Deformation Curves

Figure 5.8 shows the over-all specimen elongation plotted versus the nominal stress for a virgin specimen, a fatigue specimen cycled at the lower mean stress level, and a fatigue specimen cycled at the higher mean stress level, respectively. These curves are sensitive to the local plastic deformations because much of the over-all extension is concentrated around the hole.

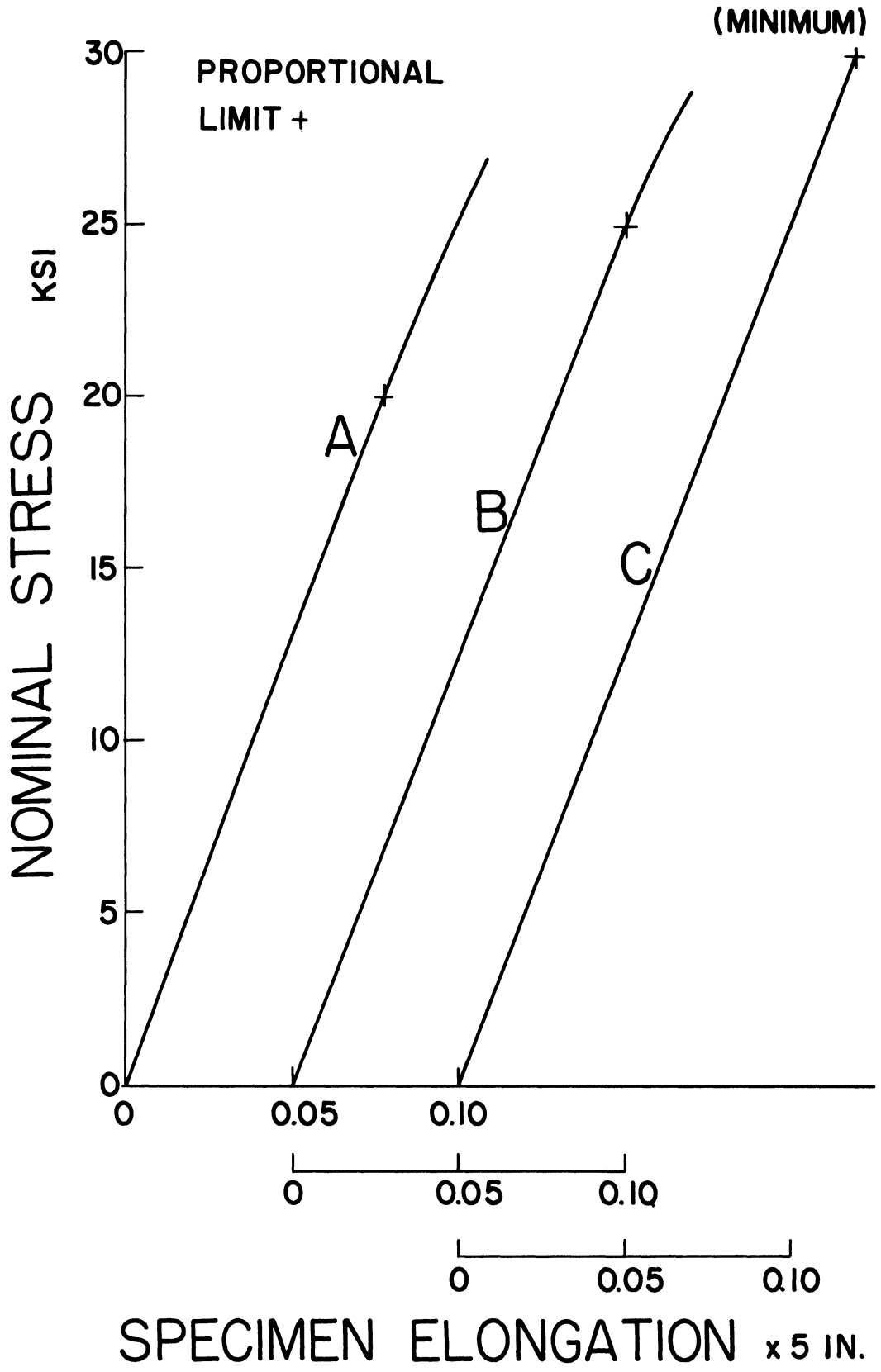

Figure 5.8 Over-all stress-strain curve. Specimen elongation determined by changes in loading platen level.

CHAPTER VI

DISCUSSION OF RESULTS

Fatigue Limits

Figures 6.1 and 6.2 show the limiting safe nominal cyclic stresses for the two series of fatigue tests. The safe range of stress is 20,000 psi nominal for each stress ratio (0.0 and 0.33) used in these tests. There ranges of stress are developed from the test data as outlined below.

Tables 5.1 and 5.2 which pertain to a stress ratio of 0.0 show that failure resulted for each of the four specimens tested under a nominal range of stress of 20,500 psi or larger. Yet, no failure occurred among the six specimens which were subjected to a nominal range of stress of 19,500 psi or smaller. Four specimens were tested with a range of 20,000 psi nominal stress: two failed, two did not. Hence, the range of stress (for approximately fifty per cent failures) is 20,000 psi nominal $\pm$ 500 psi.

Table 5.3 pertains to a stress ratio of 0.33. No failure occurred for any of the three specimens subjected to a nominal range of stress of less than 20,000 psi. Only one specimen was tested under a nominal range of stress of 20,500 psi: it failed. Four specimens were also tested under a range of stress of 20,000 psi nominal; in this case, three failed and one did not. These results also lead to an estimated nominal range of stress of 20,000 psi $\pm$ 500 psi for fifty per cent failures. (If the range were precisely 20,000 psi, the probability of obtaining 2 failures in 4 tests is .375;

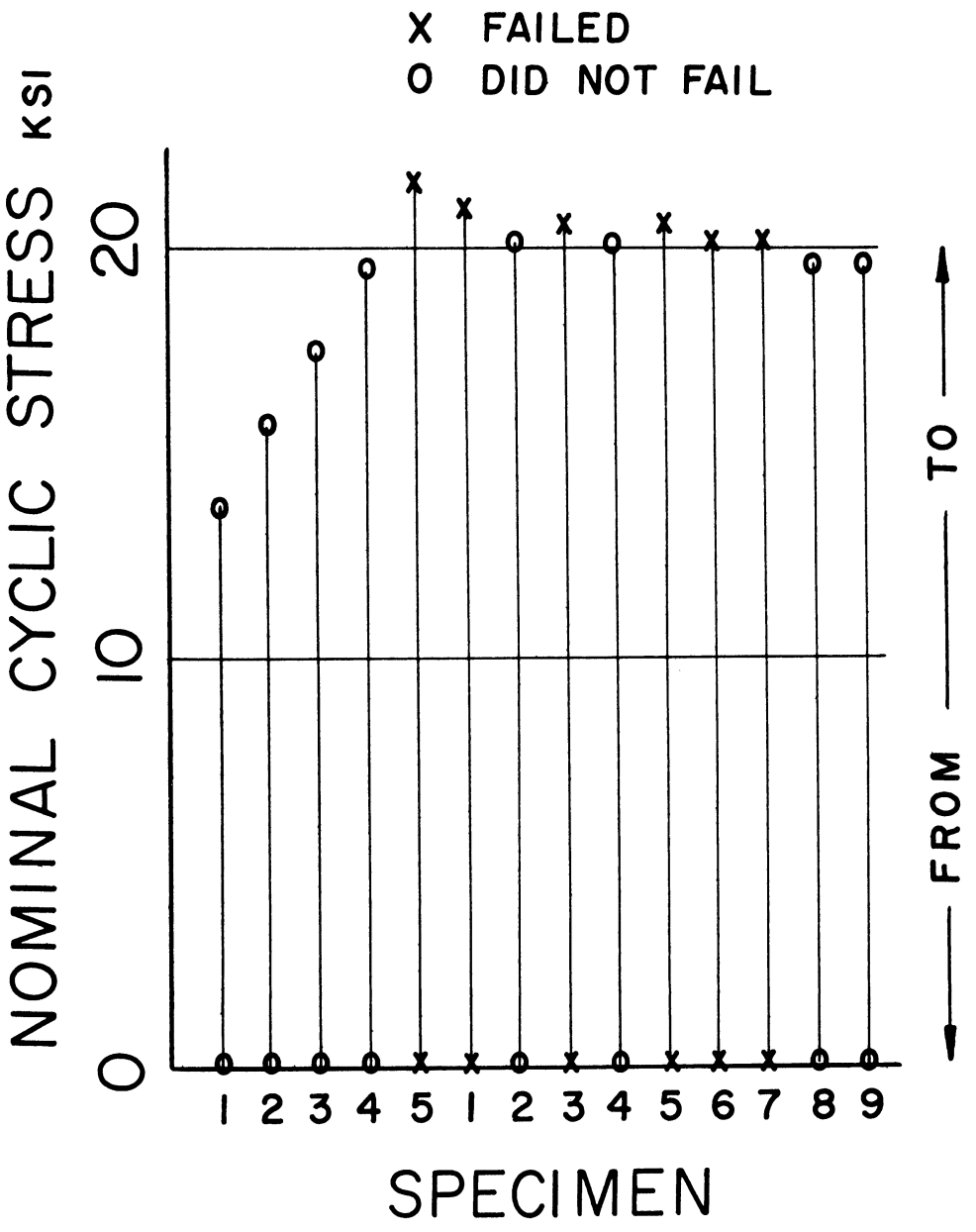

Figure 6.1 Limiting safe range of stress. Plot of data listed in Tables 5.1 and 5.2 which pertain to a stress ratio of 0.0.

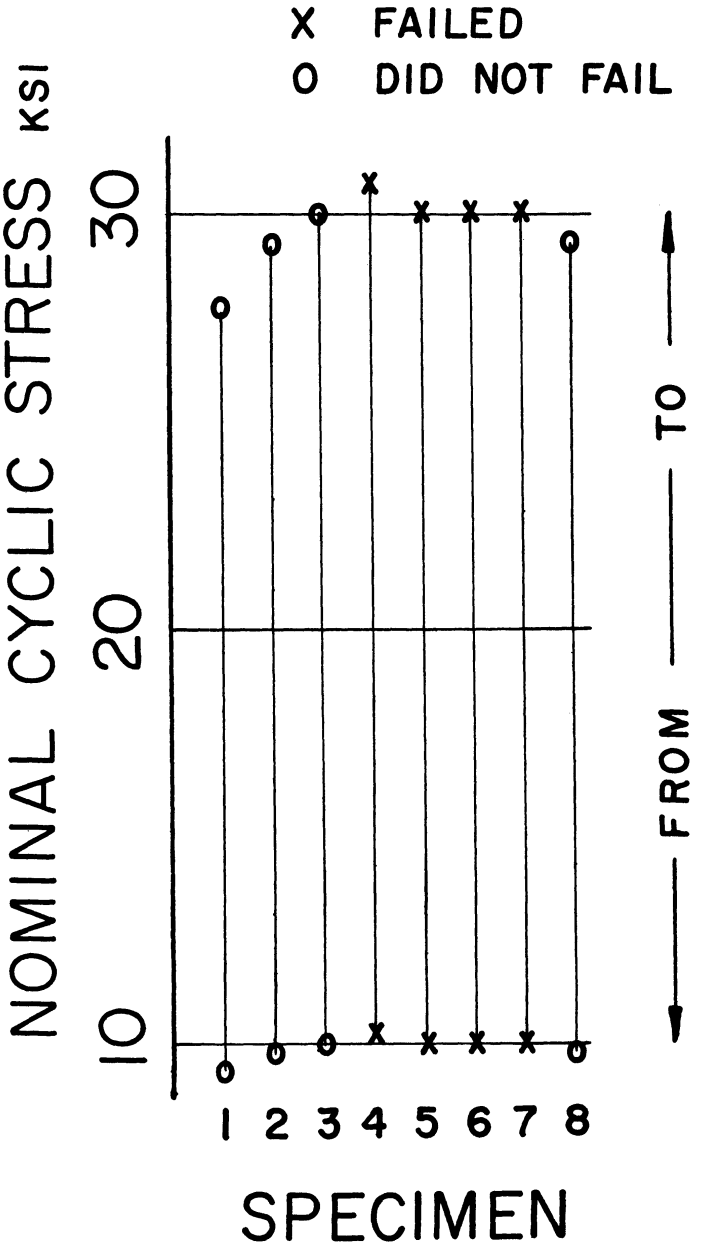

Figure 6.2 Limiting safe range of stress. Plot of data listed in Table 5.3 which pertains to a stress ratio of .33.

while the probability of obtaining 3 failures in 4 tests is .25. Hence, the "3 and 1" distribution found in these test results cannot be interpreted as indicating a range of stress significantly different than 20,000 psi nominal.)

Because the number of cycles endured by the broken specimens is larger than 2,500,000 but less than 10,000,000. the knee of the S-N curve can be presumed to occur in this range. Hence, the specimens that endured more than 10,000,000 cycles without failing can be used to determine the fatigue limits.

Figures 6.1 and 6.2 show that the fatigue limit is 10,000 psi nominal for both nominal mean stresses of 10,000 psi and 20,000 psi. In other words, these fatigue limits are identical.

A high degree of confidence can be placed in these results because eight to ten "infinite life" specimens were used to establish these values and because the scatter in the data is very small.

Fracture Appearance

The lack of pronounced scatter is evident in the fracture appearance. The fractures are so similar that it is difficult to tell one broken specimen from another (for a given mean stress).

The specimens tested with a mean stress of 10,000 psi nominal displayed fatigue cracks on each side of the hole. See Figure 5.1.

The specimens subjected to a nominal mean stress of 20,000 psi displayed only one fatigue crack. See Figure 5.2. In each series of tests, an equal number of specimens failed on each side of the hole with reference to the orientation of the specimen in the machine. This can be adduced as evidence of a lack of marked mal-alignment during testing.

The difference in fracture appearance from the lower mean stress level to the higher one is in accord with the basic understanding of crack propagation. The general notion is that the rate of crack propagation depends, at least in part, on the level of available energy on which the cracks draws for its growth. It appears that the available energy for the higher mean stress was sufficient to accelerate crack growth so much that no other significant crack had time to form.

It is quite certain that no significant crack occurred on the side of the hole opposite to the fatigue crack in Figure 5.2. When this type of failure took place, considerable plastic elongation including a small amount of necking occurred at the uncracked side of the hole due to the high maximum stress imposed on these specimens. Yet, no fatigue cracks of any length were visible in this area for any of these specimens.

In all cases the crack grew directly across the minimum section as shown in Figures 5.1 and 5.2. The deviation from the transverse center-line, within three-quarters of an inch of the edge of the hole, is less than one-sixteenth of an inch. While it can be shown analytically that the stress distribution within one-eighth of an inch of the center-line is very uniform, the fatigue cracks formed in a much narrower region. In contrast to the fatigue behavior, Piobert-Luders' bands formed in an apparently random manner in a region about one-quarter of an inch wide--verifying the uniformity of the stress distribution in the vicinity of the center-line.

The surface of a typical fatigue crack is not "silky" and no "beach-marks" are noticeable. No evidence of inclusions or flaws can be found on the surface or the edges of these cracks. Hence, it is not possible to discern where the cracks originated by examination of the fracture surface. It is not known at present whether or not the fatigue cracks originated in or at the boundary of Piobert-Luders' bands. (Attempts to locate the Piobert-Luders' bands with respect to the crack by etching techniques have not been successful).

Crack Orientation

The surface of a typical fatigue crack near the edge of the hole forms a plane which is tilted about five to ten degrees to a plane normal to the surface of the specimen. This plane is more closely associated with the plane of maximum normal stress than with the plane of maximum shear stress. However, the surfaces of some cracks are inclined up to thirty degrees with this normal plane in areas approximately one inch or more away from the holes.

Localized Yielding

The static tests show that yielding, in terms of gross plastic flow, does not occur immediately after the calculated stress reaches the yield strength. The measured strain exceeds the yield point strain by 25 to 50 per cent before prominant permanent elongation is noticeable. Close examination of the stress-strain curves show that they become slightly non-linear at approximately the yield strength and this may indicate that "restrained yielding" takes place. In other words, it is possible that this material has "yielded", but is restrained from

movement by the neighboring material which is still elastic and which still follows a definite stress-strain relationship. In addition, the deviation from the linear stress-strain relationship is time-dependent at the higher stress levels in this range of stress. Thus, this phenomena is anelastic as well as inelastic.

Since fatigue tests are usually conducted at a minimum speed of 900 CPM, this anelastic behavior is probably not very important. However, the inelastic behavior is quite important because it leads to fatigue.

Because it was observed that gross plastic flow does not occur when the calculated stress reaches the yield strength, the traditional analysis of overstrain should be modified to agree with test results. This is shown in Figure 6.3. In this model, it is assumed that the loading cycle is from zero to a maximum and that yielding, in terms of gross plastic flow, takes place upon loading to the maximum value during the first cycle. Unloading is assumed to take place elastically; consequently, this model predicts the residual stress distribution shown. This residual stress distribution is then superimposed on the original elastic stress distributions during continued cyclic loading.

Thus, the modified model shows that the local mean stress (the actual mean stress at the edge of the hole) is changed by gross plastic flow, but that the magnitude of the alternating stress is not affected because it is assumed that the alternating component of stress unloads elastically from the (constant) local yield strength. Further, it can be seen that increasing the nominal mean stress beyond that corresponding to gross localized plastic flow results in a constant

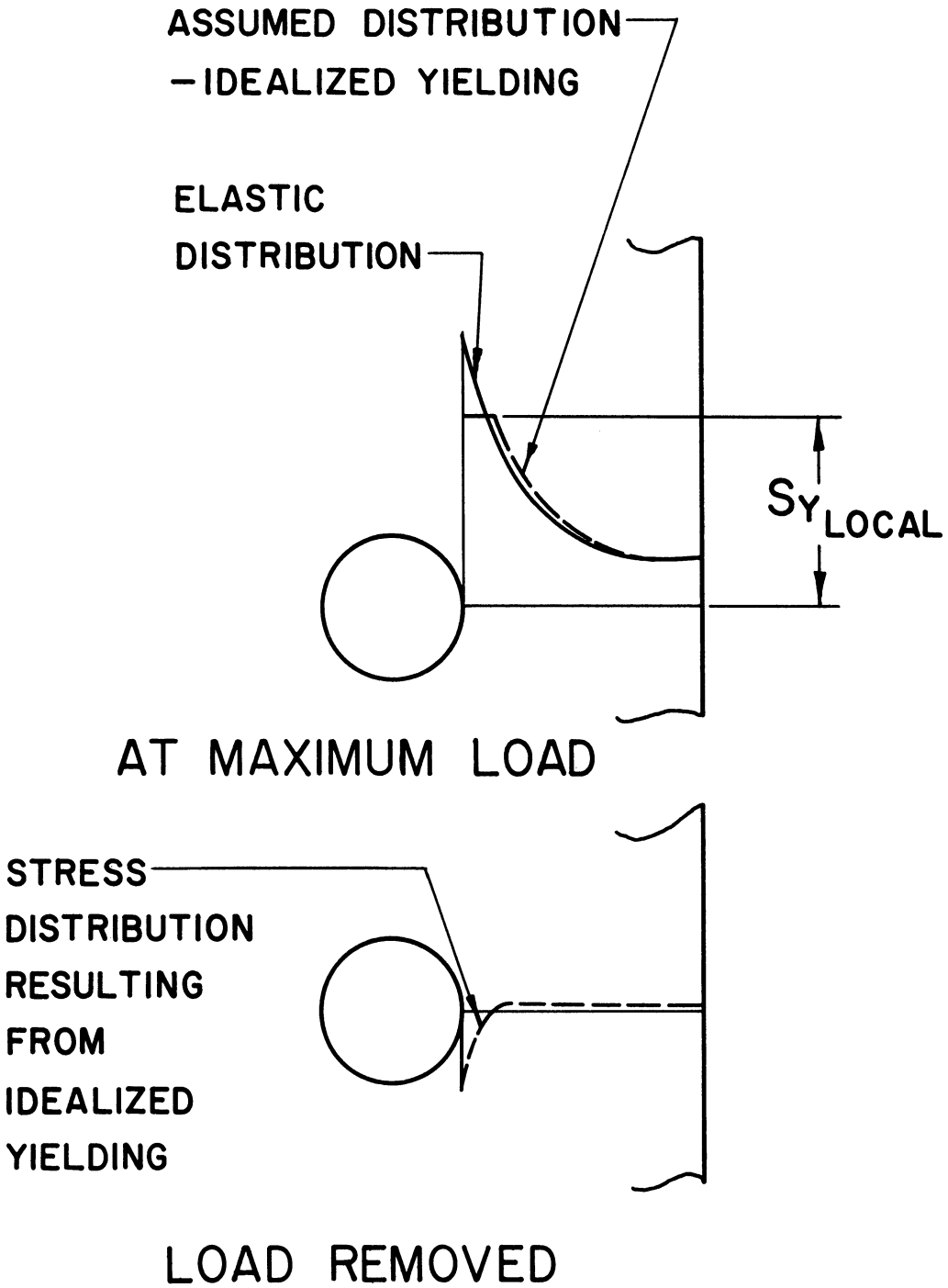

Figure 6.3 Modified ideal yielding model. Often referred to as an "overstrain" model.

value of the local mean stress (which equals the local yield strength minus the amplitude of the local alternating stress).

As can be discerned from the static test results of Chapter V, this modified model is idealized and does not correspond precisely to the observed behavior under cyclic loading. Unfortunately, not enough is known about localized yielding to permit the rationalization of a more elaborate model: hundreds of studies of static yielding under a non-uniform stress distribution have not produced a firm understanding of this phenomenon. In general, the macroscopic approach (extensometers and strain gages) indicates an increased local yield strength[126-131], while the microscopic (X-ray) tests indicate the same or a reduced "local" yield strength.[132-136] To further complicate the issue, there may be a "skin effect" involved in localized yielding.[137]

Present analytical methods of dealing with static localized yielding are limited in scope and are quite idealized.[138-140] Consequently, the development of a sophisticated model for localized yielding under cyclic loading is stimied by the difficulty in developing the requisite model for static loading.

Range of Local Strain

The calculated range of strain at the edge of the hole, based on the nominal stress, the geometric stress concentration factor and the initial value of Young's Modulus, is 1780 microinches per inch for a range of stress of 20,000 psi nominal stress. This calculated value agrees with the measured value within 3 per cent for the lower value of mean stress, see Table 6.1. However, the measured range of strain

is approximately 7 to 10 per cent higher than the calculated value for the higher value of mean stress.

The measured values show that, for small initial plastic strains, the elastic bulk governs the range of strain at the edge of the hole. However, for large initial plastic strains, the influence of the elastic bulk is not as pronounced and the strain concentration factor is increased slightly.

The range of strain is relatively constant following initial plastic flow. This range is approximately the same for the virgin specimen after a few cycles as for the fatigue specimen after 15 to 30 million cycles.

TABLE 6.1

Range of local strain. Strain measured by means of foil strain gages mounted directly on the inside surfaces of the hole (on the transverse center-line).

Specimen	Nominal Stress Cycle in ksi.	Range of Strain at edge of the hole in micro-inches/inch. RH	LH	Remarks Range measured after N cycles.
Virgin	0 - 20	1795	1810	10
		1795	1805	10,000
		1795	1825	100,000
Fatigue	0 - 20	1730	1735	5 (10×10^6 prior)
Virgin	10 - 30	1910	1990	10
		1925	----	100,000
Fatigue	10 - 30	1870	1925	5 (30×10^6 prior)

Strain Redistribution

The relationship between the mean strain at the edge of the hole and the mean strain in the elastic bulk undergoes a change during cyclic loading. The mean strain at the edge of the hole shows a marked increase during the first 100,000 stress cycles while no significant change occurs in the elastic bulk. This increase is approximately 150 to 200 micro-inches per inch at 10,000 psi nominal mean stress and approximately 300 micro-inches per inch at 20,000 psi nominal mean stress. Hence, the maximum and the minimum strain increase noticeably; but, as previously mentioned, the range of strain is approximately constant. This change can be seen in Figure 5.7.

The hysteresis loop is stable for the fatigue specimens as near as can be discerned. However, if these specimens are overloaded with respect to this hysteresis loop, then strain redistribution results again. The fatigue specimen which had been stressed from approximately zero to 20,000 psi nominal stress in both the static and fatigue tests displayed strain redistribution following one very slow cycle of stress from zero to 23,000 psi nominal. Large localized plastic strain occurred at 23,000 psi nominal stress: the corresponding local yield strength of the virgin specimen is estimated at 20,500 psi nominal . The fatigue specimen which had been stressed between 9,750 and 29,250 psi nominal stress displayed a small amount of stress redistribution under very slow loading between 10,000 and 30,000 psi nominal stress. Although gross plastic flow did not take place at the edge of the hole upon initial loading during this static test, the nominal stress-local strain curve is non-linear at the higher stress levels. This resulted in approximately

300 micro-inches per inch plastic strain upon unloading to the 10,000 psi nominal stress value. It is very likely that this specimen had undergone localized yielding in compression due to the Bauschinger effect when it was unloaded following the completion of the fatigue test and that this plastic flow destroyed the stability of the hysteresis loop. Thus, the observed strain redistribution probably results as a consequence of the specimen being unloaded between the fatigue and static tests and not as a consequence of continued redistribution under cyclic loading.

While the above uncertainty could have been avoided by mounting the strain gages on the specimen when it was still under load in the machine, this procedure is very difficult in that a temperature curing epoxy cement should be used in this situation. This problem was not pursued further because it is secondary to the principal objective of this particular test: platen level measurements and strain measurements in the elastic portion of this specimen show clearly that the over-all length of the specimen does not gradually increase under continued cyclic loading even though the average stress on the minimum cross sectional area is almost 90 per cent of the static yield strength.

Width of Hysteresis Loops

Table 6.2 lists the widths of the hysteresis loops at the edges of the hole measured at the mean stress level. These values correspond directly to the ranges of strain listed in Table 6.1.

TABLE 6.2

Width of hysteresis loop. See Table 6.1 for corresponding range of strain.

Specimen	Nominal Stress Cycle in ksi.	Width of "Average"* Hysteresis Loop at edge of the hole in micro-inches/inch. RH	LH	Remarks Average width measured after N cycles.
Virgin	0 - 20	27	36	10
		26	40	10,000
		33	48	100,000
Fatigue	0 - 20	55	30	5 (10×10^6 prior)
Virgin	10 - 30	92	103	10
		103	---	100,000
Fatigue	10 - 30	77	102	5 (30×10^6 prior)

* These values are the average value for 3 to 5 loops: the number of cycles cited under Remarks is the mean value for the loops considered.

It was found that large initial plastic flow increased the widths of the hysteresis loops in a marked manner ... by a factor of two or three. Yet, this increase has no apparent effect on the fatigue limit.

These data show that extensive localized inelastic behavior can take place without leading to fatigue failure. In particular, these data indicate that approaches of correlating the fatigue limit to the energy associated with the hysteresis loops are not valid for localized deformation at these stress levels.

Fatigue Model

Vitovec[74] has pointed out about fifteen well-established experimental observations that are neither explained or considered by most fatigue theories and models. Among the more basic objections to fatigue models are the observations that slip occurs below the fatigue limit, that fatigue starts primarily at the surface and the surface is inherently weaker that the interior material, that internal stresses are produced by fatigue stressing, that the first fatigue crack produced need not cause failure, and that stress gradients appear to influence the fatigue strength markedly. These general objections can be supplemented for any particular case: for the specimen studied here, this investigation has shown that the strain distribution changes under cyclic loading, that the local yield strength increases noticeably, and that the fracture appearance is stress-level dependent.

Yet, the need for a working fatigue model is most apparent.

At present, there is only one quantitative approach to the development of a working fatigue model: a macroscopic approach which deals with fatigue in terms of an idealized view of the actual material behavior. Unfortunately, the microscopic approach which deals with the real mechanisms of material behavior presently gives qualitative rather than quantitative correlations. Therefore, a macroscopic model must be used in the analysis of fatigue data.

Fatigue data can be analyzed by using the elastic working stress diagram of Figure 3.2 in conjunction with the modified elastic approach of treating notched specimens and with the modified ideal

yielding model of Figure 6.3. The modified ideal yielding model shows that, following initial localized yielding at the root of the notch, the local mean stress is constant and independent of the nominal mean stress. Furthermore, the amplitude of the alternating stress is not affected by localized yielding for reasonable values of the geometric stress concentration factor. Hence, the fatigue limit is not affected by further increases in the nominal mean stress beyond the particular mean stress level which first leads to localized yielding. This analysis will be illustrated in the next section.

The physical reasoning behind this model deviates somewhat from the reasoning based on idealized material behavior. As fatigue physically results from reversed slip, the critical factor involved should be one which affects the range of strain in a significant manner. However, the static tests conducted in this study indicate that the range of strain at the edge of the hole is approximately the same for all tensile mean stress levels, that is, the large elastic bulk dominates the small plastic volume and thus controls the range of strain. Therefore, the equal fatigue limits found in this study probably come about through the balancing of two opposing secondary effects. The mean strain level increases the maximum strain level and hence promotes minute inelastic behavior tending to lead to fatigue failure. On the other hand, localized plastic flow leads to localized strain hardening which tends to increase the fatigue limit. Thus, following localized plastic flow, the nominal mean stress usually has no further significant effect on fatigue within the realm of practical fatigue deformations.

Elastic Working Stress Diagrams

The elastic working stress diagram can be used to calculate the fatigue results as outlined below.

The fatigue limit (zero mean stress) for 1008 steel is approximately sixty per cent of the ultimate strength.[3,26,81] Since the ultimate strength is 47,500 psi, the fatigue limit is approximately 28,500 psi. The fatigue strength reduction factor is approximately 2.4. (The stress concentration factor is calculated as 2.55 and measured as 2.54. The notch sensitivity of this material and size of notch gives a notch sensitivity of approximately 0.90[16,141]). Hence, the fatigue limit (zero mean stress) for the notched specimen is approximately 12,000 psi nominal. See Figure 6.4.

The failure locus for notched specimens in the fatigue-limited range of stress is developed using the modified elastic approach discussed in Chapter II. This locus is extended to the level of maximum cyclic stress which first induces gross plastic flow at the root of the notch. However, as this level varies for different notches as well as for different specimens with the same notch, the maximum test value of 1.5 is used in order to be slightly conservative. (This value of 1.5 is suggested by Nakanishi[142] for localized yielding under non-uniform stress distributions.) The locus then becomes parallel to the S_m coordinate line, that is, the locus follows a line depicting a constant value of alternating stress.

Comparison of Approach to Published Data

Figure 6.5 shows this approach compared to typical data given by Grover, Bishop, and Jackson.[43] These data pertain to

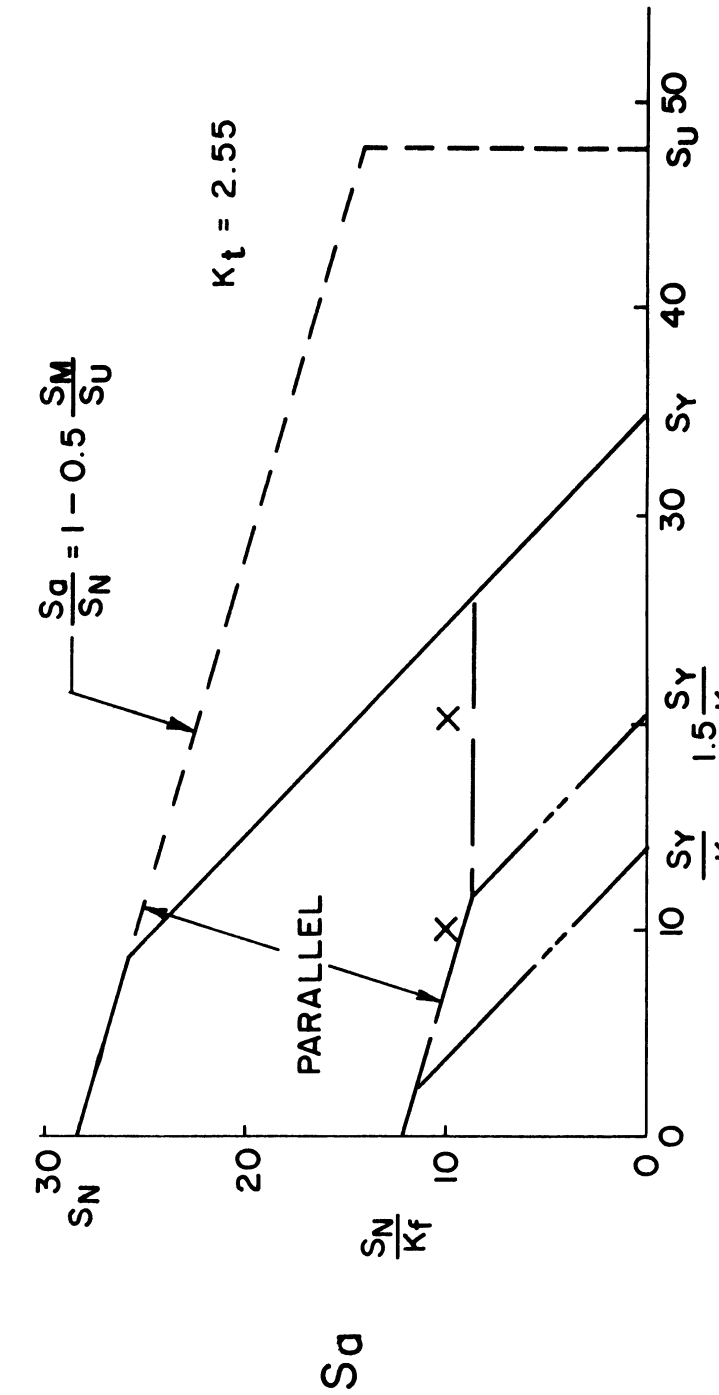

Figure 6.4 Fatigue test results. The predicted locus is slightly conservative: data corresponds to localized yielding at approximately 1.25 S_y. (Strengths in ksi.)

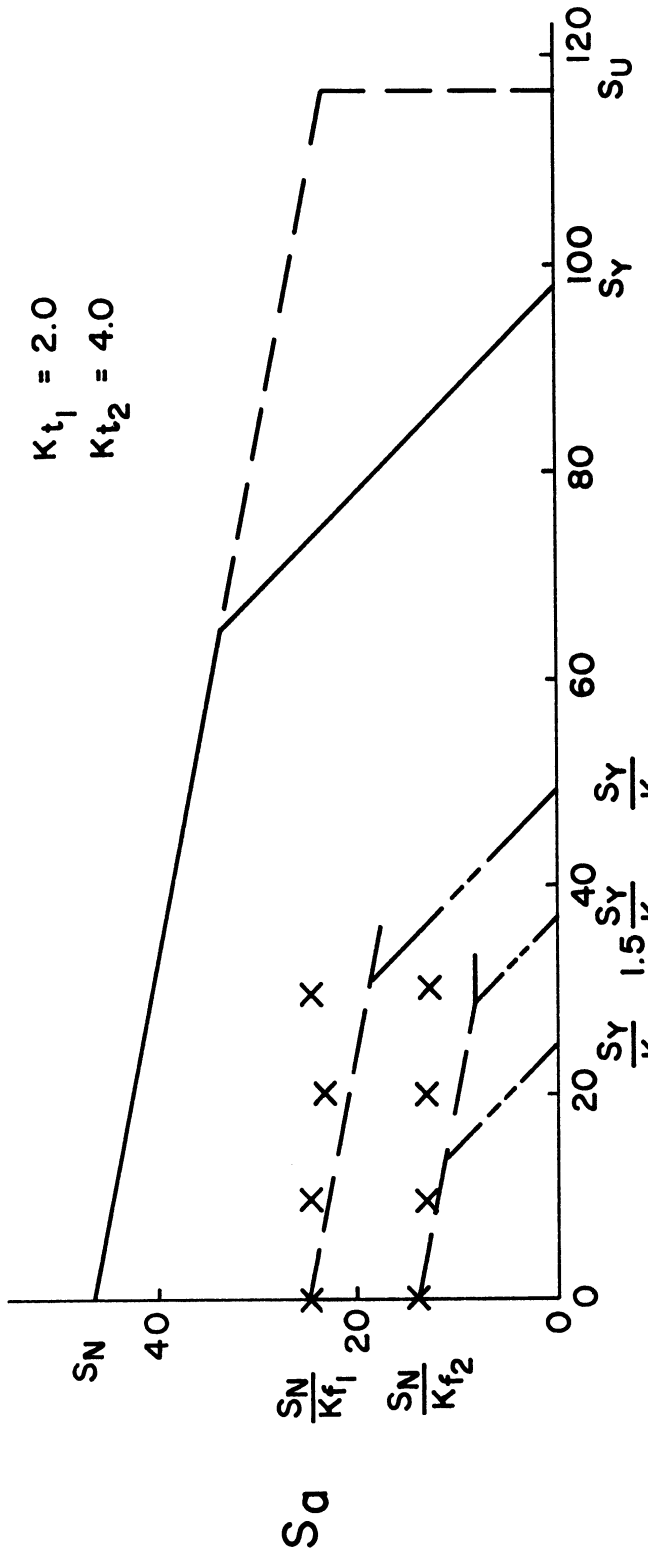

Figure 6.5 Comparison of predicted locus to published data. Reference 43. (Strengths in ksi.)

thin sheet specimens which were restrained from buckling by guides. Because no other axial mean stress test has given fatigue limits for tensile mean stresses larger than the fully reversed fatigue limit, it is likely that use of the guides resulted in somewhat low values for these fully reversed strengths. Hence, the agreement is probably better than it appears in this diagram. (A central hole was used to obtain $K_t = 2.0$ and edge notches were used to obtain $K_t = 4.0$. Other data by these investigators give about the same agreement).

Figure 6.6 shows data by Fitchie.[48] Unfortunately, these data do not pertain to mean stress levels sufficiently high to illustrate the influence of localized plastic strain. As illustrated in this diagram, the local yield strength should be estimated nearer the nominal yield strength for smaller stress concentration factors.

Figure 6.7 shows data by Trapp and Schwartz.[45] (While the point which corresponds to a maximum cyclic stress exceeding the static yield strength can be predicted accurately by using the Neuber "technical" stress concentration factor to estimate the local yield strength, this is not shown in Figure 6.7 because this particular datum point is of dubious practical value.)

Figure 6.8 shows bending data by Findley, Mergen and Rosenberg.[143] Because the radius of the circumferential V-groove is .01 inch, the Neuber[144] "technical" factor may be more appropriate for use in estimating the level at which gross plastic flow takes place. Use of this factor gives slightly better agreement than shown in Figure 6.8. The corresponding data for torsion are predicted almost

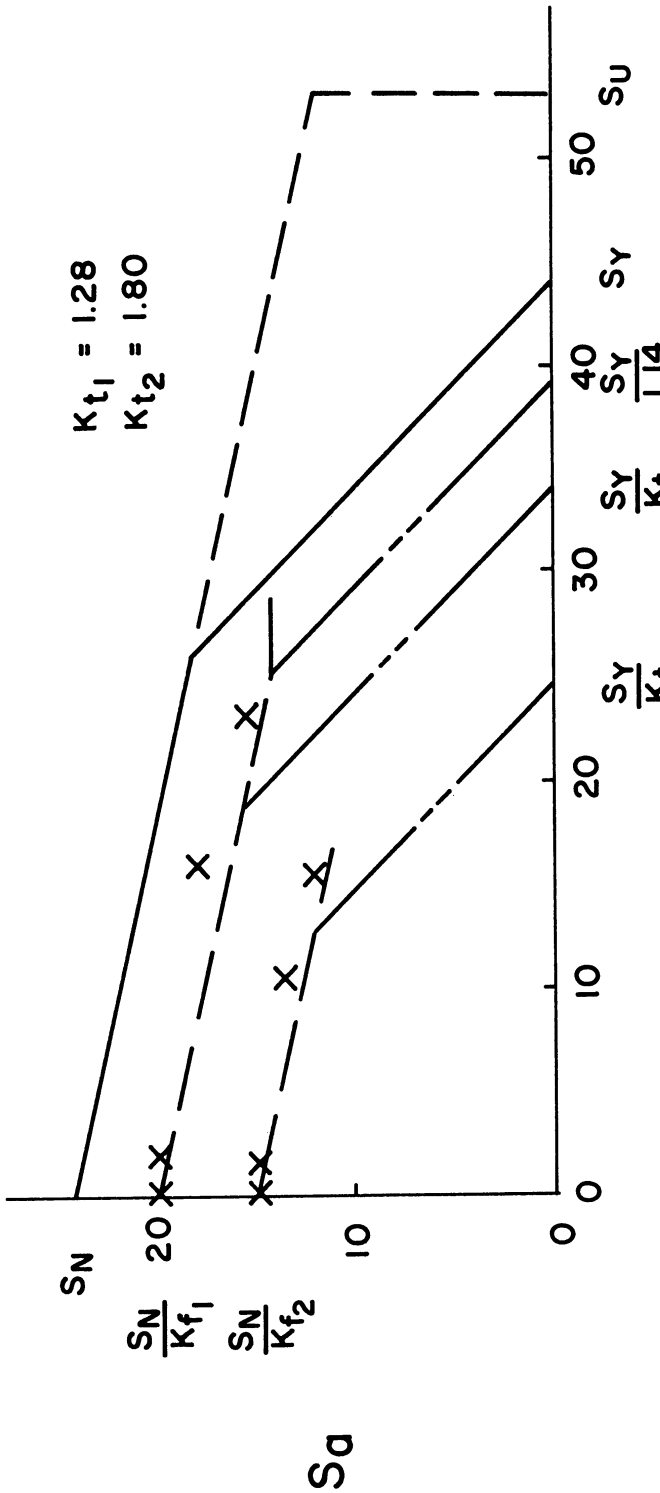

Figure 6.6 Comparison of predicted locus to published data. Reference 48. For small stress concentration factors, the local yield strength is nearer the nominal yield strength. (Strengths in tons/in^2 = 2240 psi.)

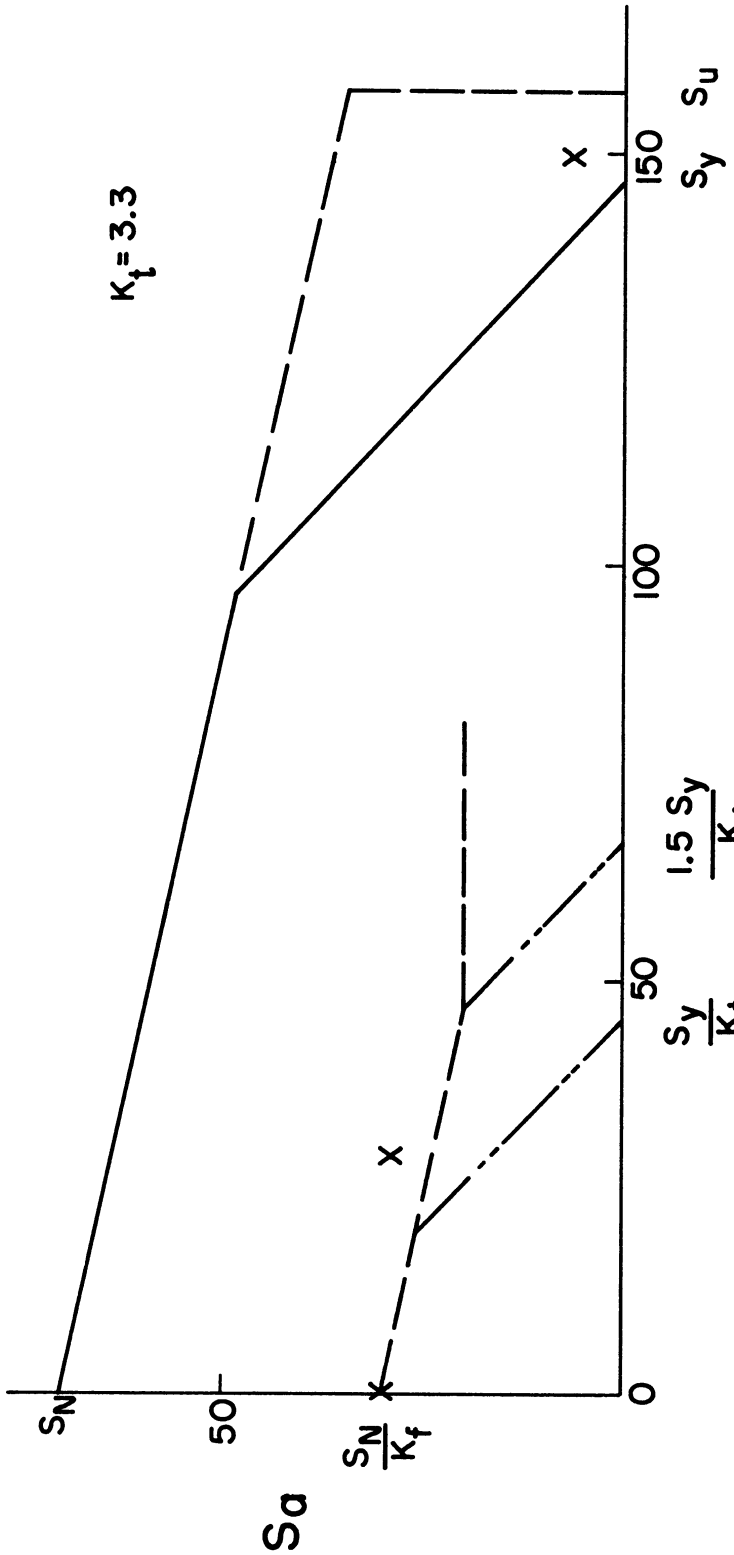

Figure 6.7 Comparison of predicted locus to published data. Reference 45. (Strengths in ksi.)

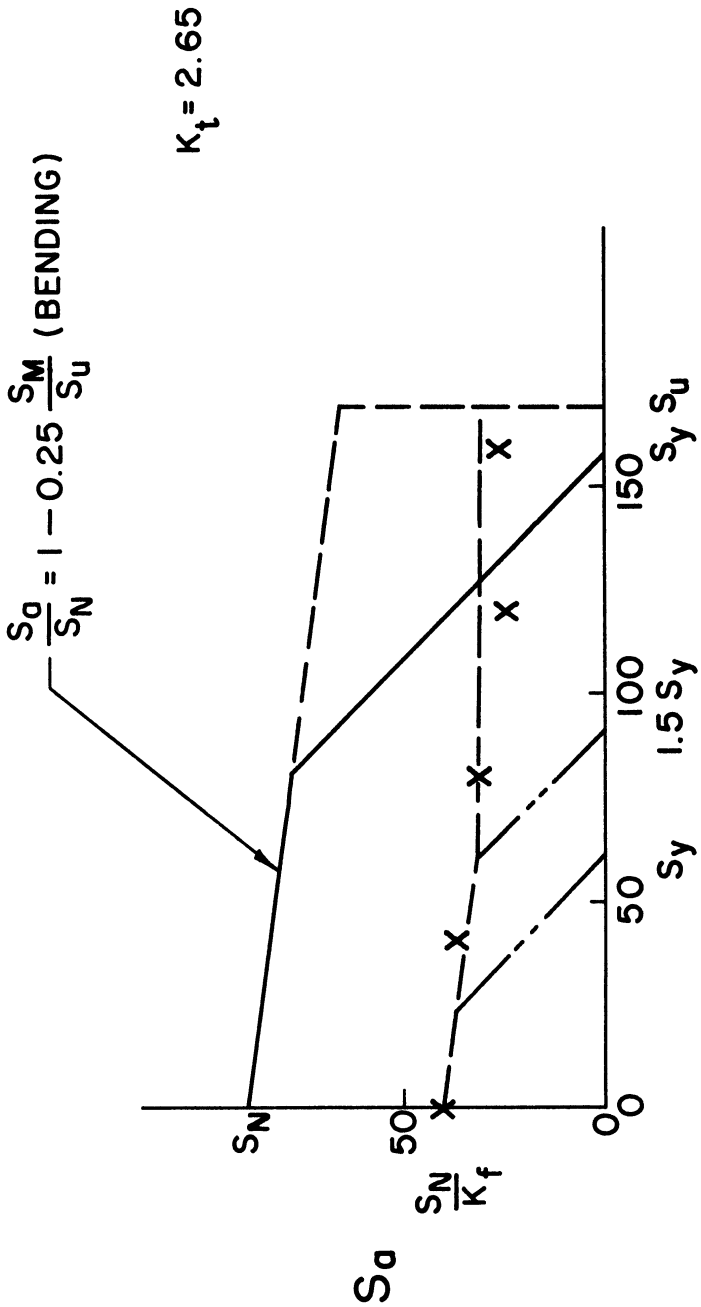

Figure 6.8 Comparison of predicted locus to published data. Reference 143. The effect of mean stress on bending is less than the effect on axial loading. (Strengths in ksi.)

precisely by the elastic working stress diagram. See Figure 6.9.

The data by Gough and Clenshaw[145], Pomp and Hempel[13,23], Smith[146], Buchmann[147], Graf[148], Nisihara and Sakurai[54], Bollenrath and Cornelius[55], and Ros[58] show agreement with the elastic diagram similar to that shown in Figures 6.4 through 6.8.

In the over-all, the horizontal line corresponding to localized yielding at 1.5 times the yield strength fits the data better than any other value when the stress concentration factor is about 1.8 or larger. This value should be lowered, however, when the geometric stress concentration factor is less than 1.5.

Summary

Fatigue tests on notched mild steel specimens show that the fatigue limit is not affected by changes in the nominal mean stress level above the level at which local plastic flow at the root of the notch first takes place. The local initial plastic strain reached a maximum value of approximately two and one-half per cent during these tests. This value is sufficiently high to treat all practical data.

This influence of local plastic flow on mean stress fatigue tests can be explained qualitatively by the traditional ideal yielding model. However, the ideal yielding model used here is modified to agree with the results of ancillary static tests. Application of the modified model to the elastic working stress diagram developed here gives quantitative agreement with the fatigue data. Furthermore, this approach agrees with the results of published mean stress studies on notched specimens under axial, bending, or torsional loading.

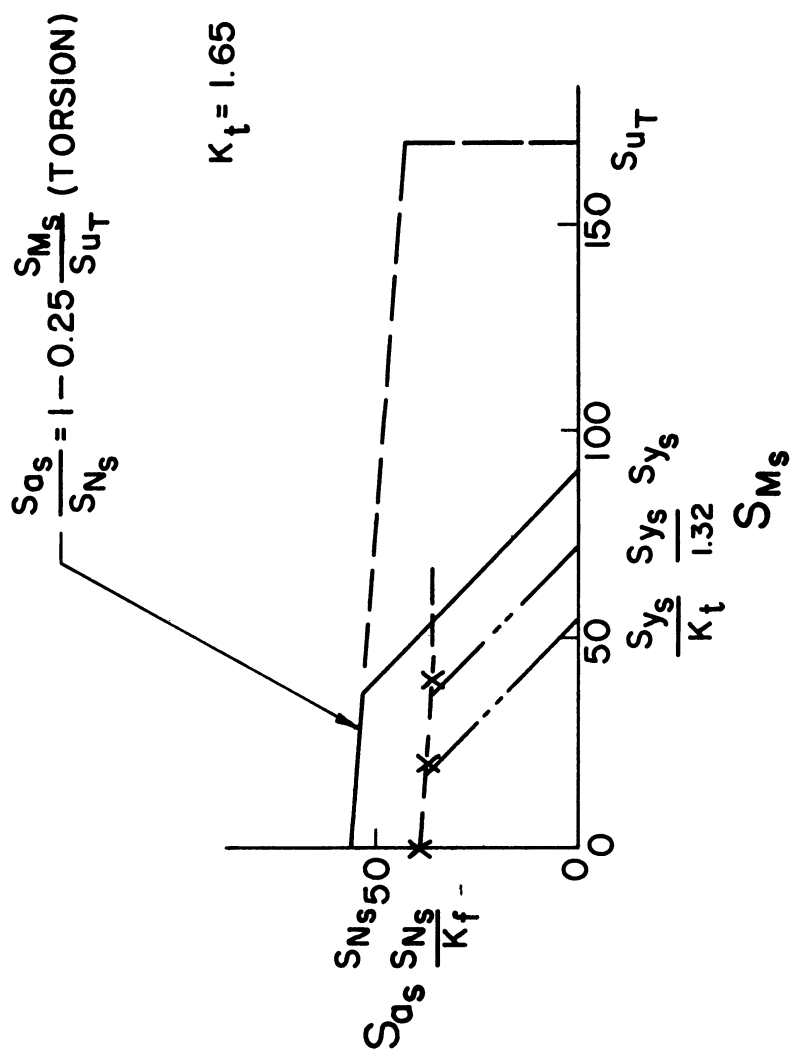

Figure 6.9 Comparison of predicted locus to published data. Reference 143. The effect of mean stress on torsion is less than the effect on axial loading. (Strengths in ksi.)

However, the modified ideal yielding model used here is too simplified to treat adequately several observed secondary factors and must be viewed as a "working" model. Further study is required to develop a "theoretical model" to explain the influence of mean stress on the observed changes in the local strain distribution, in the local static strength, and in the fracture appearance.

APPENDIX A

TERMINOLOGY

The order of presentation of these terms deviates somewhat from the presentation in the text in order to introduce more continuity into an independent review of this tabulation.

Term	Symbol	Meaning
Nominal Stress	S	The stress calculated on the minimum cross-section by simple theory such as $S = P/A$ or $S = Mc/I$ or $S_s = Tc/J$ without considering the increase in stress caused by geometric discontinuities.
Cyclic Stress	-	A general term applied to any nominal stress-time function which fluctuates periodically between fixed maximum and minimum values. In calculating cyclic stresses, it is generally assumed that static calculations represent reasonable approximations.
Maximum Stress	S_{max}	The algebraic maximum of the nominal stress in the stress cycle. Tensile stress positive.
Minimum Stress	S_{min}	The algebraic minimum of the nominal stress in the stress cycle. Tensile stress positive.
Range of Stress	S_r	The algebraic difference between the maximum and minimum nominal stress in the stress cycle. $S_r = S_{max} - S_{min}$
Alternating Stress or Variable Stress	S_a	One-half the range of stress. $S_a = S_r/2 = (S_{max} - S_{min})/2$

Term	Symbol	Meaning
Mean Stress or Steady Stress	S_m	The algebraic mean of the maximum and minimum nominal stress in the stress cycle. $S_m = (S_{max} + S_{min})/2$
Stress Ratio	R	The algebraic ratio of the minimum to the maximum nominal stress in the stress cycle. $R = S_{min}/S_{max}$
Stress Cycles Endured	N_e	The number of stress cycles which a fatigue specimen has endured at any stage of the test.
Fatigue Life	N	The number of stress cycles which a fatigue specimen has endured prior to failure.
S-N Curve	-	A plot of the alternating stress versus the fatigue life, developed by testing specimens at several alternating stress levels. The subscript "a" is dropped for simplicity.
Fatigue Strength	S_{n_N}	The amplitude of the alternating stress which leads to failure at the given fatigue life, N.
Fatigue limit or Endurance Limit	S_n	The limiting amplitude of alternating stress below which mild steel can presumably endure an infinite number of stress cycles. The stress at which the S-N curve becomes approximately horizontal.
Notch	-	A general term applied to all geometric discontinuities (stress concentrators).
Stress Concentration Factor	K_t	The ratio of the greatest stress in the region of a notch to the corresponding nominal stress. Generally stated in terms of principal normal stress ignoring so-called failure theories.

Term	Symbol	Meaning
Fatigue Strength* Reduction Factor	K_f	The ratio of the fatigue strength of an unnotched specimen at some given fatigue life to the fatigue strength of a notched specimen at the same life. It is assumed that all other test conditions are identical and S_m equals zero.
Fatigue Limit* Reduction Factor	K_f	The same as K_f above except that the fatigue limits are compared.
Notch Sensitivity Index	q	An index to measure the degree of agreement between K_t and K_f for a particular notch and material. The fatigue life must be specified when stipulating a value for this index. $q = (K_f - 1)/(K_t - 1)$
Working Stress Diagram	-	A plot of the relationship between the allowable alternating stress (S_a) and any given mean stress (S_m) or a plot of the allowable maximum stress (S_{max}) versus the mean stress (S_m). Unless otherwise indicated, these diagrams pertain to fatigue limits. Strengths are generally used as reference values in plotting these diagrams.
Elastic Working Stress Diagram	-	A working stress diagram which pertains only to fatigue data displaying no permanent deformation prior to failure. (See Chapter II, Deformation Limitations for Unnotched Specimens.)
Local Stress	-	The actual stress at the root of the notch.
Ideal Local Yield Point	(S_y/K_t)	The point on the elastic working stress diagram at which the local maximum cyclic stress equals the conventional static yield strength.
Localized Yielding	-	Localized plastic strain in an area bounded by elastic material and the surface of the specimen.

*For cases when the mean stress is not zero, see Chapter II, K_f for Nonzero Mean Stress Situations.

Term	Symbol	Meaning
Piobert-Luders' Bands	-	A series of "wedges" of plastically deformed material in which the deformation is approximately equal to the yield point elongation. These wedges are bounded by elastic material.
Cyclic Dependent Material Properties	-	Stress-strain (strength) relationships which change under repeated cyclic loading.
Anelastic Behavior	-	Time-dependent behavior.
Inelastic Behavior	-	All non-linear (stress-strain) behavior not overtly anelastic.
Cyclic Stress Sensitivity Limit	-	The stress for cyclic loading which corresponds to the proportional limit for static loading, that is, linear elastic stress-strain behavior below this stress.
Cyclic Strain Sensitivity Limit	-	The same as above except that the test is conducted in terms of strain rather than stress.
Residual Stress	-	Internal stress induced by processing or stress history.

REFERENCES

1. A. Wöhler, Uber die Festigkeitversuche mit Eisen und Stahl. A series of nine articles based on this report is found in Engineering (London), Volume XI, (1871), pages 199, 221, 244, 261, 299, 327, 349, 397 and 439. In addition, a discussion of Herr Wöhler's fatigue exhibit at the Paris Exhibition is found in Engineering (London), Volume IV, (1867), page 160.

2. J. Goodman, Mechanics applied to Engineering, Longmans, Green, and Co., London, (1899), page 453.

3. B. P. Haigh, Proceedings, Inst'n Automobile Eng'rs, Volume XXIV, (1929), page 320.

4. C. R. Soderberg, Transactions, American Society of Mechanical Eng'rs, Volume 52, Part 1, Paper APM 52-2, (1930), page 13. See also Handbook of Experimental Stress Analysis, Edited by M. Hetenyi, John Wiley and Sons, New York, Chapter 10, 1950.

5. Manual on Fatigue Testing, Prepared by Committee E-9 on Fatigue, American Society for Testing Materials Special Technical Publication No. 91, Section VI, 1949.

6. F. P. Fischer, Technische Mitteilungen Krupp, Heft 3, (1933), page 67.

7. See H. F. Moore and T. M. Jasper, Bulletin No. 136, Eng'g Experiment Station, University of Illinois, Urbana, Illinois, 1923. See also J. M. Lessells, Strength and Resistance of Metals, John Wiley and Sons, New York, Chapter 6, 1954.

8. T. Nishihara and T. Sakurai, Transactions, Society of Mechanical Eng'rs, Japan, Volume 5, (1939), page 93. Text in Japanese: English abstract page S-8. See also T. Nishihara and K. Endo, Technical Reports Eng'g Research Inst'e. Kyoto University, Volume II, (1952), page 171.

9. W. Gerber, Zeitschrift für des Bayerischen (Bavarian) Architekt und Ingenieur Vereins, 1874. See J. M. Lessells, Reference 7.

10. G. Sines, Technical Note 3495, U. S. National Advisory Committee for Aeronautics, 1955.

11. E. Orowan, Proceedings, Royal Society, London, Series A, Volume 171, (1939), page 79. An excellent discussion or Orowan's theory is given by J. A. Pope, Metal Fatigue, Chapman and Hall Ltd, London, (1959), pages 7 and 15.

12. J. O. Smith, Bulletin No. 334, Eng'g Experiment Station, University of Illinois, Urbana, Illinois, 1942.

13. A. Pomp and M. Hempel, Mitteilungen, Kaiser-Wilhelm-Institut Eisenforschung, Band XVIII, (1936), page 205. For the original data, see Band XVIII, (1936), page 1.

14. R. E. Peterson, Failure of Machine Parts, Prevention and Cure, Edited by R. Evaldson and C. Lipson, College of Eng'g, University of Michigan, Ann Arbor, Michigan, Session 2, 1955. For more comprehensive treatment, see Fatigue and Fracture of Metals, Edited by W. M. Murray, John Wiley and Sons, New York, Paper 4, (1952), page 74.

15. K. W. Gunn, Aeronautical Quarterly, Volume 6, (1955), page 277. This very interesting work is closely associated with the following references: B. P. Haigh, Reference 3; G. Fischer, Jahrbuch, der deutschen Luftfahrtforschung, (1938), page I-517; M. S. Paterson, The Failure of Metals by Fatigue, Proceedings of University of Melbourne Symposium, Melbourne University Press, Melbourne, Australia, Chapter 19, 1947; A. R. Woodward, K. W. Gunn and G. Forrest, Proceedings, International Conference on Fatigue of Metals, IME:ASME, London: New York, (1956), page 158; J. A. Pope, Reference 11, pages 82 and 203.

16. R. B. Heywood, Designing Against Fatigue, Chapman and Hall Ltd, London, (1962), page 38.

17. F. B. Stulen and H. N. Cummings, Proceedings, American Society for Testing Materials, Volume 54, (1954), page 822.

18. H. Kitagawa and T. Morohashi, Proceedings, 10th Japan National Congress for Applied Mechanics, (1960), page 155.

19. T. Yokobori, Proceedings, 1st Japan National Congress for Applied Mechanics, (1951), page 97.

20. F. Nakanishi, see Proceedings, 1st Japan National Congress for Applied Mechanics, (1951), page 107. See also Proceedings, 3rd Japan National Congress for Applied Mechanics, (1953), page 173.

21. H. J. Grover, Proceedings, International Conference on Fatigue of Metals IME:ASME, London: New York, (1956), page 85. See also B. J. Lazan and A. A. Blatherwick, Proceedings, American Society for Testing Materials, Volume 53, (1953), page 856 and Discussion page 870.

22. H. C. O'Connor and J. L. M. Morrison, Proceedings, International Conference on Fatigue of Metals, IME:ASME, London: New York, (1956), page 102.

23. A. Pomp and M. Hempel, Mitteilungen, Kaiser-Wilhelm-Institut Eisenforschung, Band XVIII, (1936), page 1.

24. H. J. Gough and W. A. Wood, Proceedings, Inst'n Mechanical Eng'rs, Volume 141, (1939), page 175.

25. F. W. Thorne, Proceedings, Inst'n Automobile Eng'rs, Volume XXIV, (1929), page 345.

26. R. Cazaud, La Fatigue des Metaux, Troisieme Edition, Dunod, Paris, (1948), page 250.

27. W. Herold, Die Wechselfestigkeit Metallischer Werkstoffe, Julius Springer, Wien, (1934), page 155.

28. J. G. Owen, Proceedings, Inst'n Mechanical Eng'rs, Volume 168, (1954), page 793.

29. See H. Tauscher, Berechnung der Dauerfestigkeit Einfluss von Werkstoff und Gestalt, Siebente verbesserte Auflange, VEB Fachbuchverlag, Leipzig, Section 15, 1961. See also Maschinteile, Teil 1, Edited by G. Köhler and H. Rögnitz, B. G. Teubner Verlagsgesellschaft, Stuttgart, Chapter 1, 1960.

30. J. H. Smith, Journal, Iron Steel Inst'e, Volume LXXXII, No. II, (1910), page 246.

31. R. M. Brown, Transactions, Inst'n Eng'rs and Shipbuilders Scotland, Volume LXXI, (1929), page 495.

32. H. J. Tapsell, Journal, Iron Steel Inst'e, Volume CXVII, No. I, (1928), page 275.

33. A. Ono, Transactions, Society Mechanical Eng'rs, Japan, Volume 2, (1936), page 457. See Japanese Journal of Eng'g Abstracts, National Research Council of Japan, Volume XIII, (1937), page 40.

34. B. P. Haigh and T. S. Robertson, Engineering (London), Volume 132, (1931), page 389.

35. L. Bairstow, Phil. Transactions, Royal Society, London, Series A, Volume 210, (1911), page 35.

36. L. C. Lidstrom and B. J. Lazan, Technical Report 56-122, Wright Air Development Center, 1956. See A. A. Blatherwick, Proceedings, Society for Experimental Stress Analysis, Volume XVIII, No. I, (1961), page 128.

37. A. A. Blatherwick and B. K. Olsen, Technical Report 61-451, Aeronautical Systems Division, Office of Technical Services, U. S. Dept Commerce, 1961.

38. M. Kawamoto and K. Nishioka, Transactions, American Society of Mechanical Eng'rs, Volume 77, (1955), page 631.

39. P. G. Forrest, Proceedings, International Conference on Fatigue of Metals, IME:ASME, London: New York, (1956), page 171.

40. B. P. Haigh, see Reference 3.

41. H. F. Moore, Proceedings, American Society for Testing Materials, Volume 33, No. II, (1933), page 362. See also H. F. Moore, N. H. Roy and B. B. Betty, Bulletin No. 244, Eng'g Experiment Station, University of Illinois, Urbana, Illinois, (1932), page 9.

42. M. Hempel and J. Luce, Mitteilungen, Kaiser-Wilhelm-Institut Eisenforschung, Band XXIII, (1941), page 53.

43. H. J. Grover, S. M. Bishop and L. R. Jackson, Technical Note 2324, U. S. National Advisory Committee for Aeronautics, 1951. For closely related work, see Technical Notes 2389 and 2390, 1951; H. J. Grover, W. S. Hyler and L. R. Jackson, Technical Note 2639, U. S. National Advisory Committee for Aeronautics, 1952.

44. B. Taylor, Transactions, Inst'e Marine Eng'rs, Volume LXIV, (1952), page 233.

45. W. J. Trapp and R. T. Schwartz, Proceedings, American Society for Testing Materials, Volume 53, (1953), page 825.

46. T. T. Oberg and E. J. Ward, Technical Report 53-256, Wright Air Development Center, 1953.

47. W. N. Findley, Proceedings, American Society for Testing Materials, Volume 54, (1954), page 836.

48. J. W. Fitchie, Proceedings, Inst'n Mechanical Eng'rs, Volume 169, (1955), page 331.

49. J. Morrow and G. M. Sinclair, see Symposium on Basic Mechanisms of Fatigue, American Society for Testing Materials Special Technical Publication No. 237, (1958), page 83.

50. F. C. Lea and H. P. Budgen, Reports and Memoranda No. 920, Great Britian Aeronautical Research Committee, 1924. See also Engineering (London), Volume CXX, (1924), pages 500 and 532; Engineering (London), Volume CXXII, (1926), page 242.

51. E. Houdremont and H. Bennek, Stahl und Eisen, Jahrgang 52, (1932), page 653. Cite data by Schenck, page 660.

52. R. B. Heywood, Designing Against Fatigue, Chapman and Hall Ltd, London, (1962), page 14. Cite data by C. F. Simpkin and W. J. Taylor. Apparently these data are the data referred to by H. Sutton, who cite data by W. D. Douglas, W. J. Taylor and G. F. Simpkin: see The Failure of Metals by Fatigue, Proceedings of University of Melbourne Symposium, Melbourne University Press, Melbourne, Australia, Chapter 4, (1947), page 42.

53. T. Nisihara and T. Sakurai, Transactions, Society of Mechanical Eng'rs, Japan, Volume 2, (1936), page 436. Text in Japanese: English abstract page S-115.

54. F. Bollenrath and H. Cornelius, Jahrbuch, der deutschen Luftfahrtforschung, (1938), page I-549. See also Zeitschrift, Vereins Deutscher Ingenieure, Band 84, (1940), page 407.

55. T. Koiwa and Y. Tada, Journal, Society Naval Arch, Japan, Volume 66, (1940), page 237. See Japanese Journal of Eng'g Abstracts, National Research Council of Japan, Volume XVII, (1941), page 51.

56. R. Wasmuht, Der Stahlbau, Beilage zur Zeitschrift, Die Bautechnik, Jahrgang 14, (1941), page 69.

57. M. Hempel and H. Krug, Mitteilungen, Kaiser-Wilhelm-Institut Eisenforschung, Band XXIV, (1942), page 71.

58. M. Ros, Memoires, Revue de Metallurgie, la Societe Francaise de Metallurgie, Volume XLVIII, (1951), page 723. See also la metallurgia italiana (Milan), Volume 43, (1951), page 512. Sines, Reference 10, cite these data and lists as a reference: M. Ros and A. Eichinger, Bericht 173, Eidgenössische Materialprufungs- und Versuchsanstalt für Industrie, Bauwesen und Gewerbe (Zürich), 1950.

59. J. E. Field, Proceedings, Inst'n Mechanical Eng'rs, Volume 168, (1954), page 795. See also C. E. Phillips and R. B. Heywood, Proceedings, Inst'n Mechanical Eng'rs, Volume 165, (1951), page 113.

60. P. E. Wiene, Transactions, Inst'e Marine Eng'rs, Volume LXVIII, (1956), page 39.

61. J. Marin, P. Borachia and U. A. Rimrott, Proceedings, American Society for Testing Materials, Volume 59, (1959), page 662.

62. A. Pomp and M. Hempel, Mitteilungen, Kaiser-Wilhelm- Institut Eisenforschung, Band XIX, (1937), page 237. See also Band XX, (1938), page 1.

63. H. F. Moore and P. E. Henwood, Bulletin No. 264, Eng'g Experiment Station, University of Illinois, Urbana, Illinois, 1934.

64. S. Luthander and G. Wallgren, Report No. 13, Flygtekniska Försöksanstalten, The Aeronautical Research Inst'e of Sweden, Stockholm, 1945.

65. R. E. Little and C. Lipson, Industry Program Paper, IP-563, University of Michigan, Ann Arbor, Michigan, 1962.

66. S. M. Shelton and W. H. Swanger, Proceedings, American Society for Testing Materials, Volume 33, No. II, (1933), page 348.

67. B. J. Lazan, see Mechanical Behavior of Materials at Elevated Temperatures, McGraw-Hill Book Co., New York, Chapter 15, 1961.

68. B. J. Lazan and T. Wu, Proceedings, American Society for Testing Materials, Volume 51, (1951), page 649.

69. A. A. Blatherwick, see Reference 36.

70. F. Wever and G. Martin, Mitteilungen, Kaiser-Wilhelm-Institut Eisenforschung, Band XXI, (1939), page 213.

71. A. Schaal, Zeitschrift, Metallkunde, Band 36, (1944), page 153.

72. H. Neerfeld and H. Möller, Archiv Eisenhüttenwesen, Jahrgang 20, (1949), page 205. For abstracts, see Stahl und Eisen, Jahrang 68, (1948), page 53, and Jahrgang 69, (1949), page 532.

73. A. Schaal, Zeitschrift, Metallkunde, Band 40, (1949), page 417. See also Zeitschrift, Metallkunde, Band 41, (1950), page 334 and Band 42, (1951), pages 147 and 279.

74. F. H. Vitovec, Technical Report 53-167, Wright Air Development Center, 1953.

75. J. A. Bennett, Proceedings, Society for Experimental Stress Analysis, Volume IX, No. II, (1952), page 105.

76. S. Taira and Y. Murakami, Bulletin, Japan Society Mechanical Eng'rs, Volume 4, (1951), page 41.

77. W. Mason and N. P. Inglis, Reports and Memoranda No. 1126, Great Britian Aeronautical Research Committee, 1927. See also Reports and Memoranda No. 838, 1922.

78. H. J. Gough and H. J. Tapsell, Reports and Memoranda No. 1012, Great Britian Aeronautical Research Committee, 1926.

79. P. H. Frith, Journal, Iron Steel Inst'e, Volume 159, (1948), page 385.

80. P. H. Frith, Proceedings, International Conference on Fatigue of Metals, IME:ASME, London: New York, (1956), page 462.

81. H. J. Gough and H. V. Pollard, Reports and Memoranda No. 2522, Part I, Great Britian Aeronautical Research Council, 1951.

82. L. F. Coffin, Jr., see Internal Stresses and Fatigue in Metals, Elsevier Publishing Co., New York, Section 4.1, 1959.

83. A. C. Low, Proceedings, International Conference on Fatigue of Metals, IME:ASME, London: New York, (1956), page 206.

84. A. Johansson, Colloquium on Fatigue, International Union of Theoretical and Applied Mechanics, Edited by W. Weibull and F. K. G. Odqvist, Springer-Verlag, Berlin, (1956), page 112.

85. L. F. Coffin, Jr. and J. F. Travernelli, Transactions, American Inst'e Mining Metal'l Eng'rs, Volume 215, (1959), page 794.

86. P. P. Benham and H. Ford, Journal, Mechanical Eng'g Science, Volume 2, (1961), page 119.

87. S. R. Valluri, Aerospace Engineering, Volume 20, (Oct. 1961), page 18.

88. R. E. Peterson, Materials Research and Standards, American Society for Testing Materials, Volume 3, No. 2, (Feb. 1963), page 122.

89. T. A. Despres, Unpublished Work, University of Michigan, Ann Arbor, Michigan, 1962-1963.

90. J. A. Ewing and J. C. W. Humfrey, Phil. Transactions, Royal Society, London, Series A, Volume 200, 1902.

91. G. T. Beilby, Proceedings, Royal Society, London, Series A, Volume 79, 1907.

92. W. Rosenhain, An Introduction to the Study of Physical Metallurgy, Second Edition, Constable and Co., London, Chapter XII, 1919.

93. B. P. Haigh, Report British Assoc., see H. J. Gough, Fatigue of Metals, Scott, Greenwood and Son, London, Chapter IV, 1924.

94. A. A. Griffith, Phil. Transactions, Royal Society, London, Series A, Volume 221, 1921.

95. C. F. Jenkin, Proceedings, Royal Society, London, Series A, Volume 103, 1923.

96. H. J. Gough and D. Hanson, Proceedings, Royal Society, London, Series A, Volume 104, 1924. See also H. J. Gough, Cantor Lectures on Fatigue Phenomena, With Special Reference to Single Crystals, Royal Society of Arts, London, Printed by F. J. Parsons, Ltd, Hastings, England, 1928.

97. W. A. Wood, see Fatigue in Aircraft Structures, Academic Press, New York, Chapter 1, 1956.

98. P. J. E. Forsyth, Nature, Volume 171, (1953), page 172.

99. A. H. Cottrell and D. Hull, Proceedings, Royal Society, London, Series A, Volume 242, (1957), page 211.

100. N. F. Mott, Acta Metallurgica, Volume 6, (1958), page 195.

101. W. A. Wood, see Fracture, Edited by B. L. Averbach, D. K. Felbeck, G. T. Hahn and D. A. Thomas, John Wiley and Sons, New York, Chapter 20, 1959.

102. R. D. McCannon and H. M. Rosenberg, Proceedings, Royal Society, London, Series A, Volume 242, (1957), page 203.

103. D. Hull, Journal, Inst'n Metals, Volume 86, (1958), page 425.

104. A. J. McEvily, Jr. and E. S. Machlin, Technical Report R-91, U. S. National Aeronautics Space Administration, 1961.

105. P. J. E. Forsyth and D. A. Ryder, Metallurgia, Volume 63, (1961), page 117.

106. C. Laird and G. C. Smith, Philosophical Magazine, Volume 7, No. 77, (1962), page 847.

107. S. Taira and K. Honda, Transactions, Japan Institute Metals, Volume 1, No. 1, (1960), page 43.

108. J. Muir and D. Binnie, Engineering (London), Volume 112, (1926), page 743.

109. H. Fowler, Engineering (London), Volume 132, (1931), page 299.

110. E. L. Robinson, Transactions, American Society of Mechanical Eng'rs, Volume 66, (1944), page 373.

111. F. V. Warnock and D. B. C. Taylor, Proceedings, Inst'n Mechanical Eng'rs, Volume 161, (1949), page 165.

112. E. W. Hart, Acta Metallurgica, Volume 3, (1955), page 146.

113. K. Farnell, Engineering (London), Volume 185, (1958), pages 92 and 788.

114. B. Jaoul, Journal, Mechanics Physics Solids, Volume 9, (1961), page 16.

115. A. J. Durelli, E. A. Phillips and C. H. Tsao, Introduction to the Theoretical and Experimental Analysis of Stress and Strain, McGraw-Hill Book Co., New York, (1958), page 203.

116. E. Sternberg and M. Sadowsky, Journal, Applied Mechanics, Volume 16, (1949), page 27. See Transactions, American Society of Mechanical Eng'rs, Volume 71, 1949.

117. M. M. Frocht and M. M. Leven, Proceedings, 14th Semi-Annual Eastern Photoelasticity Conference, Yale University, New Haven, Conn., (1941), page 15.

118. R. D. Mindlin, Experimental Mechanics, Journal of the Society for Experimental Stress Analysis, Volume 3, No. 1, (Jan. 1963), page 1.

119. Y. Pao, Journal, Applied Mechanics, American Society of Mechanical Eng'rs, Volume 29, (1962), page 299.

120. R. C. J. Howland, Phil. Transactions, Royal Society, London, Series A, Volume 229, (1930), page 49.

121. A. M. Wahl and R. Beeuwkees, Transactions, American Society of Mechanical Eng'rs, Volume 56, (1934), page 617.

122. D. A. Lemaire, Report ACA-48, Aeronautical Research Consultative Committee, Australia, 1949.

123. R. B. Heywood, Designing by Photoelasticity, Chapman and Hall Ltd, London, (1952), page 267.

124. A. J. Durelli, A. Kobayashi and K. Hofer, Experimental Mechanics, Journal of the Society for Experimental Stress Analysis, Volume 1, No. 9, (Sept. 1961), page 91.

125. A. Nadai, Theory of Flow and Fracture of Solids, McGraw-Hill Book Co., New York, (1950), page 291.

126. J. L. M. Morrison, Proceedings, Inst'n Mechanical Eng'rs, Volume 142, (1939), page 193. See also J. A. Pope, Reference 11, page 47.

127. G. E. Griffith, Technical Note 1705, U. S. National Advisory Committee for Aeronautics, 1948. See also E. Z. Stowell, Technical Note 2073, U. S. National Advisory Committee for Aeronautics, 1950.

128. H. F. Hardrath and L. Ohman, Technical Note 2566, U. S. National Advisory Committee for Aeronautics, 1951.

129. W. A. Box, Proceedings, Society for Experimental Stress Analysis, Volume VIII, No. II, (1951), page 99.

130. D. Morkovin and O. M. Sidebottom, Bulletin No. 372, Eng'g Experiment Station, University of Illinois, Urbana, Illinois, 1947.

131. M. E. Clark, H. T. Corten and O. M. Sidebottom, Bulletin No. 426, Eng'g Experiment Station, University of Illinois, Urbana, Illinois, 1954.

132. F. Bollenrath, V. Hauk and E. Osswald, Zeitschrift, Vereins Deutscher Ingenieure, Band 83, (1939), page 129. See also Welding Research Supplement, Journal of the American Welding Society, Volume 21, (1942), page 285S.

133. H. Neerfeld, Mitteilungen, Kaiser-Wilhelm-Institut Eisenforschung, Band XXVII, (1944), page 13.

134. J. T. Norton, D. Rosenthal and S. B. Maloff, Welding Research Supplement, Journal of the American Welding Society, Volume 25, (1946), page 269S.

135. G. Sachs, C. S. Smith, J. D. Lubahn, G. E. Davis and L. J. Ebert, Welding Research Supplement, Journal of the American Welding Society, Volume 26, (1947), page 26S. See also Technical Notes 986 and 987, U. S. National Advisory Committee for Aeronautics, 1947.

136. T. Nishihara and S. Taira, Proceedings, 3rd Japan National Congress for Applied Mechanics, (1953), page 183.

137. F. Nakanishi and Y. Sato, Proceedings, 5th Japan National Congress for Applied Mechanics, (1955), page 169.

138. B. Budiansky and R. J. Vidensek, Technical Note 3542, U. S. National Advisory Committee for Aeronautics, 1955.

139. G. V. Uzhik, Colloquium on Fatigue, International Union of Theoretical and Applied Mechanics, Edited by W. Weibull and F. K. G. Odqvist, Springer-Verlag, Berlin, (1956), page 112. See also G. W. Ushik (G. V. Uzhik), Festigket und Plastizitat von Metallen bei tiefen Temperaturen, VEB Deutscher Verlag fur Grundstoffindustrie, Leipzig, Section 6.3, 1961. (This book was translated from Russian to German by H. R. Bachmann.)

140. R. Hill, The Mathematical Theory of Plasticity, Oxford University Press, London, (1960), page 245. See also W. Prager, An Introduction to Plasticity, Addison-Wesley Publishing Co., Inc., Reading, Mass., (1959), page 127.

141. P. Kuhn and H. F. Hardrath, Technical Note 2805, U. S. National Advisory Committee for Aeronautics, 1952.

142. F. Nakanishi, see Reference 137.

143. W. N. Findley, F. C. Mergen and A. H. Rosenberg, Proceedings, American Society for Testing Materials, Volume 53, (1953), page 768.

144. H. Neuber, Theory of Notch Stresses, Principles for Exact Stress Calculation, Translated by F. A. Raven, Annotated by J. S. Brock for the David Taylor Model Basin, J. W. Edwards, Ann Arbor, Michigan, (1946), page 156.

145. H. J. Gough and W. J. Clenshaw, Part II of Reference 81.

146. J. O. Smith, Bulletin No. 316, Eng'g Experiment Station, University of Illinois, Urbana, Illinois, 1939.

147. W. Buchmann, Forschung auf dem Gebiete des Ingenieurwesens, Band 5, Ausgabe A, (1934), page 36.

148. O. Graf, Stahl und Eisen, Jargang 53, (1933), page 1215.

MISCELLANEOUS REFERENCES

G. Wållgren, Report No. 48, Flytekniska Försöksanstalten, The Aeronautical Research Inst'e of Sweden, Stockholm, 1953. This report on the effect of mean stress on the fatigue strengths of notched and unnotched aluminum specimens is of unusually high quality and is requisite reading in the overall area of the effect of mean stress.

T. Nishihara and M. Kawamoto, Memoirs, College of Eng'g, Kyoto Imperial University, Kyoto, Japan, Volume XI, No. 4, (1944), page 65. This outstanding report on a proposed criterion for the fatigue strengths of various materials under combined alternating stresses (in and out of phase) is perhaps the most comprehensive approach to fatigue analysis existing today. Although, unfortunately, Professor Nishihara does not deal with notched specimens, this report is of unusually high quality and is requisite reading in the over-all area of the effect of mean stress. See also Volume XI, No. 5, (1945), page 85.